IRON OXIDE REDUCTION BY A CLOSTRIDIAL CONSORTIUM: INSIGHTS FROM PHYSIOLOGICAL AND GENOME ANALYSES

by

MADHAVI SHAH

A Dissertation submitted to the

Graduate School-New Brunswick

Rutgers, The State University of New Jersey

In partial fulfillment of the requirements

for the degree of

Doctor of Philosophy

Graduate Program of Microbial Biology

written under the direction of

Dr. Nathan Yee

And approved by

_____

_____

_____

_____

New Brunswick, New Jersey

May 2013

ABSTRACT FOR THE DISSERTATION

Iron Oxide Reduction by a Clostridial Consortium:

Insights from Physiological and Genome Analyses

by MADHAVI SHAH

Dissertation Director:

Dr. Nathan Yee

Iron reducing organisms are ubiquitous and phylogenetically diverse. Their acitivity in the environment not only affects the speciation of iron in aquatic systems or sediments, but it plays a major role in iron mineral formation, sediment diagenesis, carbon cycling and the fate and transport of contaminants in the subsurface environment. Iron oxide reduction has been extensively studied with pure cultures of dissimilatory iron reducers such as *Geobacter* and *Shewanella*. However, the effects of syntrophy on iron oxide reduction and secondary mineralization by microbial consortia are poorly understood.

The research presented in this dissertation describes enrichment of an iron reducing anaerobic microbial consortium from subsurface sediments. The consortium was composed of fermentative *Clostridium sp*. strain FGH and a novel *Veillonellaceae*, strain RU4. The experimental results indicate the role of hydrogen, sulfate and growth medium in rapid reductive dissolution of iron oxides and subsequent secondary mineralization by the clostridial consortium. The data demostrated that iron oxide reduction by the consortium was catalyzed by both biotic reduction by strain FGH and

syntrophy driven biotic/abiotic reduction by strain RU4. Reductive dissolution of iron oxides by the consortium resulted in formation of solid-phase Fe(II) and poorly crystalline ferrous bearing minerals such as nanoparticulate magnetite and iron sulfides. The results of this work provide new insights in the ecological role of *Clostridia* in subsurface Fe(II) mineral formation processes.

Unlike iron respiring *Geobacter* and *Shewanella*, the mechanism of iron oxide reduction is poorly understood in iron reducing fermentative bacteria. In this study we conducted experiments with fermentative *Clostridium sp*. strain FGH to elucidate its mode of iron reduction. Experiments and genome analysis suggest an indirect, cytochrome c independent mechanism of iron reduction by strain FGH.

Veillonellaceae are recently found to be active during bioremediation studies at contaminanted sites. Genomic characterization of the novel *Veillonellaceae*, strain RU4, that could not be isolated in pure culture revealed its potential metabolic capabilities. The strain RU4 draft genome consists of fatty acid metabolism genes and pathways for sulfate, sulfite and polysulfide reduction. These results may assist in better understanding of the biogeochemical and ecological role of this novel subsurface bacterium.

ACKNOWLEDGEMENTS

First I would like to express my deepest gratitude to my teacher and mentor, Dr. Nathan Yee for his guidance and advice. I thank him for believing in me and making me the person I am today. I also extend thanks to my committee members Dr. Tamar Barkay and Dr. John Reinfelder for their endless devotion and encouragement throughout my research, and Dr. Peter Strom for his help in successfully completing this work.

I want to thank the Office of Science (BER), U.S. Department of Energy (Grant No. DE-FG02-08ER64544) for funding my research. I wish to extend my thanks to National Science Foundation for partially funding my research. I thank EMSL, a national scientific user facility sponsored by the Department of Energy's Office of Biological and Environmental Research and located at Pacific Northwest National Laboratory for supporting a portion of this research.

The following people have helped make this research possible and I thank them all. Dr. Chu-Ching Lin for setting up the iron reducing enrichment cultures, my two wonderful labmates and friends Mathew Colombo and Joanne Theisen who helped me with countless culture transfers and support. I want to thank V. Starovoytov for his assistance with transmission electron microscopy imaging and Udi Zelzion for help with genome assembly and analysis. During my years as a Graduate student at Rutgers University, I met wonderful people and made many friends. Thank you to Dr. Ines Rauschenbach, Dr. Xiuhong Zhao, Dr. Juyoung Ha, Dr. Yangping Wang, Dr. Adam Mumford, John Kim, Jessica Choi, and Jennifer Marin.

Thank you to my loving family. My mom, my biggest support and strength. My dad who recognized my potential and my siblings for their love and encouragement. I want to thank my mother-in-law and father-in-law for believing in me and supporting me

through tough times. Last but not least, thank you to my husband, to motivate me, making me smile and keeping me extremely happy. This thesis would have not been possible without their support.

I am very thankful to my uncle Himanshu Doshi and aunt Kalpana Doshi. My uncle and aunt gave me the opportunity to come to USA and achieve the best education. They love me just like their kids and have been very helpful and encouraging through out my undergradaute and graduate study at Rutgers University. I could never thank them enough for their love and devotion.

I dedicate this work to my parents, Mita and Vikram Parikh.

TABLE OF CONTENTS

Abstract of Dissertation ……...ii

Acknowledgments …… iv

List of Figures ……...viii

List of Tables …… .xii

Chapter 1 – Introduction ……..1

Chapter 2 – Syntrophic Effects in a Subsurface Clostridia Consortium on Fe(III)-(Oxyhydr)oxide Reduction and Secondary Mineralization ……...12

Abstract.....12

Introduction.....13

Materials and Methods.....15

Results…….....21

Discussion…….....28

Chapter 3 - Physiological and Genomic Characterization of an Iron-Reducing, Saprolite-derived *Clostridium* sp. Strain FGH ……...51

Abstract.....51

Introduction.....52

Materials and Methods.....54

Results…….....58

Discussion…….....63

Chapter 4 - Genomic characterization of a novel gram negative, spore forming *Veillonellaceae* derived from subsurface sediments ……75

Abstract.....75

Introduction.....76

Methods …….....77

Results and Discussion….....79

Chapter 5 – Conclusions……96

Contribution to Knowledge…….....96

Suggestions for Furture Research.....99

References.....101

LIST OF FIGURES

Figure 2.1. Neighbor joining tree of strain RU4 and strain FGH with their closest relatives belonging to order *Clostridiales.* The 16S rRNA gene of *Geothrix fermentans* was used as an outgroup. The bar represents 2 substitutions per 100 nucleotides……32

Figure 2.2. DGGE analysis of the consortium grown with fumarate (lane 1); peptone and ferrihydrite (lane 2), goethite (lane 3) or hematite (lane 4); and *Clostridium sp.* FGH grown with peptone (lane 5)……33

Figure 2.3. Experiments on the syntrophic effects on Fe(III) (oxyhydr)oxide reduction and secondary mineralization. Experiment 1: The effect of hydrogen on consortium growth; Experiment 2: Sulfide production by the consortium and pure culture of *Clostridium sp.* FGH; Experiment 3: Iron oxide reduction by pure culture of *Clostridium sp.* FGH; Experiment 4: Biotic/abiotic iron oxide reduction by the consortium; Experiment 5: Hydrogen production by pure culture of *Clostridium sp.* FGH; and Experiment 6: Characterization of secondary Fe(II) mineral products……34

Figure 2.4. Effect of hydrogen on growth of the consortium. (A) Agar slants containing ferric citrate and sulfate; defined liquid media containing (B) fumarate and sulfate; and (C) citrate and sulfate. Grey bars represent nitrogen headspace and black bars represent hydrogen headspace……35

Figure 2.5. Growth on peptone and the production of sulfide. (■) represent optical density and (●) represent acid volatile sulfide production. (A) Pure culture of *Clostridium sp.* FGH and (B) the consortium composed of *Clostridium sp.* FGH and strain RU4…..36

Figure 2.6. Reduction of iron oxides and production of Fe(II) during growth on peptone: (■) ferrihydrite, (●) goethite, and (▲) hematite. (A) Fe(II) produced by the pure culture of *Clostridium sp.* FGH and (B) Fe(II) produced by the consortium composed of *Clostridium sp.* FGH and strain RU4. 30 mM iron oxides provided to culture……..37

Figure 2.7. Role of hydrogen. (A) Gas chromatograph showing the production of H_2 gas by *Clostridium sp.* FGH when grown with peptone. Black line represents *Clostridium sp.* FGH and grey line represents sterile control. (B) Growth of strain FGH in the presence of hydrogen. Grey bars represent nitrogen headspace and black bars represent hydrogen headspace. (C) Effect of hydrogen on ferrihydrite reduction by *Clostridium sp.* FGH when grown with peptone. 100% nitrogen (●) and 100% hydrogen gas (○) in the headspace……...38

Figure 2.8. Iron oxide reduction by the consortium. (A) Ferrihydrite reducing culture; (B) Goethite reducing culture; and (C) Hematite reducing culture at day 0 and 7……..40

Figure 2.9. 2-line ferrihydrite biotransformation by the consortium when grown with peptone and sulfate. (A) X-ray diffraction patterns before (0 day) and after 7 days of incubation, F: Ferrihydrite, M: Magnetite; and the arrows are drawn as a guide to eye to indicate presence of residual "ferrihydrite" in the incubated sample; (B and C) Transmission electron micrographs with corresponding Selected Area Electron Diffractograms of the culture after 7 days of incubation showing presence of ferrihydrite (B) and magnetite (C)……41

Figure 2.10. Goethite reduction by the consortium when grown with peptone and sulfate. (A) X-ray diffraction patterns before and after 7 days of incubation. G: Goethite; (B) Transmission electron micrograph of the culture after 7 days of incubation. The arrow points to a FeS particle that formed during goethite reduction; and (C) Energy dispersive X-ray spectroscopy spectrum of the FeS particle shown in B……..…43

Figure 2.11. XPS and chemical analysis of iron oxide transformation products. (A) X-ray photoemission spectra of the S 2p region of goethite transformation products. Charge referenced using the C 1s line at 284.8 eV. Spectra of goethite samples before (green and blue) and after 7 days of incubation (black and brown); (B) Total (■) and dissolved (●) sulfide produced by the goethite reducing consortium; (C) X-ray photoemission

spectra of the S 2p region of hematite transformation products. Charge referenced using the C 1s line at 284.8 eV. Spectra of hematite samples before (green and blue) and after 7 days of incubation (black and brown); and (D) Total (■) and dissolved (●) sulfide produced by the hematite reducing consortium……..……44

Figure 2.12. Hematite reduction by the consortium when grown with peptone and sulfate. X-ray diffraction patterns before and after 7 days of incubation. H: Hematite....45

Figure 2.13. Characterization of crystalline iron oxide transformation product. Oxidation of goethite (A) and hematite (B) transformed products when exposed to air……46

Figure 3.1. (A) Transmission electron micrographs of strain FGH, showing a gram positive cell wall; (B) Neighborhood joining tree of strain FGH with its closest relatives. The 16S rRNA gene of *Shewanella oneidensis* was used as an outgroup. The bar represents 5 substitutions per 100 nucleotides……67

Figure 3.2. Ferrihydrite (1 mM) reduction by *Clostridium sp.* FGH when grown with 30 mM pyruvate(A), 30 mM glucose (B), or 110 mM glucose (C). Cells were incubated with ferrihydrite in presence [■] or absence [□] of carbon source. Points and error bars represent the means and standard deviations of duplicate cultures……..……68

Figure 3.3. Ferrihydrite bead reduction by *Clostridium sp.* FGH during glucose (110 mM) fermentation. 1 mM ferrihydrite beads were provided. Cells were incubated with iron oxide in presence [■] or absence [□] of glucose. Points and error bars represent the means and standard deviations of triplicate cultures……..……....69

Figure 3.4. Extracellular flavin production by *Clostridium sp.* FGH. *Shewanella oneidensis* MR-1 was used as a positive control. Error bars represent the standard deviations of duplicate cultures……..……..70

Figure 3.5. Schematic representation of genes and metabolism pathways in the genome of *Clostridium sp.* FGH……71

Figure 4.1. Transmission electron micrographs of Strain RU4. (A) Exponential phase culture showing gram-negative cell wall with a IM-Inner Membrane and OM-Outer Membrane; and (B) Stationary phase culture showing endopsore formation……89

Figure 4.2. Beta oxidation pathway in strain RU4……..…..90

Figure 4.3. Schematic representation of genes and metabolism pathways in the genome of strain RU4……..…….91

Figure 4.4. Sulfate reduction operon structure in (A) strain RU4, (B) *Desulfotomaculum reducens* strain MR-1 and (C) *Desulfovibrio vulgaris* strain Hildenborough. *apr*AB, alpha and beta subunit of the APS reductase; *sat*AB, alpha and beta subunit of the sulfate adenylyltransferase; *qmo*ABC, alpha, beta and gamma subunits of the quinone-interacting membrane-bound oxidoreductase; *hdr*B, heterodisulfide reductase; and hyp, hypothetical protein……92

Figure 4.5. Sulfite reductase operon structure in (A) strain RU4, (B) *Desulfotomaculum gibsoniae* strain DSM 7213 and (C) *Desulfotomaculum nigrificans* strain DSM 574. dsrABC, sulfite reductase subunit A, B and C……93

Figure 4.6. Polysulfide reduction operon structure in (A) strain RU4 and (B) *Wolinella succinogenes* strain DSM 1740. psrABC, polysulfide reductase subunit A, B and C…..94

LIST OF TABLES

Table 2.1. Substrate utilization by the consortium……..……..47

Table 2.2. Growth of consortium on various substrates……..…48

Table 2.3. Effect of sulfate on iron oxide reduction by the consortium……..……49

Table 2.4. Dissolved and total Fe(II) production during iron oxide reduction by the consortium……50

Table 3.1. Growth of *Clostridium sp*. FGH on various substrates in presence or absence of sulfate……..……72

Table 3.2. Spend media reaction with ferrihydrite (30 mM)……..…..73

Table 3.3. c-type cytochromes in the genome of *Clostridium sp*. FGH and in the complete genome of other organisms……..…74

Table 4.1. G+C content and tetranucleotide frequency analysis of contigs in the genome assembly. The G+C content of *Clostridium sp*. FGH is 30%. Contigs in bold have G+C content close to *Clostridium sp.* FGH. Contigs highlighted in grey have similar tetranucleotide frequencies…..……..…….95

CHAPTER 1

INTRODUCTION

Iron Reduction

On the surface of the Earth, iron primarily exists in two oxidation states, ferrous (Fe^{2+}) and ferric (Fe^{3+}). Fe^{2+} is soluble and mobile in contrast to Fe^{3+}, which is highly insoluble and exists in solid phase minerals. However, Fe^{2+} is unstable under oxic conditions at neutral pH and is readily oxidized to Fe^{3+}. Therefore, at pH values at or above a circumneutral pH, iron exists primarily as insoluble, solid-phase minerals (Schwertmann and Cornell, 1991). In soil and sediment environments, Fe^{3+} oxides and oxyhydroxides can be present as amorphous minerals such as ferrihydrite or as well-crystallized minerals such as hematite (Fe_2O_3) and goethite (FeOOH) (Schwertmann and Cornell, 1991).Decreasing pH values increase the solubility of Fe^{3+} as well as enhance the stability of Fe^{2+}, and below pH 4.0, Fe^{2+} primarily exists as an aqueous species, even in the presence of oxygen (Stumm and Morgan, 1996). In nature, iron cycling involves oxidation and reduction reactions between the ferrous and ferric forms. The oxidation of Fe^{2+} can be catalyzed either chemically or by microorganisms. Fe^{2+} oxidation results in precipitation of Fe^{3+} as iron oxides. These iron oxides can either serve as electron acceptors for microorganisms or can reduced to Fe^{2+} chemically.

The microbial reduction of Fe(III) oxides produces a biogeochemically active pool of Fe that includes Fe(II)aq , Fe(II) adsorbed on Fe(III) mineral surfaces, and Fe(II) minerals. One of the major pathways for transformation of mercury, uranium, chromium, technictium and organic contaminants in the subsurface is through reactions with biogenic Fe(II)-containing minerals (Elsner et al., 2004; Fredrickson et al., 2004; Gregory et al., 2004; Hyun et al., 2012; Klausen et al., 1995; Lee and Batchelor, 2002; Liger et al., 1999; McCormick et al., 2002; Peretyazhko et al., 2012; Scott et al., 2005; Wiatrowski et al., 2009). These transformation reactions affect the fate and transport of toxic metals (contaminants) in groundwater and the subsurface. In addition to contaminant transformations, iron oxide mineral transformations can strongly affect the ecology of subsurface geological habitats, by altering the crystallinity, structural form, and bioavailable surface area of iron mineral substrates.

Iron reducing microorganisms

Iron respiration has been proposed as one of the first forms of microbial metabolism (Lovley et al., 2004; Vargas et al., 1998). It is thought to have evolved preceding the development of oxygen, nitrate and sulfate respiration. Iron oxide reduction has been observed in archaea (Kashefi and Lovley, 2000, 2003; Vargas et al., 1998) and is widely distributed among the bacteria (Caccavo et al., 1996; Caccavo et al., 1994; Carlson et al., 2012; Dobbin et al., 1999; Lovley et al., 2004). Iron plays a key role in environmental microbe-metal interaction due to its abundance in the Earth's crust and the ability of microbes to reduce ferric ion (III) to ferrous ion (II). Fe(III) oxides such as ferrihydrite, goethite, and hematite are commonly found in the Earth's crust. Bacteria preferentially reduce amorphous Fe(III) oxyhydroxides such as ferrihydrite (Lovley and Phillips, 1986; Munch and Ottow, 1980, 1983) because it is energetically more favorable than reducing crystalline iron oxides.

Dissimilatory iron reducing microbes couple reduction of Fe(III) to oxidation of organic matter. This ability enables prokaryotes that respire ferric iron to thrive in anoxic subsurface geologic environments. Members of the family *Geobacteriaceae* and genus *Shewanella* are model dissimilatory iron reducing bacteria. Most of our knowledge about iron reduction capabilities, secondary mineral transformation and the mechanism of Fe(III) oxide reduction is based on these model iron reducing bacteria. Dissimilatory iron reduction ability is not limited to gram negative bacteria, but has been determined in a few gram positive bacteria. Recently, *Thermicola potens*, a gram positive Firmicute was characterized for its iron oxide respiration ability (Carlson et al., 2012).

In addition to iron respiring bacteria, other iron reducing microorganisms that do not respire iron are increasingly being recognized as an environmentally and ecologically important group. Very diverse groups of microorganisms are involved in iron reduction in the environment. The mechanism of iron oxide reduction by these iron reducers remains poorly understood.

Mechanisms of Microbial Iron Reduction

The insoluble nature of Fe(III) oxides poses difficulty for iron reducing microorganisms to utilize Fe(III). Microbes have developed several strategies to transfer electrons to extracellular Fe(III) oxide minerals. Microbes either require direct contact with the extracellular Fe(III) oxide or must produce extracellular redox active compounds (such as humic acids) or electron shuttling compounds to reduce Fe(III). Direct contact between the microorganism and the solid-phase Fe(III) oxides is required for the reduction of insoluble Fe(III) oxides in *Geobacter* (Nevin and Lovley, 2000). Recent studies proposed that pili (also referred to as conductive nanowires) function as an

electrical conduit for the transfer of electrons to insoluble Fe(III) oxides in *Geobacter* and, potentially, other solid-phase terminal electron acceptors (Reguera, 2005).

Some iron reducing microorganisms can reduce soild phase Fe(III) oxides without establishing direct contact with the insoluble Fe(III) mineral. They can produce exogenous (Lovley et al., 1996) or endogenous (Kotloski and Gralnicka, 2013; Marsili et al., 2008; Nevin and Lovley, 2002; Newman and Kolter, 2000; Turick et al., 2002) soluble external electron shuttles that can transfer electrons to insoluble Fe(III) oxides. *Shewanella* and *Geothrix* produce flavins that function as electron shuttles to Fe(III) oxides (Mehta-Kolte and Bond, 2012; von Canstein et al., 2008). Other than using an electron shuttle, microbes can also produce Fe(III) chelators that can facilitate iron oxide reduction.

Since Fe(III) exists as insoluble oxides at neutral pH values, the reduction of extracellular Fe(III) is likely to proceed via mechanisms substantially different from those for the reduction of soluble electron acceptors such as oxygen, nitrate, fumarate, or sulfate. The mechanism of iron oxide reduction has been studied extensively in two gram negative Proteobacteria, *Geobacter sulfurreducens* PCA and *Shewanella oneidensis* MR-1. To transfer electrons to extracellular solid-phase Fe(III), these bacteria have to transfer electrons derived from central metabolism in the cytoplasm and inner membrane to an insoluble, extracellular electron acceptor via the periplasm and outer membrane.

Multihaem c-type cytochromes are the major electron carrier proteins found in *Geobacter* and *Shewanella*. These c-type cytochromes are strategically located in the bacterial cell envelop to facilitate the electron transfer from the quinine/quinol pool in the inner membrane to the periplasm and then to the outer membrane, where they interact with the iron oxides (Shi et al., 2009). The outermembrane c-type cytochromes can transfer electrons to iron oxides either directly or indirectly.

In *Geobacter*, the outer membrane tetrahaem *c*-cytochrome OmcE and hexahaem *c*-cytochrome OmcS are thought to be located on the cell surface where they are thought to transfer electrons to pili. Pili are hypothesized to relay electrons directly to Fe(III) oxides (Reguera, 2005). OmcE and OmcS receive the electrons originating from the quinone/quinol pool in the inner membrane (IM). A key periplasmic cytochrome, MacA, was identified in the inner membrane and is predicted to function as an intermediate carrier (Butler et al., 2004) and therefore might pass electrons to other periplasmic proteins such as PpcA, a tri-heme periplasmic *c*-type cytochrome involved in electron transport to outer membrane proteins (Lloyd et al., 2003). OmcB is an outer membrane protein determined to have an important role in Fe(III) reduction (Leang et al., 2005; Leang et al., 2003). Disruptions in *omcB* by gene replacement impaired the ability of *G. sulfurreducens* to reduce Fe(III) by approximately 94–97% (Leang et al., 2003).

Multiheme c-type cytochromes can transfer electrons directly to solid phase Fe(III) or flavins in *Shewanella oneidensis* MR-1. Proteins that are known to be directly involved in the reduction include the following multiheme c-type cytochromes. The tetrahaem *c*-cytochrome CymA that is a homologue of the NapC/NirT family of quinone dehydrogenases is located in the cytoplasmic membrane that can transfer electrons from quinone pool to periplasm (Myers and Myers, 1993, 1997; Myers and Myers, 2000). The periplasmic decahaem *c*-cytochrome MtrA is thought to accept electrons from the cytoplasmic membrane electron carrier CymA, and transfer these electrons to outer membrane proteins. MtrA has also been proposed to be involved in soluble Fe(III) reduction as a terminal reductase in the periplasm (Pitts et al., 2003). The outer membrane decahaem *c*-cytochromes MtrC and OmcA can transfer electrons directly to the surface of solid Fe(III) oxides (Beliaev et al., 2001). MtrC and OmcA might also reduce Fe(III) oxides indirectly by transferring electrons to either flavin-chelated Fe(III) or oxidized flavins.

Recently, multiheme c-type cytochromes were also proposed to be involved in dissimilatory iron reduction by a gram positive Firmicute. Genome sequencing and analysis of *Thermincola potens* revealed the presence of 32 multiheme c-type cytochromes (Carlson et al., 2012). A few c-type cytochromes were identified as cell wall/surface c-type cytochromes that might have implication for electron transfer to insoluble Fe(III) oxides. A terminal iron reductase has yet to be identified in iron reducing microorganism.

Microbial Secondary Iron Biomineralization

Secondary iron mineralization is primarily studied with members of the family *Geobacteraceae* and the genus *Shewanella* (Fredrickson et al., 1998; Hansel et al., 2005; Hansel et al., 2003). The production of Fe(II) and its subsequent reaction with the parent iron mineral substrate induces the reductive dissolution of iron oxides and the precipitation of secondary iron minerals. The products of Fe(II)-induced ferrihydrite transformation were commonly goethite, lepidocrocite, magnetite, vivianite, siderite or green rust depending on the Fe(II) concentration, pH, and the presence of stabilizing ligands (Fredrickson et al., 1998; Hansel et al., 2005; Hansel et al., 2003). Secondary iron biomineralization was driven by Fe(II) concentration. At low concentrations (<0.3 mM), ferrihydrite was rapidly converted to goethite. Goethite precipitation occurred via dissolution and reprecipitation reactions. If Fe(II) concentrations were high (> 0.3 mM), both goethite and magnetite precipitate.

Studies with *Shewanella alga* revealed that AQDS (Anthraquinone-2,6-disulfonate) and presence of ligands such as phosphate or carbonate or organic ligands also determine what secondary iron minerals are formed during ferrihydrite reduction (Fredrickson et al., 1998). The presence of AQDS in media facilitated bacteria to produce more Fe(II). Biogenic solids in the bicarbonate buffered media were

predominantly siderite ($FeCO_3$), whereas vivianite and magnetite were formed in phosphate and PIPES buffered media, respectively. When phosphate was present in the PIPES buffer with AQDS, poorly crystalline green rust was formed (Fredrickson et al., 1998). Current knowledge about secondary iron mineralization is based on ferrihydrite reduction by *Shewanella* and *Geobacter*, but very little is known about secondary iron minerals produced during goethite or hematite reduction by bacteria. Further investigation is also required to determine secondary iron mineralization by microbial consortia.

Importance of microbial consortia

In natural habitats, microbes occur in communities rather than pure culture. Microbial community interactions in the environment are poorly understood. Recent studies have shown that microbial interactions can enable functions that a single cell type cannot, for example, anaerobic methane oxidation (Boetius et al., 2000). In subsurface ecosystems, microbial communities are known to participate in syntrophic interactions. Syntrophy is a community-level process that involves interspecies exchange of metabolites between organisms. Syntrophic metabolism may require close physical contact or metabolic synchronization of the syntrophic partners (McInerney et al., 2009). A recent study by Summers et al. (2010) demonstrated that a syntrophic microbial consortium composed of iron-reducing bacteria is able to catalyze electron transfer reactions that a single cell type cannot. Cooperative exchange of electrons and hydrogen in microbial communities is known to play an important role in the conversion of complex natural organic matter to CO_2 and CH_4 (Stams et al., 2006; Stams and Plugge, 2009).

In some microbial consortia, fermentation of the organic matter generates H_2, which is consumed by a lithotrophic partner. The initial substrate reactions are catalyzed

by the fermentative bacterial species, but the growth of the fermenters and the metabolic products that are formed are strongly affected by the hydrogen consumer. When the fermentative bacteria are isolated and grown in pure culture without the syntrophic partner, H_2 accumulates to high levels (ΔG° of the reaction is positive), NADH oxidation becomes thermodynamically unfavorable and organic matter degradation stops. Hydrogen consumption by a hydrogen utilizing partner lowers the hydrogen partial pressure, making the conversion exergonic (ΔG° of the reaction is negative), thus enabling proton reduction and energy conservation (McInerney et al., 2008; Schink and Stams, 2006; Stams, 2006; Stams and Plugge, 2009). Intact syntrophic microbial consortia have been shown to oxidize organic compounds that the individual species cannot utilize alone (McInerney et al., 2009; McInerney et al., 2008). To date and to the best of our knowledge, the reduction of crystalline iron oxides by syntrophic microbial consortia has not been examined.

Fermentation and its effects on iron reduction

Fermentations are cytosolic oxidation-reduction pathways. During fermentation, NADH or some other reduced electron acceptor that is generated by oxidation reactions in the pathway is reoxidized by metabolites produced within the fermentative pathway. These reactions occur in cytosol rather than in the membranes. ATP production in fementation occurs via substrate level phosphorylation (White, 2007). In contrast to respiration, fermentation takes place in the absence of an exogenous electron acceptor. Therefore, the fermentation pathway must produce the electron acceptors to dispose of the electrons produced during oxidation reactions. These electron acceptors function as an electron sink for removal of electrons whereas the reduced products formed during fermentation are excreted into the media. Hydrogen, carbon dioxide, acetate and formate are common fermentation products formed by microorganisms. These

fermentation products might serve as growth substrates for environmentally important groups of microorganisms such as sulfate, iron or metal reducers in subsurface environments.

Apart from dissimilatory iron reducers, fermentative bacteria can also catalyze iron reduction (Dobbin et al., 1999; Lovley et al., 1991). Iron is not required for growth of these fermentative bacteria and they are thought to transfer only a small fraction of reducing equivalent to Fe(III) (Lovley, 1987; Lovley et al., 1991). The diversion of reducing equivalents to Fe(III) might provide an energetic advantage, utilizing the oxidation of NADH coupled to soluble Fe(III) reduction to yield ATP (Dobbin et al., 1999) or by shift in the fermentation end products. Iron oxide reduction by fermentative bacteria is poorly understood and mechanisms of iron oxide reduction require further research.

Reductive dissolution of iron oxides by sulfide

Sulfate reducers are commonly found in anoxic sediments and subsurface environments. Some sulfate reducers (Coleman et al., 1993; Lovley et al., 1993) are also capable of Fe(III) reduction. Sulfate reducing bacteria can reduce Fe(III) either enzymatically or nonenzymatically (Li et al., 2006; Tebo and Obraztsova, 1998). The nonenzymatic reduction of Fe(III) reduction by sulfate reducing bacteria involves reduction of Fe(III) by sulfide. During reduction of Fe(III) oxides by sulfide, sulfide is oxidized to elemental sulfur, which can be reduced back to sulfide by activity of sulfur reducing bacteria. This type of sulfur cycling can enable extensive amounts of iron oxide reduction. Iron oxide reduction by sulfur cycling (S0/S2- redox couple) was observed in *Sulfurospirillum deleyianum* (Straub and Schink, 2004). This process plays an important role in sulfidogenic sediment.

Applications of genome sequencing to iron reducing bacteria

Advances in shotgun cloning, automation of DNA sequencing and the development of powerful computational methods for DNA sequences have provided tools to reveal the molecular basis for environmentally important microbial processess. Genome sequencing of the dissimilatory iron reducing bacteria *Shewanella* (Heidelberg et al., 2002) and *Geobacter* (Methe et al., 2003) unravelled the presence of numerous c-type cytochromes in these metal reducing bacteria. Genome sequencing also assisted gene expression and mutagenesis studies to determine the function of these c-type cytochromes in transfer of electrons to insoluble iron oxides. Genome sequencing of other iron reducing bacteria that do not respire iron can provide insight in metabolism and mechanism of iron reduction by these organisms.

Goal and Objectives of this study

The overall goal of this disseration was to characterize an iron reducing consortium enriched from subsurface sediments.

- Chapter 2 investigates Fe(III) (oxyhydr)oxide reduction and secondary mineralization by a subsurface clostridia consortium. The objectives were to determine amorphous and crystalline iron oxide reduction by the consortium; elucidate the role of hydrogen, sulfate and growth medium on rates and extent of iron oxide reduction by the consortium, and identify the secondary minerals produced by the microbial consortium.
- Chapter 3 examines the mode of iron oxide reduction by strain FGH through physiological and genome analysis. The objectives were to examine if direct contact was necessary for iron reduction by fermentative *Clostridium sp*. FGH; determine if c-type cytochromes are present in the genome of strain FGH; and identify the genes involved in metabolism.
- Chapter 4 investigates the metabolic ability of strain RU4 via genome sequencing and analysis. The objective of this study was to reveal the genes encoding for metabolic pathways in strain RU4 to understand its potential biogeochemical and ecological role in the subsurface environment.

CHAPTER 2

Syntrophic Effects in a Subsurface Clostridia Consortium on Fe(III)-(Oxyhydr)oxide Reduction and Secondary Mineralization

Submitted to Geomicrobiology Journal

ABSTRACT

In this study, we cultivated from subsurface sediments an anaerobic clostridia consortium that was composed of a fermentative Fe reducer *Clostridium* species (designated as strain FGH) and a novel sulfate-reducing bacterium belonging to the clostridia family *Vellionellaceae* (designated as strain RU4). In pure culture, *Clostridium sp*. strain FGH mediated the reductive dissolution/transformation of iron oxides during growth on peptone. When *Clostridium sp.* FGH was grown with strain RU4 on peptone, the rates of iron oxide reduction were substantially higher. Iron reduction by the consortium was mediated by multiple mechanisms, including biotic reduction by *Clostridium sp.* FGH and biotic/abiotic reactions involving biogenic sulfide formed by strain RU4. The *Clostridium* sp. FGH produced hydrogen during fermentation, and the presence of hydrogen inhibited growth and iron reduction activity. The sulfate reducing partner strain RU4 was stimulated by the presence of H_2 and generated reactive sulfide, which promoted the chemical reduction of the iron oxides. Characterization of Fe(II) mineral products showed the formation of nanoparticulate magnetite during ferrihydrite reduction, and the precipitation of iron sulfides during goethite and hematite reduction. The results suggest an important pathway for iron reduction and secondary mineralization by fermentative and sulfate reducing microbial consortia through syntrophy-driven biotic/abiotic reactions with biogenic sulfide.

1. INTRODUCTION

Clostridia are common subsurface spore forming anaerobes (Klouche et al., 2007; Lin et al., 2006; Liu et al., 1997; Moser et al., 2003; Rastogi et al., 2010) that are known to play an important role in the biogeochemical cycling of carbon, sulfur and iron (Castro et al., 2000; Daumas et al., 1988; Lin et al., 2007; Rosnes et al., 1991; Senko et al., 2009; Tebo and Obraztsova, 1998; Widdel and Pfenning, 1977). In laboratory studies, pure cultures of clostridia were among the first organisms shown to reduce Fe(III) oxides (Hammann and Ottow, 1974; Starkey and Halvorson, 1927). A growing body of literature suggests that clostridia are key microbial drivers in iron reduction in estuarine sediments and acid mine drainage environments (Lin et al., 2007; Senko et al., 2009; Tebo and Obraztsova, 1998). Many clostridia reduce iron during fermentative growth (Dobbin et al., 1999; Hammann and Ottow, 1974; Lovley, 1995; Starkey and Halvorson, 1927). Subsurface clostridia frequently occur in complex communities (Akob et al., 2007; Cardenas et al., 2010; Gihring et al., 2011; Nevin et al., 2003), and are often associated with microbes that consume fermentation products. The community interactions in fermentative consortia that affect iron reduction are poorly understood.

In subsurface ecosystems, microbial communities are known to participate in syntrophic interactions (McInerney et al., 2009; McInerney et al., 2008). Cooperative exchange of electrons and hydrogen in microbial communities is known to play an important role in the microbial fermentation of polysaccharides and proteins (Stams, 2006; Stams and Plugge, 2009), and in degradation of organic contaminants. Microbial consortia composed of clostridia have also been shown to couple the oxidation of methanol (Daniel et al., 1999) and benzene (Kunapuli et al., 2007) to the reduction of

soluble Fe(III) to Fe(II). The interactions between members of clostridia within consortia, and their impact on the reductive dissolution of iron oxides, have not been studied.

The Integrated Field Research Center in Oak Ridge (IFRC-OR), TN, is an U.S. Department of Energy operated site where *in situ* stimulation of bacterial activity has been studied as a potential approach to mitigate the subsurface migration of mobile radionuclide contaminants. Bioremediation experiments with uranium-contaminated groundwater at IFRC-OR found that *Desulfosporosinus* and unknown genera belonging to the *Clostridiales* are important indicator species in areas where iron reduction occurs (Cardenas et al., 2010). Pyrosequencing of 16S rRNA genes in an ensuing biostimulation experiment at this field site showed that members of the clostridia family *Vellionellaceae* dominated the bacterial communities during the initial phase of iron reduction (Gihring et al., 2011). Selective chemical extractions and variable temperature ^{57}Fe-Mössbauer spectroscopy studies indicated that the IFRC-Oak Ridge sediments contain varying amounts of goethite, hematite, and poorly-crystalline Fe-oxides (Fredrickson et al., 2004; Kukkadapu et al., 2006; Wu et al., 2012). Hence understanding the factors that affect the activity of clostridia towards Fe-oxides may have important implications for the effective design of field-scale bioremediation strategies.

One of the major pathways of contaminant transformation in the subsurface is through reactions with biogenic Fe(II) containing minerals (Elsner et al., 2004; Gregory et al., 2004; Klausen et al., 1995; Lee and Batchelor, 2002; McCormick et al., 2002; Peretyazhko et al., 2012; Qafoku et al., 2009; Wiatrowski et al., 2009). Secondary iron(II) phases are known to form during dissimilatory reduction of Fe oxides (Hansel et al., 2003; Liu et al., 2001b). Most of the studies, however, focused on biotransformation of poorly crystalline Fe(III) oxide, ferrihydrite. Also, the subsequent reaction of soluble Fe(II) with residual ferrihydrite may induce precipitation of relatively more crystalline Fe oxides. For example, recent laboratory studies have shown sequestration of uranium in

Fe(II) induced ferrihydrite mineral transformation products, magnetite or goethite (Nico et al., 2009; Stewart et al., 2009). To date, the formation of secondary iron(II) bearing phases in the subsurface sediments has been mainly attributed to members of the family *Geobacteraceae* and the genus *Shewanella* (Fredrickson et al., 1998; Hansel et al., 2003; Lovley et al., 1987). Very little is known about the chemical forms of Fe(II) and secondary iron minerals produced by clostridia.

In this study, we cultivated an anaerobic consortium from subsurface sediments collected at the IFRC-OR, Tennessee. We characterized the phylogenetic composition of the consortium, examined its iron oxide reduction activity under different growth conditions, and analyzed the secondary iron mineral products. We found that the consortium, which was composed of two strains of clostridia, rapidly reduced iron oxides and generated extensive amounts of Fe(II)-containing minerals. The results of this work provide new insights into the ecological role of clostridia in iron oxide reduction and Fe(II) mineralization pathways.

2. MATERIALS AND METHODS

2.1. Enrichments. The sediment inoculum for the enrichment cultures was obtained from the uncontaminated Background Area of the United States Department of Energy's IFRC-OR. A sediment core composed of unconsolidated clay-rich saprolite was collected on August 24, 2006 (Borehole FB628 at Site A; Lat=35.94, Long=84.33) and aseptically sectioned under strict anaerobic conditions in a glove box (Coy Labs, Grass Lake, MI). Sediment samples were stored anaerobically and refrigerated in a gas-tight container prior to overnight shipment to Rutgers University, New Jersey, USA.

Sediment material from a core section that was recovered from 4.5-6.0 m below surface was used as the enrichment inoculum. Enrichments were made with 90 mL of

anoxic defined artificial groundwater (AGW) medium, formulated to represent the principal chemical components revealed by an on-site monitoring well (FW300 and FW301) close to the core sampling location. AGW contained 0.2 mM NH_4Cl, 0.1 mM NaCl, 0.04 mM KH_2PO_4, 0.04 mM $MgSO_4.7H_2O$, 0.03 mM $CaCl_2.2H_2O$, 10 mM acetate, 30 mM ferrihydrite, 0.2 mM cysteine, 0.05 g/L yeast extract, and Wolfe's vitamins and minerals (as in ATCC medium 1957). The final pH of the medium, buffered by 10 mM PIPES, was adjusted to 6.8 using 1N NaOH. Medium preparation and culture transfer were performed using strict anaerobic (purged with 100% nitrogen gas) and aseptic techniques.

Prior to use as inoculum, sediment was homogenized using acid-washed, autoclaved agate mortar and pestle. All procedures were conducted in a Coy anaerobic chamber with an atmosphere of ~95% N_2 and ~5% H_2. Inoculated serum bottles were incubated statically at 28°C in the dark. Autoclaved sediment served as an abiotic control. After three successive transfers, an enrichment producing Fe(II) was used to inoculate anaerobic agar shake (Balch) tubes made with 3 mL of 1.8% BD Difco™ noble agar and 6 mL of AGW medium containing ferric citrate instead of ferrihydrite. An active consortium culture composed of two microorganisms was obtained from anaerobic agar shake tubes. The consortium culture was maintained in serum bottles by periodic transfer to medium containing fumarate (30 mM) and yeast extract (0.05 g/l) at 28°C. The pure culture of *Clostridium sp.* FGH was isolated (Shah et al., submitted) and maintained in medium containing 2% peptone at 28°C.

2.2. Electron microscopy. For visualizing mineral morphology, thin sections were prepared by fixing the cells in 2.5% glutaraldehyde, gradually dehydrating in an ethanol series, and embedding in London Resin (LR) white. The polymerized samples were sectioned on a microtome and observed using a JEOL 2010 transmission electron

microscope (TEM) operating at 200 KV. Samples were prepared in an anaerobic chamber to prevent oxidation of Fe(II)-containing solids. High-resolution TEM is fitted with selected area electron diffraction (SAED). A 10 µm objective aperture was used for imaging. A 10 µm selected-area aperture and various camera lengths were used to obtain selected area electron diffraction patterns.

2.3. Phylogenetic analysis. Genomic DNA was extracted from the consortium and pure cultures by using the PowerSoil DNA Kit (MoBio, Carlsbad, CA). The 16S rRNA gene was PCR amplified using bacterial 16S universal primers 27F (5'-AGAGTTTGATCMTGGCTCAG-3') and 519R (5'- GWATTACCGCGGCKGCTG-3'). PCR products were visualized following electrophoresis in 1% agarose gels in 1xTAE (40 mM Tris, 5 mM sodium acetate, 1 mM EDTA [pH 7.8]). Agarose gel was run at 125 V for 30 min. PCR products were purified using Ultraclean PCR kit (MoBio, Carlsbad, CA) and purified PCR products were then sequenced by Genewiz (South Plainfield, NJ). The most closely related sequences to the 16S rRNA gene were identified by blastn searches (Altschul et al., 1997) of the NCBI database and downloaded from GenBank. The sequences were aligned by using ClustalW2.0 (Chenna et al., 2003), trimmed in ClustalX, and the neighbor-joining phylogenetic trees were constructed using MEGA 4 (Tamura et al., 2007).

2.4. Denaturing gradient gel electrophoresis. Exponential phase cultures were analyzed using denaturing gradient gel electrophoresis (DGGE). Genomic DNA was extracted by a phenol-chloroform method (Kerkhof and Ward, 1993), and the extracted DNA was PCR amplified for DGGE analysis using primers and protocols described by Muyzer et al (1993). Purified PCR products (193 bp) were then separated by DGGE as described by Muyzer and Smalla (1998) using a DCode^{TM}Universal Mutation Detection

System (Bio-Rad Laboratories, CA). DGGE gels contained 8% (w/v) polyacrylamide gels and a 40-80% denaturant gradient consisting of 7 M urea and 40% (v/v) formamide stock solution according to Geets et al (2006). Electrophoresis was performed in 1×TAE buffer at 55 V for 16 h at 60 °C.

DGGE gels were stained with ethidium bromide for 20 min and rinsed quickly with Milli-Q water. Gel images were then acquired under UV light. Gel slices containing DNA bands were excised, and the DNA eluted into Milli-Q water by an overnight incubation at 4°C and subjected to another cycle of PCR amplification. PCR products were purified using Ultraclean PCR kit and purified PCR products were sequenced by Genewiz. DGGE is a qualitative technique that provided an estimate of which organism is dominant under different conditions.

2.5. Growth experiments. Cultures were grown with different carbon sources in minimal medium and incubated at 28°C for 7 days. Fumarate, citrate, acetate, formate, propionate, butyrate and succinate were provided at a concentration of 30 mM or peptone was added as 2% (w/v) to test for fermentation of these carbon sources. Then both the consortium and pure culture of *Clostridium sp.* FGH were tested for their ability to utilize sulfate (30 mM) as an electron acceptor and hydrogen (100% in the headspace) as an electron donor when provided with various carbon sources. To test for autotrophic growth, cultures were grown with hydrogen, carbon dioxide (H_2:CO_2 ratio was 80:20 v/v), and sulfate in minimal media. Growth was measured by optical density (A_{600}).

2.6. Iron oxide reduction experiments. Fe(III)-(oxyhydr)oxides were prepared using methods from Schwertmann and Cornell (1991). Briefly, ferrihydrite was prepared by neutralization of $Fe(NO)_3.9H_2O$ solution with KOH. Goethite was synthesized by first

precipitating ferrihydrite by neutralization of $Fe(NO)_3.9H_2O$ solution with KOH, and then holding ferrihydrite in a closed flask at 70°C for 60 h. Hematite was prepared by adding $Fe(NO)_3.9H_2O$ to 2 mM HCl solution at 98 ^oC and heating this solution at 98 ^oC for 7 days. Synthesis of iron oxides was followed by 7-8 washes with deoxygenated deionized water in the anaerobic chamber until the washed suspension reached neutral pH. The mineralogical identity of the iron oxides was confirmed by powder X-ray diffraction (XRD) and Mössbauer spectroscopy. Surface area was determined with an 11-pt BET-Nitrogen isotherm (Micromeritics Gemini 2375). XRD and BET measurements were conducted on dry samples. Ferrihydrite was dried at room temperature, whereas goethite and hematite were dried at 60°C before analysis. The surface areas of goethite, hematite and ferrihydrite were 35, 36 and 310 m^2/g, respectively.

A modified artificial groundwater medium was used for the iron oxide reduction experiments. It contained 0.75 mM NH_4Cl, 0.1 mM NaCl, 0.34 mM KH_2PO_4, 0.38 mM $MgCl_2.6H_2O$, 0.34 mM $CaCl_2.2H_2O$, 10 mM PIPES buffer, 0.05 g/L yeast extract, Wolfe's vitamin mix and a modified mineral solution [10 ml per liter of medium]. The modified mineral solution contained (g/L): Nitrilotriacetic acid, 1.5; $MnCl_2.4H_2O$, 0.5; $FeCl_2.4H_2O$, 0.1; $CoCl_2.6H_2O$, 0.1; $ZnCl_2$, 0.1; $CuCl_2.2H_2O$, 0.01; H_3BO_3, 0.01; $Na_2MoO_4.2H_2O$, 0.01; $NaSeO_3$, 0.01; $NiCl_2.6H_2O$, 0.01; $Na_2WO_4.2H_2O$, 0.01. The final pH of the medium was adjusted to 6.8 with 1 N NaOH and then supplemented with 30 mM fumarate or 2% peptone as the carbon source. Ion chromatography analysis indicated that 2% peptone contained 2.6 mM sulfate.

Iron reduction experiments were conducted with 30 mM of goethite, hematite or ferrihydrite. Cells were pre-washed by centrifugation (9167g for 10 mins); the supernatant was decanted, and pellets resuspended in fresh medium devoid of electron donors and acceptors in the anaerobic chamber. The washed cell suspension was adjusted to an optical density ($O.D._{600}$) of 0.1, and then used to inoculate the medium at

a 1:10 (v:v) dilution. The final cell density was 3×10^7 cells/ml as determined by DAPI staining and epifluorescence microscopy. Triplicate cultures were set-up and incubated under strict anaerobic conditions in the dark at 28°C on a shaker (New Brunswick Scientific, NJ) and agitated at 150 rpm.

2.7. Chemical analyses. At selected time points, samples were removed from iron oxide reducing cultures, reacted with 0.5 N HCl (trace metal grade) for 1 h, and analyzed for Fe(II) using the ferrozine assay (Viollier et al., 2000). Acetate, fumarate and citrate were measured by high performance liquid chromatography (HPLC) with a 0.013 M H_2SO_4 solution as the mobile phase using a System Gold 166 detector and Aminex HPX-87C column. HPLC analyses were conducted at a flow rate of 0.6 ml min^{-1} and column temperature of 65°C. Production of hydrogen was determined by gas chromatography. The gas chromatograph was equipped with a molecular sieve 5A column and a thermal conductivity detector (TCD) for hydrogen analysis. The column and detector temperatures were set to 100°C and 150°C, respectively. Nitrogen gas (10 ml/min) was used as a carrier gas for measurements. Acid volatile sulfide was measured in sulfate reducing cultures by adding 2 ml of 12 N HCl to the 20 ml of remaining culture. The reaction vessel was purged with 100% nitrogen gas and then placed in a water bath at 95°C for 90 min. Two traps with 1% zinc acetate solution were connected to the reaction vessel to absorb H_2S formed from the reaction. H_2S trapped by the zinc acetate solution was analyzed for total sulfide production using the Cline method (Cline, 1969).

2.8. X-ray diffraction. Powder XRD patterns were obtained under anoxic conditions using a Rigaku MicroMax^{TM}-007HF diffractometer with a chromium source operating at 35 KV and 25 mA. Samples were dried under nitrogen atmosphere in an anaerobic chamber, and then ground to powder before packing into a capillary (0.5 mm diameter)

and sealed air-tight. The JADE+, V5 (Materials Data Inc., Livermore, California) software package was used for data analysis.

2.9. X-ray *Photoelectron Spectroscopy*. XPS measurements were performed with a Physical Electronics Quantera Scanning X-ray Microprobe. Inside a nitrogen recirculated glove box, samples were pressed onto double sided Scotch tape supported by clean flat Si 100 wafers, and introduced to the ultra high vacuum XPS system. A monochromatic Al Kα X-ray (1486.7 eV) source was used for excitation. A 100 W X-ray beam, focused to 100 μm diameter, was rastered over a 1.3 mm x 0.1 mm rectangle on the sample. High-energy resolution spectra were collected using a pass-energy of 69.0 eV with a step size of 0.125 eV. For the Ag 3d5/2 line, these conditions produced a FWHM of 0.91 eV. The sample experienced variable degrees of charging. Low energy electrons at ~1 eV, 20 μA and low energy Ar^+ ions were used to minimize this charging.

3. RESULTS

3.1. Characterization of the consortium. An anaerobic microbial consortium composed of two different bacteria was cultivated from Oak Ridge sediments. The culture did not use the acetate provided to the medium during the early stages of the enrichment (Table 2.1). Instead, the consortium first grew by fermentation of citrate in the AGW Fe-citrate medium, and in later incubations by fermenting fumarate. Cultures grown by anaerobic fermentation of fumarate were analyzed by 16s rRNA gene analysis. PCR amplification of the16s rRNA gene revealed a single DNA sequence of an organism belonging to the *Vellionellaceae* family, most similar to *Sporomusa sphaeroides* DSM 2875, *Sporomusa paucivorans* DSM 3697^T, *Propionispora hippie* KS, *Propionispora vibriodes* FKBS1, and *Desulfosporomusa polytropa*, all at a relatively low

similarity (91% identity) (Figure 2.1). This novel bacterium was designated as strain RU4. A PCR amplification of the 16S rRNA genes of the culture grown in the peptone cultures showed the predominance of a bacterium most similar (99% identity) to *Clostridium tunisiense* $E1^T$. We refer to this bacterium as *Clostridium sp.* FGH. We have isolated *Clostridium sp.* FGH in pure culture (Shah et al., submitted). In contrast, strain RU4 did not grow in isolation, and after numerous dilution-to-extinctions and repeated transfers of single colonies on anaerobic agar shake tubes containing AGW medium supplemented with fumarate, we were unable to disrupt its association with *Clostridium sp.* FGH. However, by growing the consortium in fumarate medium, strain RU4 was enriched to dominate the consortium cultures.

3.2. Substrates utilized for growth. The consortium composed of *Clostridium sp.* FGH and strain RU4 grew with peptone, fumarate and citrate as carbon sources (Table 2.2). Denaturing gradient gel electrophoresis (DGGE) indicated that *Clostridium sp.* FGH was the dominant member during growth on peptone, whereas strain RU4 dominated the consortium under fumarate grown conditions (Figure 2.2, lane 1). PCR amplification of the16s rRNA gene also showed that strain RU4 dominated the consortium during growth on citrate. When grown on fumarate or citrate, the addition of hydrogen enhanced growth. Sulfate was not required for growth, but its addition to the media resulted in nominally higher cell densities after a period of 7 days. A small increase in cell density was also observed in the basal medium alone containing only 0.05 g/L yeast extract. The addition of acetate, formate, propionate, butyrate or carbon dioxide as the carbon source did not stimulate growth above the levels measured in the basal medium. The pure culture of *Clostridium sp*. FGH grew with peptone but did not grow with fumarate or citrate as the carbon source. *Clostridium sp.* FGH was also unable to grow

autotrophically using H_2 as an electron donor and sulfate as an electron acceptor (data not shown).

3.3. Syntrophic Effects on Fe(III)-(oxyhydr)oxide (bio)reduction and secondary mineralization. 6 sets of experiments were conducted to examine the effect of hydrogen, sulfate, and growth medium on rates and extent of Fe(III)-(oxyhydr)oxide (bio)reduction and secondary mineralization by the clostridia consortium. These experiments are outlined in Figure 2.3. Experiment 1 examined the effect of hydrogen on the growth of the consortium. In experiment 2, we quantified sulfide production by the consortium and pure culture of *Clostridium sp.* FGH. In experiment 3, we investigated Fe(III)-(oxyhydr)oxide reduction by pure culture of *Clostridium sp*. FGH. We then examined biotic/abiotic Fe(III)-(oxyhydr)oxide reduction by the consortium in experiment 4. In experiment 5, we measured hydrogen production by pure culture of *Clostridium sp*. FGH. Finally, experiment 6 was conducted to characterize the secondary Fe(II) mineral products produced by the clostridia consortium.

3.3.1. Experiment 1: Effect of hydrogen on growth of the consortium. When strain RU4 and *Clostridium sp.* FGH were grown together on agar slants containing ferric citrate and sulfate, the addition of hydrogen gas stimulated Fe(III) and sulfate reduction, resulting in extensive precipitation of black iron sulfide on these agar slates (Figure 2.4A). DNA was obtained from single colonies on the agar slants and from the liquid cultures for PCR amplification of the 16s rRNA gene. Sequencing of 16s rRNA gene revealed a single DNA sequence of strain RU4. We also repeated these growth experiments using liquid media in the absence of Fe(III). The addition of hydrogen gas in the headspace promoted growth by sulfate reduction and resulted in higher cell densities (Figure 2.4B, C). Because the pure culture of *Clostridium sp.* FGH does not grow

autotrophically using H_2 (data not shown), we infer that the growth of strain RU4 was stimulated by the presence of hydrogen.

3.3.2. Experiment 2: Sulfide production. The pure culture of *Clostridium sp.* FGH did not reduce sulfate to sulfide when grown with peptone (Figure 2.5A). When provided with 2.6 mM of sulfate, *Clostridium sp.* FGH grew to high cell densities but did not produce any detectable acid volatile sulfide during 7 days of incubation. In contrast, the consortium composed of *Clostridium sp.* FGH and strain RU4 produced 1.8 mM sulfide during 7 days of growth (Figure 2.5B). Because the pure culture of *Clostridium sp.* FGH does not reduce sulfate, we infer that strain RU4 is the sulfate reducing member of the consortium.

3.3.3. Experiment 3: Iron oxide reduction by pure culture of *Clostridium sp.* FGH. The pure culture of *Clostridium sp.* FGH reduced solid-phase Fe(III) oxides (Figure 2.6A). After 5 days of incubation *Clostridium sp.* FGH produced nearly 9.0 mM, 1.1 mM, and 1.2 mM of Fe(II) during ferrihydrite, goethite and hematite reduction, respectively. The pure culture of *Clostridium sp.* FGH extensively reduced ferrihydrite in comparison to goethite and hematite. Although sulfate was present in the peptone medium, *Clostridium sp.* FGH did not reduce the sulfate and no sulfide was detected in these experiments.

3.3.4. Experiment 4: Iron oxide reduction by the consortium. When *Clostridium sp.* FGH was grown with strain RU4, iron oxide reduction was much faster. After 5 days of growth in peptone medium, the consortium composed of both bacteria produced 12.3 mM, 5.3 mM, and 7.3 mM of Fe(II) during reduction of ferrihydrite, goethite and hematite, respectively (Figure 2.6B). Notably, the reduction of crystalline iron oxides was faster

with the consortium than the pure culture *Clostridium sp.* FGH. DGGE analysis indicated that both organisms were growing under these conditions, with *Clostridium sp.* FGH as the dominant member of the consortium (Figure 2.2, lanes 2, 3 and 4). The consortium produced 1.2 mM sulfide during 5 days of growth.

In fumarate medium, the presence of sulfate increased the rates of iron reduction by the consortium. While sulfate had a negligible effect on *Clostridium sp.* FGH, its presence in the culture medium affected the activity of strain RU4. In the absence of sulfate, the fumarate grown consortium dominated by strain RU4 weakly reduced goethite and hematite. Under this condition, the consortium produced approximately 0.2 mM and 0.7 mM Fe(II) after 7 days during goethite and hematite reduction, respectively. In contrast, when sulfate was added to the medium, iron reduction rates increased substantially, the RU4 dominated consortium produced 2.7 mM and 4.8 mM Fe(II) during goethite and hematite reduction, respectively (Table 2.3). The production of biogenic sulfide also occurred over this period. After 7 days, approximately 1.5 mM and 3 mM acid volatile sulfide was measured in the goethite and hematite experiments, respectively.

3.3.5. Experiment 5: Production of hydrogen by *Clostridium sp.* FGH. Analysis of the gaseous products in the pure culture of *Clostridium sp.* FGH culture showed the production of hydrogen with growth on peptone (Figure 2.7A). We then tested if the addition of hydrogen gas to the headspace of *Clostridium sp.* FGH cultures would hinder its growth and iron reduction activity. The experimental results showed that the presence of H_2 inhibits growth, with cell densities of *Clostridium* sp. FGH grown for 7 days under hydrogen headspace 60% lower than those obtained under N_2 headspace (Figure 2.7B). The lower cell densities also corresponded to slower iron reduction rates than those

observed for the N_2 grown culture, as the addition of hydrogen gas to ferrihydrite reducing cultures resulted in decreased Fe(II) production (Figure 2.7C).

3.3.6. Experiment 6. Characterization of secondary mineral products. The secondary iron mineral products formed by the anaerobic clostridia consortium were analyzed. During ferrihydrite reduction in peptone with sulfate, the visual coloration of the parent iron oxides changed from brown to black (Figure 2.8A). The Fe(II) produced by the consortium was predominately retained in the solid-phase. After 7 days, the consortium produced 20.8 mM total Fe(II), of which 4.7 mM Fe(II) was in the dissolved phase and approximately 77% of total Fe(II) produced was accumulated in the solids. X-ray diffraction analysis of the reaction product showed the partial transformation of 2-line ferrihydrite to nanoparticulate magnetite, with copious amounts of residual “ferrihydrite” (Figure 2.9A). The presence of ferrihydrite-like and magnetite phases was also evident from TEM-SAED work (Figure 2.9B and 2.9C). TEM analysis of the reacted-ferrihydrite showed the presence an electron dense secondary phase. Selected area electron diffraction of an electron dense particle (~20 nm) indicated the formation of nanoparticulate magnetite (Figure 2.9C).

Goethite reduction by the consortium also resulted in significant amounts of solid-phase Fe(II). After 7 days of incubation, the consortium produced 5.5 mM Fe(II), of which 5.2 mM was bound in the solid phase, corresponding to about 85 - 95% of the total ferrous iron (Table 2.4). The accumulation of solid phase ferrous iron was concurrent to a change in visual coloration of the parent iron oxides from yellow to dark green (Figure 2.8B). X-ray diffraction analysis of the reaction products showed only diffraction peaks for goethite (Figure 2.10A). Other than the residual iron oxide substrate, no crystalline phases were identified by XRD in the reacted samples. TEM analysis of the reaction products showed the presence of sparsely distributed fine grained

secondary particles approximately 10 nm in size (Figure 2.10B). Energy dispersive X-ray spectroscopy indicated that these secondary particles were composed of iron and sulfur (Figure 2.10C). X-ray photoelectron spectra of the reacted samples detected the presence of reduced sulfur, with characteristic sulfide peaks at 161.4 and 160.4 eV (Figure 2.11A). Chemical analysis of the secondary minerals precipitated during the goethite incubations also showed the formation of solid-phase sulfide, with the accumulation of approximately 1.2 mM sulfide in the solid-phases as AVS after 7 days of incubation (Figure 2.11B). The ferrous iron and secondary minerals produced by the goethite reducing consortium were highly reactive towards oxygen and were rapidly oxidized to parent iron oxide within 90 mins of exposure to air (Figure 2.13A). After exposure to air, the green coloration of the mineral suspension reverted back to a yellow color.

The accumulation of solid phase Fe(II) was also observed in the hematite reduction experiments. After 7 days of incubation, the consortium produced 7.4 mM Fe(II), of which 6.2 mM was bound in solid phase (Table 2.4), corresponding to about 85 - 95 % of the total ferrous iron produced indicating that most of the Fe(II) produced sorbs to the parent mineral or cells. The formation of solid phase Fe(II) was concurrent with a change in visual coloration of the parent iron oxides from red to dark brown (Figure 2.8C). X-ray photoelectron spectra of the reacted samples exhibited sulfide peaks at 161.8 and 160.9 eV (Figure 2.11C). Chemical analysis of the secondary minerals precipitated during the hematite incubations also showed the formation of solid-phase sulfide, with approximately 1.2 mM sulfide accumulating in the solid-phases as AVS after 7 days of incubation (Figure 2.11D). X-ray diffraction analysis of the reaction products showed only diffraction peaks for hematite, suggesting that sulfide precipitates were poorly crystalline. Characteristic peaks of hematite were observed before and after the incubation period, and no other crystalline phase was detected (Figure 2.12). The

biogenic Fe(II) formed in the hematite reduction experiments was highly reactive towards oxygen with rapid oxidization to parent iron oxide within 60 – 90 mins of exposure to air (Figure 2.13B). After exposure to air, the dark brown coloration of the mineral suspension rapidly changed back to a red color.

4. DISCUSSION

Rates of iron oxide reduction were much faster when *Clostridium sp.* FGH was grown with strain RU4 (Figure 2.6B). Iron reduction by the microbial consortium was likely mediated by two different pathways (figure 2.3). First pathway involves biotic reduction by *Clostridium sp.* FGH where the reductant is unknown. Whereas the second pathway involves production of biogenic sulfide that acts as a reductant for biotic/abiotic iron reduction by the consortium. First, the biotic reduction by *Clostridium sp.* FGH may have been affected by the presence of strain RU4 via syntrophic interactions. Because syntrophic interactions are known to facilitate carbon degradation by fermenting bacteria (Schink and Stams, 2006), we postulate that the consumption of H_2 by strain RU4 may also affect the iron reducing activity of *Clostridium sp.* FGH. *Clostridium sp.* FGH produced H_2 gas during fermentation of amino acids (Figure 2.7A). While this bacterium was able to reduce iron oxides in pure culture, without its syntrophic partner, H_2 accumulates to high levels. With elevated hydrogen concentrations, oxidation of intracellular redox mediators such as NADH and $FADH_2$ can become energetically unfavorable (Stams, 2006). When these intracellular redox mediators are not oxidized, their accumulation slows down the corresponding extracellular electron transfer reactions. As such, hydrogen accumulation in the pure cultures of *Clostridium sp.* FGH may limit the kinetics of iron oxide reduction. Conversely, hydrogen consumption by an H_2 utilizing partner lowers the hydrogen partial pressure, thereby rendering the

fermentation reaction exergonic, and enabling proton reduction and energy conservation (McInerney et al., 2008; Schink and Stams, 2006; Stams, 2006; Stams and Plugge, 2009). Our experimental data is consistent with the occurrence of syntrophic hydrogen consumption during crystalline iron oxide reduction by this fermentative microbial consortium (Figure 2.3).

Another possible pathway for iron reduction by the consortium is through biotic/abiotic reactions involving biogenic sulfide. Sulfide can chemically reduce iron oxides (Poulton et al., 2004; Raiswell and Canfield, 1998). Our experiments show that the production of sulfide by strain RU4 was stimulated by hydrogen gas (Figure 2.4). Because H_2 easily diffuses away from the fermenting *Clostridium sp.* FGH, hydrogen can act as an extracellular electron carrier between organisms that was utilized by strain RU4 to fuel sulfate reduction (Figure 2.3). The hydrogen oxidizing sulfate-reducing bacterium *Desulfosporomusa polytropa* is the most closely related organism to strain RU4. Although several strains of *Desulfosporomusa polytropa* can weakly reduce ferric iron during homoacetogenesis (Sass et al., 2004), we were unable to grow strain RU4 under homoacetogenic conditions in the presence of iron oxides. To date, the other organisms closely related to strain RU4 (*Sporomusa sphaeroides, Sporomusa paucivorans, Propionispora hippie,* and *Propionispora vibriodes*) have not been tested for iron oxide reduction activity. Conversely, our experimental data show that strain RU4 reduces sulfate to sulfide, and the presence of H_2 increases this activity (Figure 2.4). The rate and extent of iron reduction by the microbial consortium was strongly affected by increasing sulfate concentrations in the medium. In the presence of sulfate, the reductive dissolution of iron oxides is controlled by the strong interplay between growth of the sulfate reducer and extracellular redox-reactions between the biogenic sulfide and iron oxide mineral surfaces (Li et al., 2006). Sulfur-reducing bacteria that are unable to reduce ferric iron directly are known to grow by the reduction of iron oxides via sulfur

cycling with sulfide as the reductant (Straub and Schink, 2004). Similarly, strain RU4 may indirectly transfer electrons to iron oxide surfaces while oxidizing hydrogen (Figure 2.3).

The formation of FeS(s) in the culture medium suggests the two bacteria in the consortium may have been interacting with each other in a mutualistic fashion. When grown in isolation, Fe^{2+} produced by iron reduction can bind onto cell surfaces and inhibit metabolism, and sorb onto mineral surfaces to block electron transfer sites (Liu et al., 2001a). Likewise, elevated levels of sulfide produced by sulfate reduction are known to cause cellular stress and decrease the growth rate of sulfate reducing bacteria (Caffrey and Voordouw, 2010). When grown together, mutalistic interactions between the iron and sulfate reducing bacteria can alleviate some of these inhibitory effects by FeS(s) precipitation. In our experimental system, we observed the formation of FeS(s) precipitation, indicating that some of the cell associated ferrous iron and dissolved sulfide was removed and bound in a less toxic phase. Furthermore, FeS(s) precipitation also decreased the concentration of the reaction products, allowing $\Delta G_{reaction}$ to maintain negative values, thereby keeping iron and sulfate reduction thermodynamically favorable.

The consortium produced oxygen sensitive Fe(II) phases that have important implications for contaminant reactions in subsurface environments. First, during ferrihydrite reduction, extensive amounts of sorbed Fe(II) and nanoparticulate magnetite were formed (Figure 2.9). Because these Fe(II) bearing mineral phases can chemically reduce a wide range of metal contaminants, including U(VI) and Hg(II) (Scott et al., 2005; Wiatrowski et al., 2009), their formation in contaminated waters can result in biotic/abiotic metal reduction. Secondly, poorly crystalline FeS(s) precipitated during hematite and goethite reduction (Figures 2.10 & 2.11). This secondary FeS(s) phase was highly reactive to oxygen (Figure 2.13), and previous laboratory experiments have

also shown that FeS(s) can also reduce U(VI) (Hyun et al., 2012). Finally, a substantial amount of sorbed Fe(II) likely accumulated in the solid phase during iron reduction (Table 2.4). Fe(II) is known to sorb onto bacterial cells and mineral surfaces (Liu et al., 2001a) and total solid phase Fe(II) greatly exceeded the concentration of acid volatile sulfide in the goethite and hematite systems. Because surface bound Fe(II) can reduce U(VI) and Tc(VII) (Fredrickson et al., 2004; Liger et al., 1999), the formation sorbed Fe(II) by the consortium may further contribute to contaminant reduction and immobilization in subsurface environments.

In their natural habitat, the fermentative growth of *Clostridium sp.* FGH, when coupled to hydrogen driven sulfate reduction by *Vellionellaceae* RU4, may potentially contribute to the in situ iron reduction activity, particularly in sediments containing crystalline Fe(III) where fermenters may compete effectively with respiratory Fe(III) reducers. Recent emulsified vegetable oil injections at Oak Ridge, TN, resulted in the stimulation of organisms in the family *Veillonellaceae* (Gihring et al., 2011). During the bioremediation experiment, the *Veillonellaceae* were positively correlated with dissolved Fe concentrations. In this saprolitic sediment, Fe(III) oxides exist as crystalline goethite and hematite (Fredrickson et al., 2004; Kukkadapu et al., 2006), iron oxide phases that our laboratory fermentative consortium is able to rapidly reduce. Our data suggest that fermentative and sulfate reducing bacteria may play an important role in the reduction of crystalline iron oxides, and potentially of other metals, during the subsurface injection of fermentable carbon substrates.

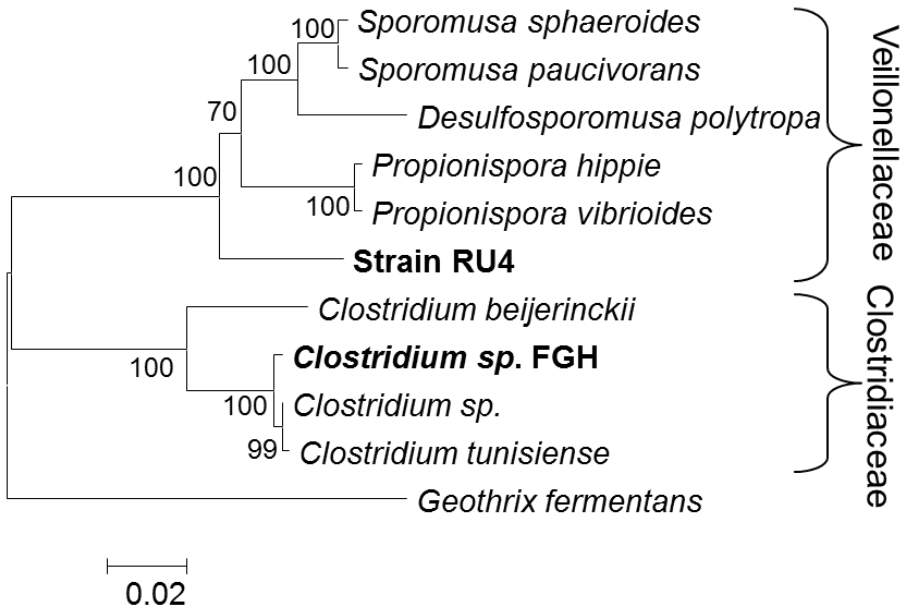

Figure 2.1. Neighbor joining tree of strain RU4 and strain FGH with their closest relatives belonging to order *Clostridiales.* The 16S rRNA gene of *Geothrix fermentans* was used as an outgroup. The bar represents 2 substitutions per 100 nucleotides.

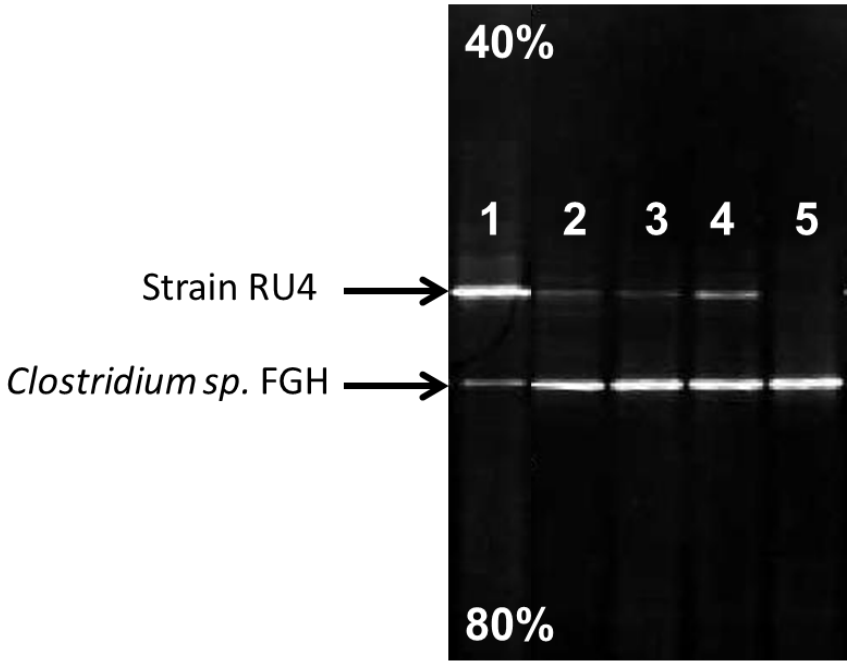

Figure 2.2. DGGE analysis of the consortium grown with fumarate (lane 1); peptone and ferrihydrite (lane 2), goethite (lane 3) or hematite (lane 4); and *Clostridium sp.* FGH grown with peptone (lane 5).

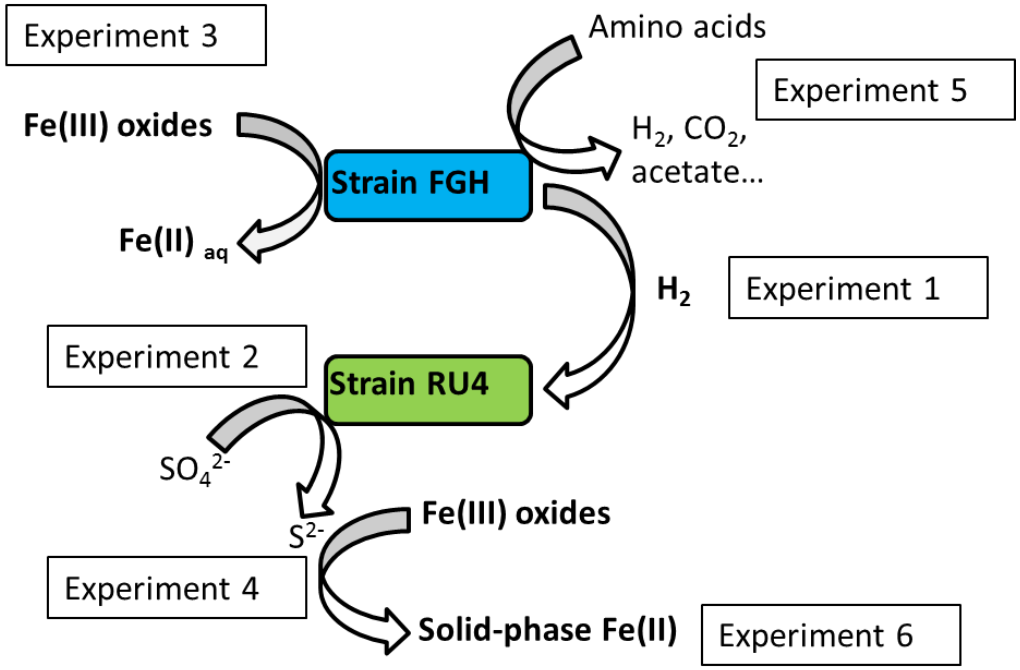

Figure 2.3. Experiments on the syntrophic effects on Fe(III) (oxyhydr)oxide reduction and secondary mineralization. Experiment 1: The effect of hydrogen on consortium growth; Experiment 2: Sulfide production by the consortium and pure culture of *Clostridium sp.* FGH; Experiment 3: Iron oxide reduction by pure culture of *Clostridium sp.* FGH; Experiment 4: Biotic/abiotic iron oxide reduction by the consortium; Experiment 5: Hydrogen production by pure culture of *Clostridium sp.* FGH; and Experiment 6: Characterization of secondary Fe(II) mineral products.

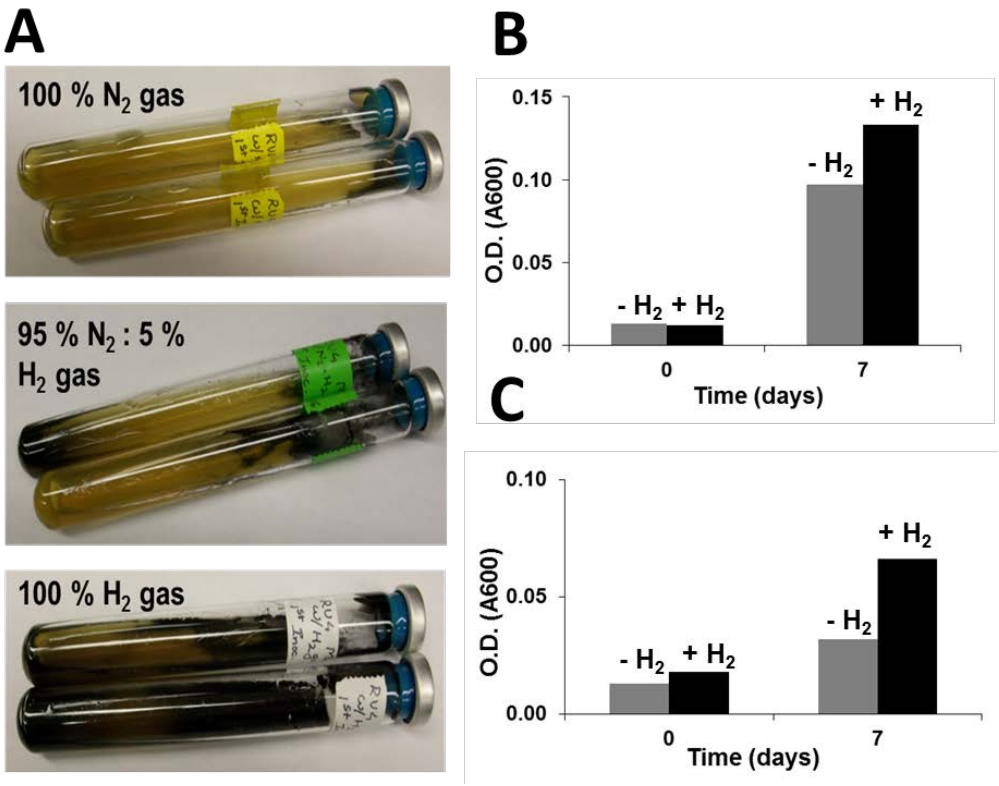

Figure 2.4. Effect of hydrogen on growth of the consortium. (A) Agar slants containing ferric citrate and sulfate; defined liquid media containing (B) fumarate and sulfate; and (C) citrate and sulfate. Grey bars represent nitrogen headspace and black bars represent hydrogen headspace.

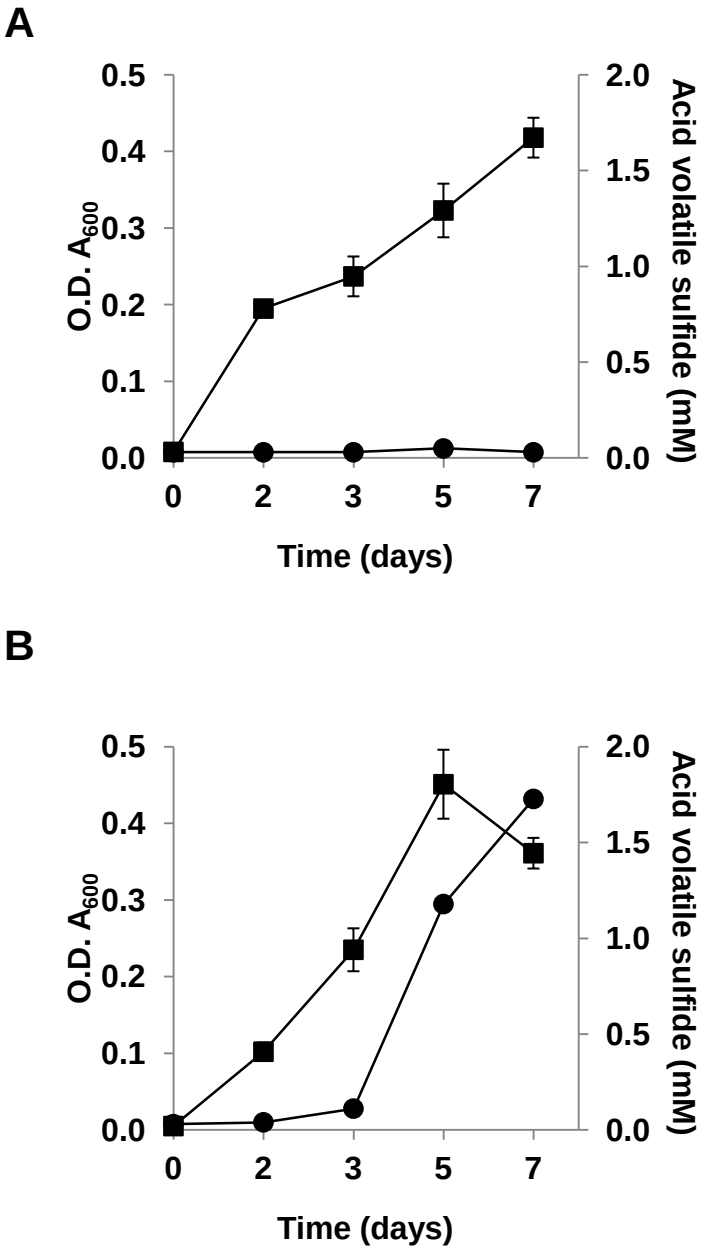

Figure 2.5. Growth on peptone and the production of sulfide. (■) represent optical density and (●) represent acid volatile sulfide production. (A) Pure culture of *Clostridium sp.* FGH and (B) the consortium composed of *Clostridium sp.* FGH and strain RU4.

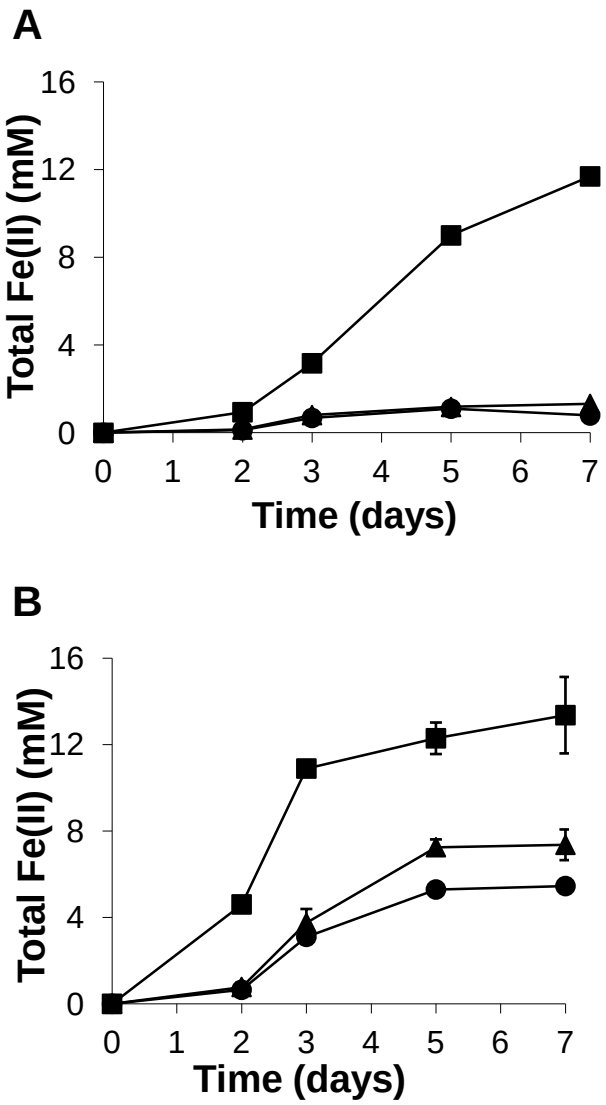

Figure 2.6. Reduction of iron oxides and production of Fe(II) during growth on peptone: (■) ferrihydrite, (●) goethite, and (▲) hematite. (A) Fe(II) produced by the pure culture of *Clostridium sp.* FGH and (B) Fe(II) produced by the consortium composed of *Clostridium sp.* FGH and strain RU4. 30 mM iron oxides provided to culture.

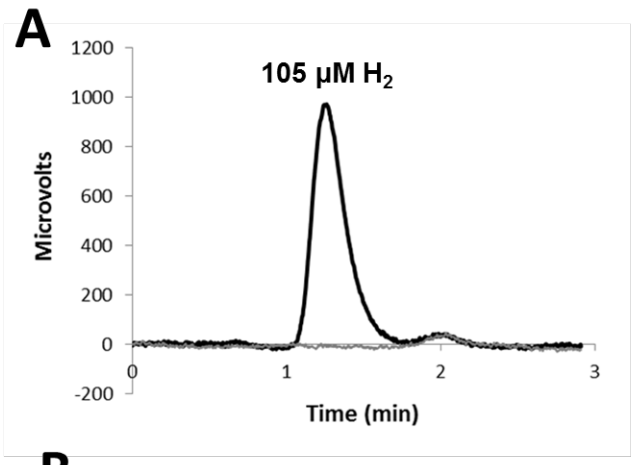
A
105 µM H_2
Microvolts
1200
1000
800
600
400
200
0
-200
0
1
2
3
Time (min)

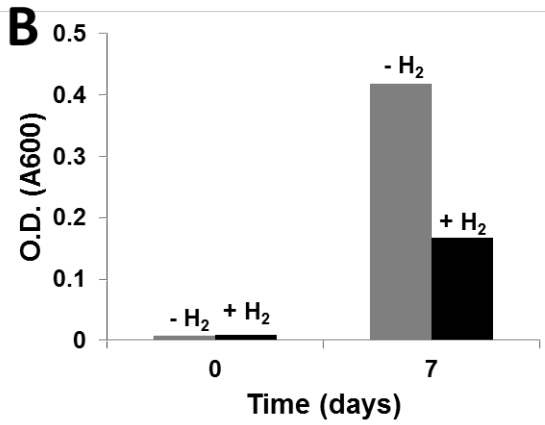
B
O.D. (A600)
0.5
0.4
0.3
0.2
0.1
0
- H_2
+ H_2
- H_2
+ H_2
0
7
Time (days)

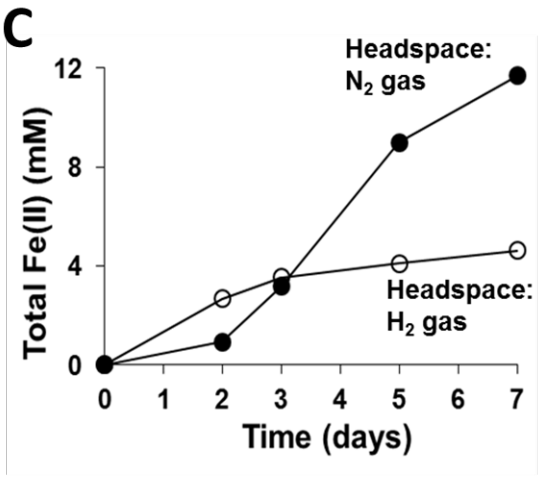
C
Total Fe(II) (mM)
12
8
4
0
Headspace:
N_2 gas
Headspace:
H_2 gas
0
1
2
3
4
5
6
7
Time (days)

Figure 2.7. Role of hydrogen. (A) Gas chromatograph showing the production of H_2 gas by *Clostridium sp.* FGH when grown with peptone. Black line represents *Clostridium sp.* FGH and grey line represents sterile control. (B) Growth of strain FGH in the presence of hydrogen. Grey bars represent nitrogen headspace and black bars represent hydrogen headspace. (C) Effect of hydrogen on ferrihydrite reduction by *Clostridium sp.* FGH when grown with peptone. 100% nitrogen (●) and 100% hydrogen gas (○) in the headspace.

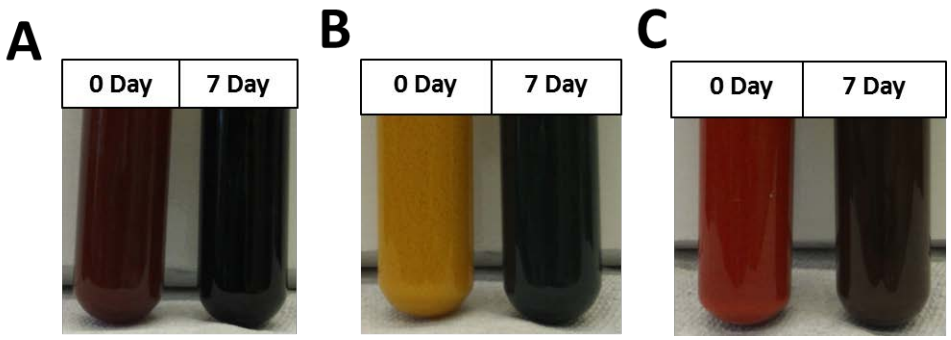

Figure 2.8. Iron oxide reduction by the consortium. (A) Ferrihydrite reducing culture; (B) Goethite reducing culture; and (C) Hematite reducing culture at day 0 and 7.

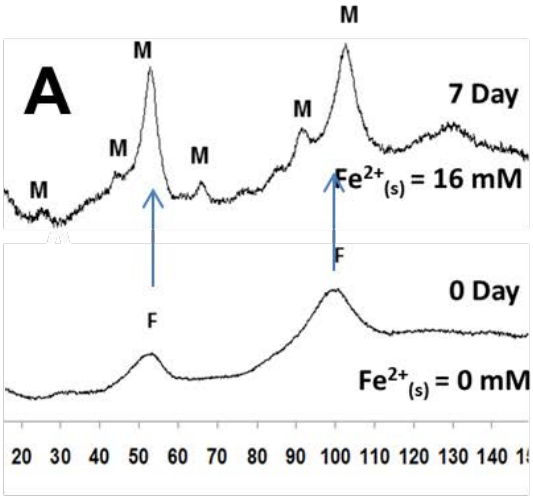
A
7 Day
M
F
$Fe^{2+}_{(s)}$ = 16 mM
0 Day
$Fe^{2+}_{(s)}$ = 0 mM
20 30 40 50 60 70 80 90 100 110 120 130 140
degrees., 2θ

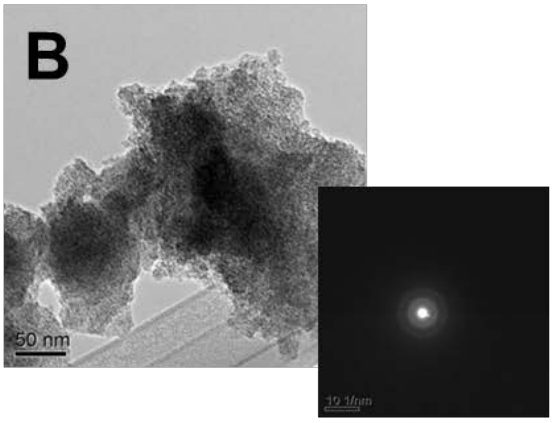
B
50 nm

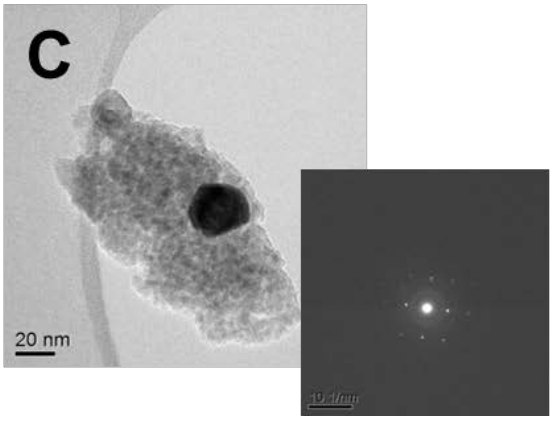
C
20 nm

Figure 2.9. Ferrihydrite (2-line) biotransformation by the consortium when grown with peptone and sulfate. (A) X-ray diffraction patterns before (0 day) and after 7 days of incubation, F: Ferrihydrite, M: Magnetite. The arrows are drawn as a guide to the eye to indicate presence of residual “ferrihydrite” in the incubated sample; (B and C) Transmission electron micrographs with corresponding Selected Area Electron Diffractograms of the culture after 7 days of incubation showing presence of ferrihydrite (B) and magnetite (C).

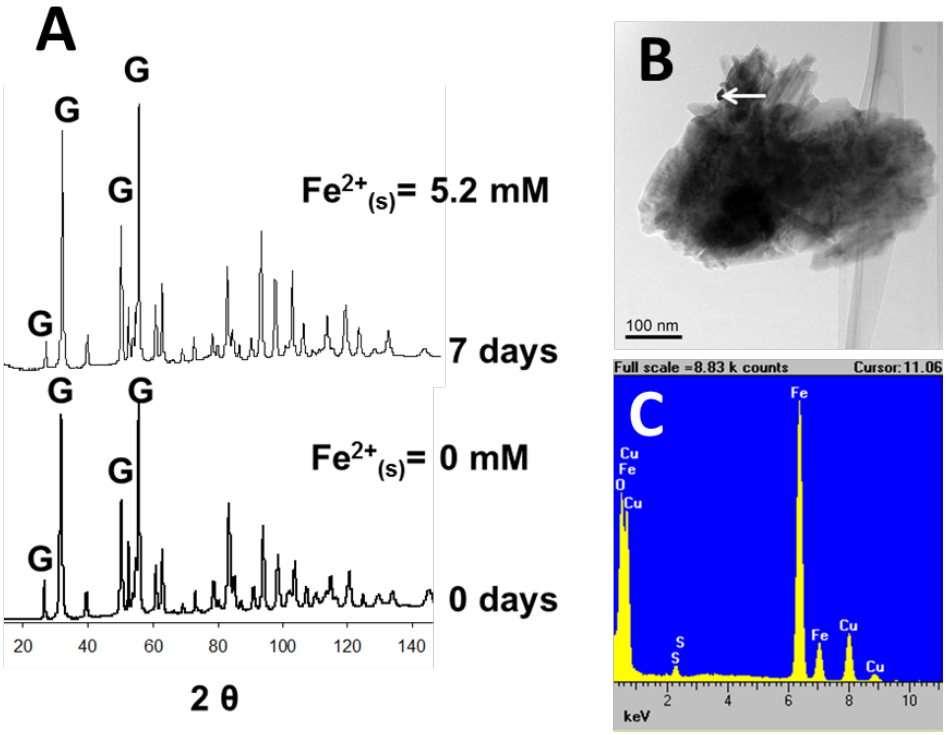

Figure 2.10. Goethite reduction by the consortium when grown with peptone and sulfate. (A) X-ray diffraction patterns before and after 7 days of incubation. G: Goethite; (B) Transmission electron micrograph of the culture after 7 days of incubation. The arrow points to an FeS particle that formed during goethite reduction; and (C) Energy dispersive X-ray spectroscopy spectrum of the FeS particle shown in B.

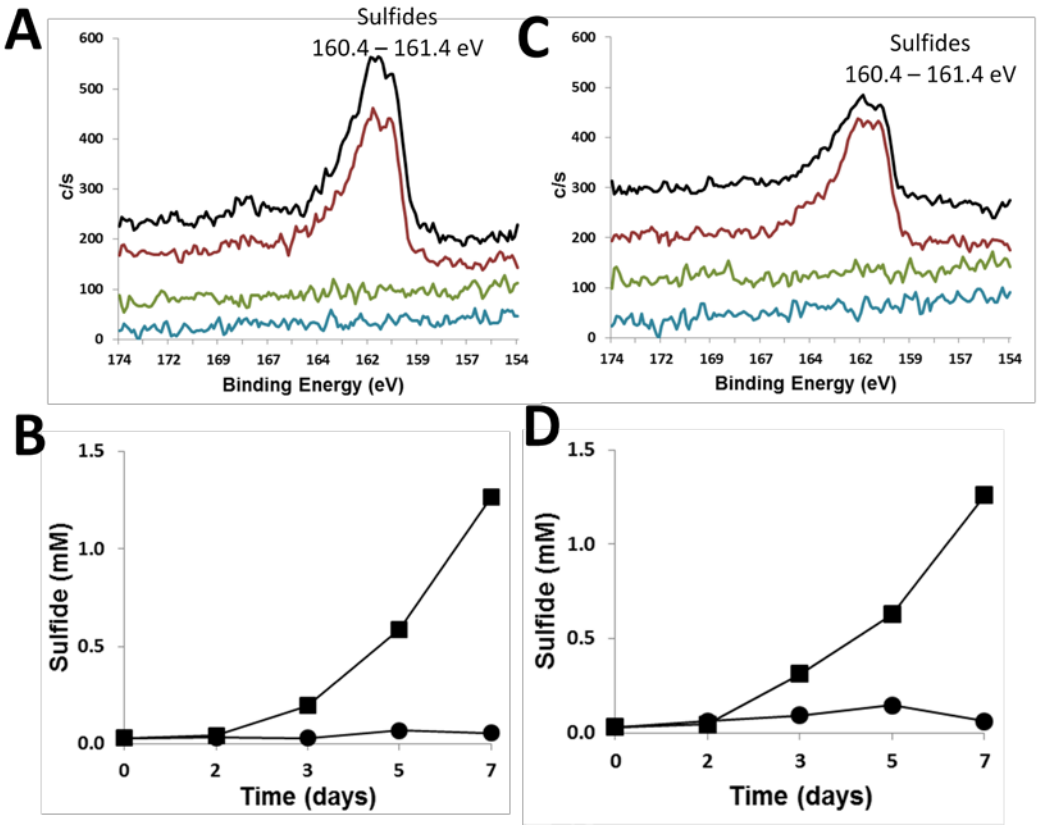

Figure 2.11. XPS and chemical analysis of iron oxide transformation products. (A) X-ray photoemission spectra of the S 2p region of goethite transformation products. Charge referenced using the C 1s line at 284.8 eV. Spectra of goethite samples before (green and blue) and after 7 days of incubation (black and brown); (B) Total (■) and dissolved (●) sulfide produced by the goethite reducing consortium; (C) X-ray photoemission spectra of the S 2p region of hematite transformation products. Charge referenced using the C 1s line at 284.8 eV. Spectra of hematite samples before (green and blue) and after 7 days of incubation (black and brown); and (D) Total (■) and dissolved (●) sulfide produced by the hematite reducing consortium.

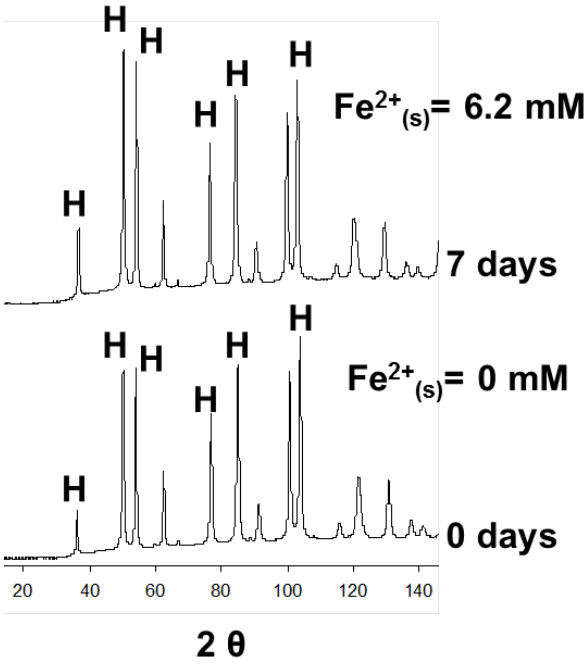

Figure 2.12. Hematite reduction by the consortium when grown with peptone and sulfate. X-ray diffraction patterns before and after 7 days of incubation. H: Hematite

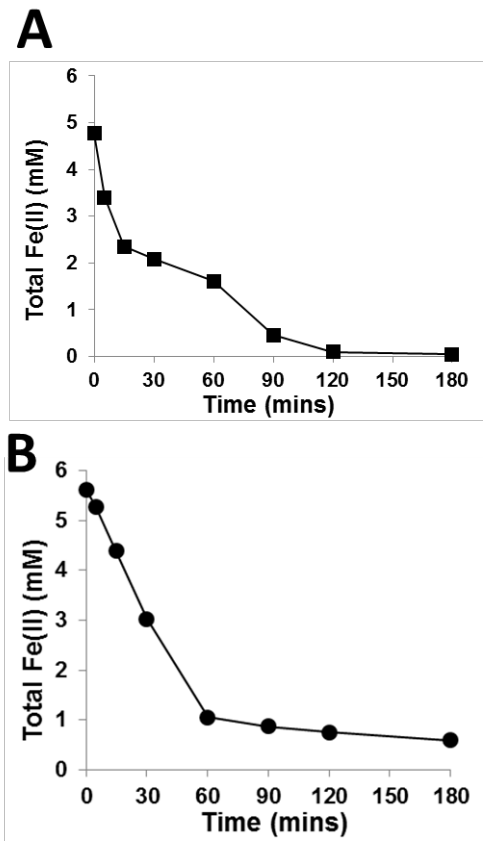

Figure 2.13. Characterization of crystalline iron oxide transformation product. Oxidation of goethite (A) and hematite (B) transformed products when exposed to air.

Table 2.1. Substrate utilization by the consortium.

Time (days)	Substrate Concentration (mM)		
	Acetate[1]	Citrate[2]	Fumarate[2]
0	21	10	32
4	19	7	10
25	21	0	0

[1] Fumarate provided as the electron acceptor

[2] Cultures grown under fermentative conditions

Table 2.2. Growth of consortium on various substrates.

Carbon source	Hydrogen	Sulfate	Consortium (O.D. A_{600})		
			0 D	3 D	7 D
Peptone	-	+	0.005	0.235	0.361
Fumarate	+	+	0.012	0.084	0.133
Fumarate	-	+	0.013	0.093	0.097
Fumarate	-	-	0.017	0.098	0.083
Citrate	+	+	0.018	0.047	0.066
Citrate	-	+	0.013	0.028	0.032
Citrate	-	-	0.010	0.021	0.021
Acetate	+	+	0.008	0.023	0.025
Formate	+	+	0.009	0.026	0.011
Propionate	+	+	0.006	0.015	0.014
Succinate	+	+	0.007	0.016	0.015
Butyrate	+	+	0.006	0.014	0.015
Carbon dioxide	+	+	0.015	0.025	0.034
Basal media	-	+	0.010	0.024	0.027

Table 2.3. Effect of sulfate on iron oxide reduction by the consortium[1].

Iron oxides[2]	Sulfate (mM)	Total Fe(II) (7 D) (mM)	Acid volatile sulfide (7D) (mM)
Goethite	0.0	0.2	0.0
Goethite	30.0	2.7	1.5
Hematite	0.0	0.7	0.0
Hematite	30.0	4.8	3.0

[1] 30 mM fumarate provided as the carbon source.

[2] 30 mM iron oxides provided to the culture.

Table 2.4. Dissolved and total Fe(II) production during iron oxide reduction by the consortium[1].

	Ferrihydrite		Goethite		Hematite	
Time (d)	$Fe(II)_D$	$Fe(II)_T$	$Fe(II)_D$	$Fe(II)_T$	$Fe(II)_D$	$Fe(II)_T$
0	0.0 ± 0.0	0.0 ± 0.0	0.0 ± 0.0	0.0 ± 0.0	0.0 ± 0.0	0.0 ± 0.0
2	1.3 ± 0.3	4.6 ± 0.0	0.1 ± 0.0	0.7 ± 0.3	0.2 ± 0.1	0.8 ± 0.2
3	2.4 ± 0.1	10.9 ± 0.4	0.2 ± 0.0	3.1 ± 0.2	0.2 ± 0.1	3.8 ± 0.6
5	2.5 ± 0.6	12.3 ± 0.7	0.4 ± 0.1	5.3 ± 0.2	0.6 ± 0.2	7.3 ± 0.4
7	2.7 ± 0.6	13.4 ± 1.8	0.3 ± 0.1	5.5 ± 0.3	1.2 ± 0.1	7.4 ± 0.7

[1] 30 mM iron oxides provided to the culture.

CHAPTER 3

Physiological and Genomic Characterization of an Iron-Reducing, Saprolite-derived *Clostridium* sp. Strain FGH

Submitted to Geobiology Journal

ABSTRACT

Clostridia are obligate anaerobes commonly found in ferruginous soils and sediments. In this study, we describe the physiology and genome of a clostridia isolate that reduces Fe(III) oxides during fermentative growth. From unconsolidated saprolite, we isolated a gram-positive iron-reducing bacterium, designated as strain FGH. Based on its 16S rRNA gene sequence, strain FGH is closely related to *Clostridium* species in the phylum Firmicutes. This anaerobic bacterium ferments glucose and pyruvate, but was unable to grow on succinate, lactate, malate or citrate. In defined media, strain FGH reduces Fe(III) oxides during glucose and pyruvate fermentation. Direct contact between cells and mineral surfaces was not required for iron oxide reduction. Experiments conducted with cell-free spent media indicate that strain FGH does not produce ligands to solubilize Fe(III), and does not secrete extracellular flavins to mediate electron transfer to iron oxides. We sequenced the genome of strain FGH and found genes that encode for complete glycolysis and pyruvate fermentation pathways. Genes for sugar uptake, hydrogen production, iron metabolism, and spore-formation were also identified in the genome sequence. Notably, strain FGH lacks the genes for multiheme c-type cytochromes, which are known to be abundant in dissimilatory iron-reducing bacteria. Comparison of genomes with related species indicates that deficiency in multi-heme c-type cytochromes is common amongst *Clostridium.* These results suggest that strain FGH reduces Fe(III) oxides by a cytochrome-independent extracellular mechanism.

INTRODUCTION

Clostridia are prominent members of microbial communities in sedimentary environments, and play an important role in the reductive dissolution of Fe(III)-bearing minerals (Akob et al., 2008; Kostka et al., 2002; Lehours et al., 2009; Lin et al., 2007; Lovley et al., 1991; Petrie et al., 2003; Scala et al., 2006). Although bacteria belonging to the genus *Clostridium* have been identified as the principal agents of iron reduction in certain sediments (Lin et al., 2007), relatively few pure cultures of Fe(III)-reducing *Clostridium* species have been isolated from natural geologic systems (Dobbin et al., 1999). In laboratory investigations, anaerobic *Clostridium* species were among the first organisms to be shown to reduce iron oxides (Hammann and Ottow, 1974; Starkey and Halvorson, 1927). A characteristic feature of Fe(III)-reducing *Clostridium* is their ability to mediate iron reduction during fermentative metabolism (Dobbin et al., 1999; Lovley, 1995). This mode of iron reduction is different from anaerobic Fe(III) respiration, as *Clostridium* does not reduce iron for energy generation or growth (Lovley et al., 1991). Currently, the mechanisms of iron reduction employed by fermentative *Clostridium* remain poorly understood.

In dissimilatory iron reducing bacteria (DIRB), multi-heme c-type cytochromes are an important component of the electron transport chain in Fe(III) respiration (Carlson et al., 2012; Shi et al., 2009). The genome sequences of the gram-negative DIRB *Shewanella onedensis* MR-1 and *Geobacter sulfurreducens* PCA have revealed remarkably large numbers of putative c-type cytochrome genes (Heidelberg et al., 2002; Methe et al., 2003). Experimental studies have demonstrated that *S. onedensis* uses the tetraheme c-type cytochrome CymA and the decaheme c-type cytochromes MtrA, OmcA and MtrC to facilitate extracellular electron transfer to insoluble iron oxides (Beliaev et al., 2001; Myers and Myers, 1997; Pitts et al., 2003; Shi et al., 2009). Extracellular

electron transfer in *G. sulfurreducens* involves the periplasmic c-type cytochromes PpcA and MacA, and outermembrane tetraheme c-type cytochrome OmcE and hexaheme c-type cytochrome OmcS (Butler et al., 2004; Holmes et al., 2006; Lloyd et al., 2003; Mehta et al., 2005). In both *S. onedensis* and *G. sulfurreducens*, deleting genes that encode for cytochromes impairs the ability for extracellular electron transfer (Bretschger et al., 2007; Coursolle et al., 2010). Recent studies with the Firmicute *Thermicola potens* indicate that gram-positive DIRB also carries abundant multiheme c-type cytochromes genes, and cell-wall associated cytochromes are responsible for electron transfer to solid phase substrates (Carlson et al., 2012). To date, the number of multiheme c-type cytochromes genes in Fe(III)-reducing gram-positive *Clostridium* species has not been studied in detail.

Some iron reducers are known to release extracellular compounds to mediate electron transfer to solid phase iron oxide minerals (Kappler and Straub, 2005). While *Geobacter* and *Thermicola* reduce solid phase iron via direct contact with the mineral surfaces (Leang et al., 2003; Nevin and Lovley, 2000; Shi et al., 2009)*, Shewanella* and iron-reducing species of *Geothrix* can reduce iron oxides at a distance (Lies et al., 2005; Nevin and Lovley, 2002). *Shewanella* produces flavins that function as electron shuttles to reduce iron oxides at a distance (Lies et al., 2005; Marsili et al., 2008; von Canstein et al., 2008), and *Geothrix* produces both Fe(III) chelators and redox active molecules that enable indirect iron oxide reduction (Mehta-Kolte and Bond, 2012; Nevin and Lovley, 2002). It is currently unknown if iron-reducing *Clostridium* species produce extracellular flavins for Fe(III) reduction, or instead requires direct contact for electron transfer to poorly soluble iron oxides.

In this study, we isolated an obligate anaerobic gram-positive bacterium from subsurface saprolitic sediments, designated as strain FGH. Based on its 16S rRNA gene sequence, strain FGH belongs to the genus *Clostridium.* We investigated the

mechanisms of iron reduction by strain FGH under fermentative growth conditions, and found that strain FGH can reduce the iron oxide ferrihydrite at a distance while fermenting glucose. We sequenced the genome of this bacterium and identified genes that encode for glycolysis and fermentation pathways. Notably, the genome of strain FGH lacks the genes for multiheme c-type cytochromes. The results suggest that iron oxide reduction by this fermentative bacterium does not require direct contact and is mediated by a cytochrome-independent mechanism.

MATERIALS AND METHODS

Isolation of strain FGH. Unconsolidated clay-rich saprolite sediment core from the uncontaminated Background Area (Borehole FB628 at Site A; Lat=35.94, Long=84.33) of Oak Ridge, TN was collected at a 4.5 – 6.0 m depth and used as inoculum. Homogenized sediments were suspended in artificial groundwater, and an enrichment culture was plated on anaerobic LB plates in a glove box. Single colonies were picked from these LB plates and streaked three times on fresh LB plates to isolate a pure culture. Isolate was then transferred to anaerobic minimal media containing 0.75 mM NH_4Cl, 0.1 mM NaCl, 0.34 mM KH_2PO_4, 0.38 mM $MgCl_2.6H_2O$, 0.34 mM $CaCl_2.2H_2O$, 100 mM PIPES buffer, Wolfe's vitamin mix and a modified Wolfe's mineral solution [10 ml per liter of media]. The modified mineral solution was devoid of sulfate and contained (g/L): Nitrilotriacetic acid, 1.5; $MnCl_2.4H_2O$, 0.5; $FeCl_2.4H_2O$, 0.1; $CoCl_2.6H_2O$, 0.1; $ZnCl_2$, 0.1; $CuCl_2.2H_2O$, 0.01; H_3BO_3, 0.01; $Na_2MoO_4.2H_2O$, 0.01; $NaSeO_3$, 0.01; $NiCl_2.6H_2O$, 0.01; $Na_2Wo_4.2H_2O$, 0.01. The final pH of the medium was set to 6.8 by addition of 1 N NaOH. The isolate was then routinely maintained anaerobically in minimal media containing peptone (2%) and incubated at 28°C.

Electron microscopy. Transmission electron micrographs were obtained from peptone grown strain FGH culture. Cells were collected during exponential phase (24 h) by centrifugation at 9167 g for 10 min in the glove box. Cell pellet was washed with minimal media devoid of carbon source and fixed in Karnovsky's fixative (formaldehyde, 4% v/v and glutaraldehyde, 1% v/v, in 0.1 M Millonig's phosphate buffer, pH 7.3) for 3 h. After fixation, cells were incubated in 1% osmium tetroxide for 1 h. Fixed cells were dehydrated by sequential washes in a graded ethanol series. The cells were then resuspended in Epon-Araldite (Electron Microscopy Sciences) and embedded. The embedded samples were thin sectioned with a diamond knife (LKB 2088 ultramicrotome; LKB Produkter). Cells were first stained with a 5% (w/v) uranyl acetate solution in 50% ethanol for 15 min. Then they were stained again with a 0.5% (w/v) lead citrate solution in distilled water for 2 min. For imaging, grids were transferred into a transmission electron microscope (JEOL JEM-100CX) to collect images.

Phylogenetic analysis. Genomic DNA was obtained from peptone grown strain FGH cultures at exponential phase (24 h). Cells were collected for DNA extraction by centrifugation at 9167 g at 10 min in a glove box. PowerSoil DNA Kit (MoBio, Carlsbad, CA) was used to extract DNA from these cells. Bacterial 16S universal primers 27F (5'-AGAGTTTGATCMTGGCTCAG-3') and 519R (5'- GWATTACCGCGGCKGCTG-3') were used to amplify 16S rRNA gene from the samples. The amplified PCR products were then ran on a 1% agarose gel in 1X TAE (40 mM Tris, 5 mM sodium acetate, 1 mM EDTA [pH 7.8]) at 125 V for 30 min. This electrophoresis analysis determined if the PCR was able to successfully amplify the right size of products from the DNA. Ultraclean PCR kit (MoBio, Carlsbad, CA) was used to purify the PCR products, which were then, send for sequencing to Genewiz (South Plainfield, NJ). The gene sequence obtained from Genewiz was used to find the most closely related 16S rRNA gene sequences by blastn

search (Altschul et al., 1997) of the NCBI database. All of the closely related 16S rRNA gene sequences were downloaded from Genbank and uploaded to ClustalW2.0 (Chenna et al., 2003) for alignment with the 16S rRNA gene sequence from strain FGH. The sequences were then trimmed in ClustalX and used to build a neighbour-joining phylogenetic tree using MEGA 4 (Tamura et al., 2007).

Growth experiments. Strain FGH cultures were grown with different carbon sources in minimal media at 28°C. Glucose, pyruvate, succinate, lactate, malate and citrate were provided at the concentration of 30 mM, peptone was added as 2% (w/v), and yeast extract at 0.05 g/L. When strain FGH was tested for its ability to utilize sulfate as an electron acceptor during growth with various carbon sources, sulfate was provided at 5 mM concentration. Inoculum was grown with 2% peptone for 1 day. Cells were washed by centrifugation at 9167 g for 10 mins under anoxic conditions in a glove box. The supernatant was then decanted, and the cells were resuspended in fresh medium. The washed cell suspensions were used for all experiments at a 1:10 (v:v) dilution. Optical densities (A_{600}) of the cultures were measured to determine growth. Substrate utilization was also measured by high performance liquid chromatography (HPLC).

Iron oxide reduction experiments. Ferrihydrite was synthesized in the laboratory based on the protocol described by Schwertmann and Cornell (1991). The ferrihydrite containing nanoporous beads were synthesized using the procedure described in Lies et al. (2005). Synthesized mineral suspensions were then washed with deoxygenated deionized water for 7-8 times in the glove box. These washed mineral suspensions were purged with 100% nitrogen gas and sealed in a serum bottle. Power X-ray diffraction (XRD) was performed with air dried ferrihydrite samples to confirm its identity.

Ferrihydrite's surface area was determined as 310 m^2/g based on 11-pt BET-Nitrogen isotherm (Micromeritics Gemini 2375) measurments.

Iron reduction experiments were conducted with pyruvate (30 mM) or glucose (30 mM or 110 mM) as the carbon source and ferrihydrite (1 mM) in minimal medium. For Fe-bead experiments, glucose (110 mM) was provided as the carbon source and ferrihydrite or ferrihydrite beads (1 mM). Cultures were incubated under strict anaerobic conditions in the dark at 28°C on a shaker and agitated at 150 rpm. For spent media experiments, strain FGH was grown with glucose (110 mM) for 2 days and filtered through a 0.2 µm filter anaerobically. The filtrate was reacted with 1 mM ferrihydrite under anoxic conditions and samples were collected for Fe(II) and Fe(III) measurements at selected time intervals.

To test for flavin production by strain FGH, cultures were grown anaerobically with 110 mM glucose at 28°C and the supernatant was collected for analysis. The control strain, *Shewanella oneidensis* MR-1 was anaerobically grown in *Shewanella* basal medium (SBM) with 20 mM lactate and 40 mM fumarate at 30°C. After 18 h of incubation, samples were taken and cells were removed by centrifugation. Fluorescent flavins in the supernatant were analyzed using a clear 96-well plate and read in a Molecular Devices SpectraMax M2 plate reader at 440 nm excitation, 525 nm emission (Covington et al., 2010). Riboflavin was used as the standard, and a calibration curve was made using a riboflavin stock solution diluted in defined medium at concentrations ranging from 0.125 to 10 µM.

Chemical analyses. Samples were removed from iron oxide reducing cultures and analyzed for substrate loss and formation of metabolic products at specific time intervals. For measuring dissolved Fe(II) and Fe(III), samples were first filtered through a 0.45 µm filter, and the filtrate was reacted with 1 N HCl (trace metal grade). Whereas for total

Fe(II) measurements, samples were reacted with 1N HCl for 1 h before Fe(II) concentration was quantified using the ferrozine assay (Viollier et al., 2000). The ferrozine assay was sensitive enough to detect as low as 5 µM Fe(II) concentration. Sulfide production was measured using the Cline method (Cline, 1969). The formation of hydrogen and carbon dioxide gas was determined by gas chromatography with a thermal conductivity detector and electron capture detector, respectively. Pyruvate, succinate, lactate, malate, acetate, formate and citrate were measured by HPLC (Beckman) with a 0.013 M H_2SO_4 mobile phase at a flow rate of 0.6 ml min^{-1} and column temperature of 65°C. Aminex HPX-87C column was used for analysis and the HPLC consisted of a System Gold 166 detector.

Genome sequencing and analysis. Genomic DNA of strain FGH was extracted from peptone grown cultures using the PowerSoil DNA Kit (MoBio, Carlsbad, CA). A paired end library was constructed using an Illumina Nextera kit, and sequencing was performed using an Illumina Genome Analyzer IIX (Illumina Inc., San Diego, CA). Sequence assembly was performed using CLC Genomics Workbench 5.1 (CLC Bio, Cambridge, MA). Gene annotation and protein sequence analysis was performed based on National Center for Biotechnology Information (NCBI) database and Basic Local Alignment Search Tool (BLAST) (Altschul et al., 1997). Metabolic pathway reconstructions were performed using KEGG Automatic Annotation Server (Moriya et al., 2007) and Rapid Annotation using Subsystem Technology (RAST) (Aziz et al., 2008). Genomic data has been submitted to NCBI as Bioproject SUB139619. We searched for cytochrome c genes in the draft genome of strain FGH and complete genomes of other organisms by querying for genes that are annotated as c-type cytochromes in GenBank. Then heme motifs (CXXCH) were queried in this list of genes to calculate the number of heme motifs and determine the number of multiheme c-type cytochromes.

RESULTS

Physiological characterization of strain FGH. An anaerobic iron-reducing bacterium designated as strain FGH was isolated from the unconsolidated Oak Ridge saprolitic sediments. At exponential growth phase, cells were rod shaped, approximately 2 µm in length and 0.5 µm in width (Figure 3.1A). These cells stained gram positive, and transmission electron micrograph showed the presence of a thick cell wall. Based on PCR amplification and sequence analysis of the 16S rRNA gene, strain FGH was most similar (99% identity) to *Clostridium tunisiense* $E1^T$ and *Clostridium sp*. CYP5 (Figure 3.1B).

Strain FGH is an obligate anaerobe that grew in minimal medium with glucose or pyruvate as the carbon source (Table 3.1). No external electron acceptor was required for growth, indicating strain FGH grows by fermentation. Growth on glucose and pyruvate yielded high optical densities within 3 day of incubation. Strain FGH was unable to ferment succinate, lactate, malate or citrate. The addition of sulfate did not result in growth on these substrates, and no substrate loss was detected with or without sulfate (Table 3.1). Furthermore, sulfate reduction and sulfide production were also not detected in glucose and pyruvate grown cultures.

Iron oxide reduction. Strain FGH reduced ferrihydrite during growth on glucose and pyruvate (Figure 3.2). The presence of ferric iron was not required for growth. When grown with 30 mM pyruvate, strain FGH reduced about 40% of the ferrihydrite in 7 days (Figure 3.2A). The rate of ferrihydrite reduction was 0.05 mM/d during pyruvate fermentation. When provided with 30 mM of glucose, ferrihydrite was reduced at faster rates, approximately 0.15 mM/d, resulting in 1 mM Fe(II) production in 7 days (Figure

3.2B). The rate of iron reduction was increased when the concentration of glucose was increased from 30 mM to 110 mM (Figure 3.2C). Strain FGH reduced 1 mM ferrihydrite within 36 h of incubation with 110 mM glucose with maximum reduction rate of 0.91 mM/d. In all experiments, ferrous iron production did not occur when cells were incubated in the absence of a carbon source.

An experiment was conducted to determine if strain FGH required direct contact to reduce Fe(III). Ferrihydrite precipitated inside nanoporous glass beads that was unavailable for direct cellular contact (Lies et al., 2005) was incubated with strain FGH in minimal medium. Strain FGH was able to mediate the complete reduction of ferric iron in the Fe-bead system (Figure 3.3). Although the rates of iron reduction were slower, strain FGH fully reduced 1 mM of Fe(III) inside the glass beads after 36 h. Ferrihydrite reduction and ferrous iron production was not observed when cells were incubated in the absence of glucose**.**

Reaction of cell-free spent medium with ferrihydrite did not result in iron reduction (Table 3.2). Spent media harvested from 110 mM glucose incubations and reacted with ferrihydrite in the absence of cells did not produce Fe(II). Furthermore, the formation of dissolved Fe(III) was also not observed, indicating that strain FGH does not produce ligands to solubilize Fe(III). Finally, we analyzed for the presence of fluorescent compounds (440 nm excitation/525 nm emission) indicative of flavins in the spent medium. Strain FGH produced negligible amounts of flavins (0.07 µM/OD_{600}) in comparison to positive control *S. oneidensis* MR-1 (0.8 µM/OD_{600}) (Figure 3.4).

Genomic characterization of strain FGH. Genomic sequencing of strain FGH resulted in the assembly of 75 contiguous sequences (contigs) containing a total of 4,882,233 base pairs. The draft genome displayed a G+C content of 30.67%, and 4621 open reading frames (ORFs) were identified. Genome analysis of strain FGH revealed

complete pathways for glucose metabolism and pyruvate utilization (Figure 3.5). Genes for the entire glycolysis pathway were present in FGH genome, including the glucokinase (FGH_3973), glucose-6-phosphate isomerase (FGH_1372), 6-phosphofructokinase (FGH_3839), fructose bisphosphate aldolase (FGH_2980), glyceraldehyde 3-phosphate dehydrogenase (FGH_4487), phosphoglycerate kinase (FGH_4486), phosphoglycerate mutase (FGH_3537), phosphopyruvate hydratase (FGH_4483) and pyruvate kinase (FGH_504) genes. Glucose fermentation led to the production of acetate, formate, hydrogen and carbon dioxide, which were detected by HPLC and gas chromatography (data not shown). Genes for pyruvate metabolism were also present in the genome, including the pyruvate ferrodoxin oxidoreductase (FGH_1812) and pyruvate formate-lyase (FGH_2431) genes. In the fermentation pathway, pyruvate is converted into acetyl-CoA by pyruvate-ferredoxin oxidoreductase, producing CO_2 and reduced ferredoxin. Identification of these genes provides a molecular basis for understanding the growth of strain FGH on glucose and pyruvate, as illustrated in table 3.1.

Analysis of the genome sequence indicates that strain FGH is able to ferment a variety of sugar compounds, as well as amino acids and alcohols. We found genes for numerous glycolytic enzymes, including β-galactosidase (FGH_1391), β-glucosidase (FGH_2156) and α-mannosidase (FGH_1396), which enable the utilization of complex sugar molecules by degrading the compounds into simpler sugars that enter the main glycolysis pathway. The genome of strain FGH also contained genes for metabolizing amino acids, including the glutamate mutase (FGH_2089) and tryptophanase (FGH_1849). Alcohol metabolism can also be performed by strain FGH with the action of Fe-containing alcohol dehydrogenase (FGH_503 and FGH_3385), alcohol dehydrogenase (FGH_247), short-chain alcohol dehydrogenase (FGH_312), butanol dehydrogenase (FGH_2145) and methanol dehydrogenase (FGH_2959 and

FGH_3800). Similar to *C. perfringens* (Shimizu et al., 2002), genes coding for the tricarboxylic acid (TCA) cycle were absent in the genome of strain FGH.

Transporter genes for sugars and branched amino acid uptake were identified in the genome sequence. In strain FGH, sugar uptake is mediated by an ABC-type transporter (FGH_4491, FGH_4492 and FGH_4493), glycoside-pentoside-hexuronide transporter for polysaccharide uptake (FGH_2543), and a mannose-fructose-sorbose family transporter for monosaccharide uptake (FGH_90). We also found specific ABC transporter genes for amino acid uptake, including histidine/glutamic acid/glutamine/arginine transporters (FGH_727 and FGH_728) and leucine/isoleucine/valine transporters (FGH_2333 and FGH_2336). Strain FGH catalyzes peptide transport through branched amino acid transporters (FGH_550, FGH_551 and FGH_553) and oligopeptide/dipeptide transporters (FGH_248, FGH_249 and FGH_250).

Hydrogenase genes that commonly occur in *Clostridium* species were also found in the genome sequence of strain FGH. The genes for ferredoxin hydrogenase (FGH_656), [Fe] hydrogenase (FGH_225, FGH_458 and FGH_3910) and [NiFe] hydrogenase (FGH_279) were identified in the genome sequence. These ferredoxin dependent hydrogenases are known to catalyze electron transfer from reduced ferredoxin to protons resulting in the production of H_2, which is released from the cell together with CO_2. Ferredoxin hydrogenase (FGH_656) protein present in strain FGH is 67% similar to Fe-hydrogenase protein in *Clostridium* sp. JC122, and the [Fe] hydrogenase (FGH_3910) protein sequence is 75% similar to [Fe] hydrogenase in *C. sporogenes* PA 3679. [NiFe] hydrogenase (FGH_283) protein found in strain FGH is 74% similar to Ni,Fe-hydrogenase III large subunit I in *C. clariflavum* DSM 19732. Finally, the [NiFe] hydrogenase proteins HypA (FGH_281), HypB (FGH_282), HypF (FGH_283), HypC (FGH_284), HypD (FGH_285), and HypE (FGH_286) were identified

in an operon in the genome of strain FGH. These proteins are involved in hydrogenase biosynthesis, nickel incorporation into hydrogenase, assembly chaperone, maturation and expression.

Genome analysis of strain FGH indicates that this bacterium assimilates iron and produces a diverse range of Fe-S proteins. Strain FGH carries an iron chelate uptake gene (FGH_1314, FGH_1315 and FGH_ 1316) and a ferrous iron transport protein (FGH_3174). Strain FGH uses iron to synthesize a large variety of Fe-S oxidoreductase enzymes (FGH_2861, 4096, 3921, and 452) and 4Fe-4S ferredoxin proteins (FGH_ 4103, 831, 1013, 117, 1513, 2113, 2358, 2547, 280, 294, 3532, and 3869). These iron-sulfur proteins play a central role in electron transfer within the cell. The nifU gene which encodes for an iron-sulfur cluster assembly scaffold protein in the nitrogen fixation pathway was also identified in the genome of strain FGH.

Finally, analysis of the genome sequence reveals that strain FGH is a spore-former. Strain FGH has about 40 sporulation and germination related genes. Genes encoding sporulation-related sigma factor (FGH_2874) and sporulation related transcriptional regulator (FGH_3929) are also found in the genome of strain FGH. Many stage specific sporulation genes in strain FGH are present in operons. Presence of stage specific sporulation genes (stages II, III, IV, and V) indicate that sporulation would proceed to stage V when sporulation is initiated. The sporulation genes in the genome of strain FGH were very similar to genes found in *C. kluyveri*, *C. carboxidivorans*, *C. tetani*, *C. bolutinum*, and *C. sporogenes*.

DISCUSSION

Strain FGH is phylogenetically related to *C. pasteuranium* and *C. beijerinckii* (Dobbin et al., 1999; Lovley, 1995), two *Clostridium* species known to be iron reducers. Similar to strain FGH, *C. pasteuranium* and *C. beijerinckii* reduce iron oxides during

glucose fermentation. The closest relative of strain FGH in pure culture is *C. tunisiense* $E1^T$, a gram positive, fermentative spore-former that has not been tested for iron reducing activity (Thabet et al., 2004). Strain FGH is also more distantly related to the iron-reducing clostridia *Desulfotomaculum reducens*, *Pelosinus fermentans,* and *Thermoterrabacterium ferrireducens* (Gavrilov et al., 2007; Shelobolina et al., 2007; Tebo and Obraztsova, 1998).

Strain FGH does not require direct contact for iron reduction (Figure 3.3). The ability of strain FGH to reduce Fe(III) oxides at a distance suggests that an extracellular factor is involved in the reduction processes. The cell-free spent medium experiments showed that the extracellular compound is not a chemical reductant that abiotically reduces Fe(III) oxides (Table 3.2). Furthermore, we did not detect dissolved Fe(III) indicating that the compound is not a ligand that solubilizes the Fe(III) oxide. Fluorescent flavins, which have recently been proposed to be the dominant extracellular electron shuttle for iron oxide reduction by *Shewanella* and *Geothrix* (Mehta-Kolte and Bond, 2012; von Canstein et al., 2008), were not detected in the spent medium (Figure 3.4). Moreover, the recently identified flavin secretion gene *bfe* (Kotloski and Gralnicka, 2013) was not found in the genome of strain FGH, further arguing against a flavin mediated iron reduction mechanism.

Comparative analysis of strain FGH with the complete genome sequences of other members of the *Clostridium* genus reveals a common deficiency of cytochrome genes. In general, cytochrome genes are rarely found in *Clostridium* genomes (Table 3.3). Close relative of strain FGH such as *C. cellulolyticum* H10, *C. lentocellum*, *C. phytofermentans* ISDg, *C. saccharolyticum* WM1, *C. sp.* BNL1100, and *C. thermocellum* ATCC27405 do not possess any cytochromes (Table 3.3). In *Clostridium* species that do carry cytochromes (e.g., *C. beijerinckii* and *C. cellulovorans*), no cytochrome gene has more than a single heme motif (CXXCH). Based on genome sequences currently

available in microbial genome databases, members of *Clostridium* appear to be devoid of multiheme c-type cytochrome genes.

The lack of multiheme c-type cytochromes in strain FGH is not surprising as clostridia do not respire iron for energy generation. Cytochromes are membrane-associated electron carriers involved in respiration. Based on the genome analysis, we found no evidence that iron reduction in strain FGH is linked to a membrane-bound electron transport chain. This is in contrast to DIRB (*Geobacter*, *Shewanella* and *Thermicola)*, which harbor a network of multiheme c-type cytochromes that connects the inner membrane to the external cell surface for electron transfer and the generation of proton motive force. DIRB have numerous multiheme c-type cytochromes with the average number of heme per cytochrome ranging from 6.4 to 11.8 (Table 3.3). The dearth of cytochrome genes and absence of the multiheme signature in *Clostridium* genome sequences suggest that fermentative clostridia employ a fundamentally different mechanism for iron oxide reduction. This calls into question the biological function of iron reduction in strain FGH and other metal reducing fermenters.

The physiological reason for iron reduction by strain FGH is unclear. It has been proposed that iron reduction by fermentative bacteria might be advantageous as an excess electron sink or shift the proportions of fermentation end products to provide a slightly greater energy yield (Dobbin et al., 1999; Lovley and Phillips, 1989; McInerney and Beaty, 1988). But while fermentative metabolism can divert a proportion of electron flow to Fe(III) reduction, the electron transfer reaction does not generate energy for growth (Lovley, 1995; Lovley et al., 1991). Strain FGH might also be reducing iron oxides for Fe(II) solubilization and assimilation rather than dissimilatory reduction. The genome of strain FGH encodes for abundant and diverse iron-sulfur proteins that have a critical function in electron transfer processes in the cell. Alternatively, iron reduction

may have no physiological role at all, but instead may be a side reaction of fermentative growth that confers no biological benefit.

Strain FGH was isolated from sediments adjacent to a uranium contaminant plume at Oak Ridge National Lab. Analysis of 16S rRNA gene sequences extracted from sediments at this field site have shown that members belonging to genus *Clostridium* are stimulated during uranium bioremediation experiments (Madden et al., 2009; North et al., 2004; Petrie et al., 2003). Phylogenetically, strain FGH is closely related to several *Clostridium* species that have been shown to reduce soluble U(VI) to poorly soluble U(IV) (Dalla Vecchia et al., 2010; Francis et al., 1994; Gao and Francis, 2008). Recently, an unknown extracellular factor was found to be required for U(VI) reduction by *Clostridium* spores (Dalla Vecchia et al., 2010). In that study, *Clostridium acetobutylicum* spores reduced U(VI) when incubated with spent media and hydrogen. The extracellular factor produced mediated U(VI) reduction by transferring electrons from hydrogen to uranium and the hydrogenase was proposed to be located on the surface of the exosporium. These observations were also consistent with *Desulfotomaculum reducens* spores, that reduced U(VI) and Fe(III) by an unknown extracellular factor (Junier et al., 2009). Therefore, the production of extracellular factors by Firmicutes may have important implications for metal reduction ability of these organisms. An interesting question is whether or not Fe(III) and U(VI) reduction share a common mechanism in *Clostridium* species. Elucidation of the extracellular electron transfer mechanisms by strain FGH merits further investigation, and will be important not only for understanding subsurface iron reduction in clostridia dominated environments, buy may also have practical applications for contaminant bioremediation.

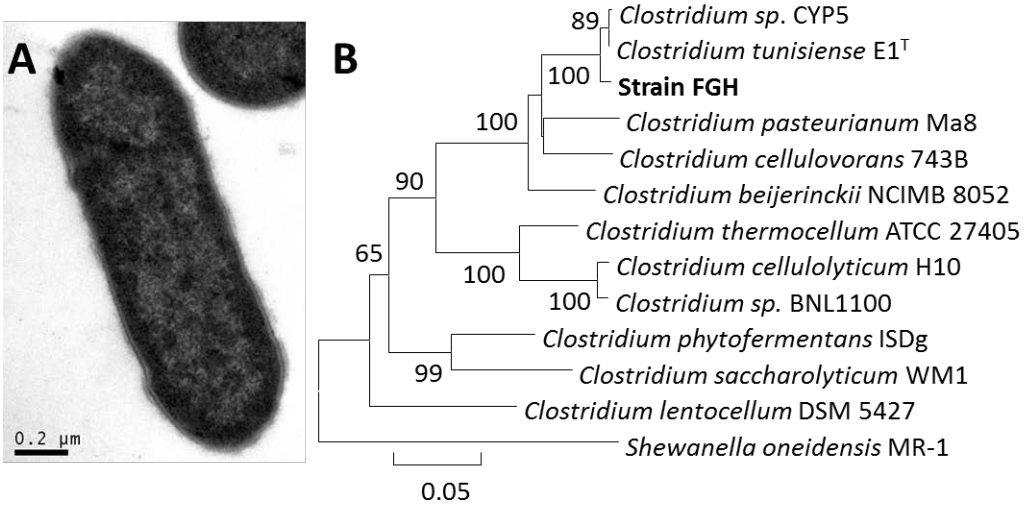

Figure 3.1. (A) Transmission electron micrographs of strain FGH, showing a gram positive cell wall; (B) Neighborhood joining tree of strain FGH with its closest relatives. The 16S rRNA gene of *Shewanella oneidensis* was used as an outgroup. The bar represents 5 substitutions per 100 nucleotides.

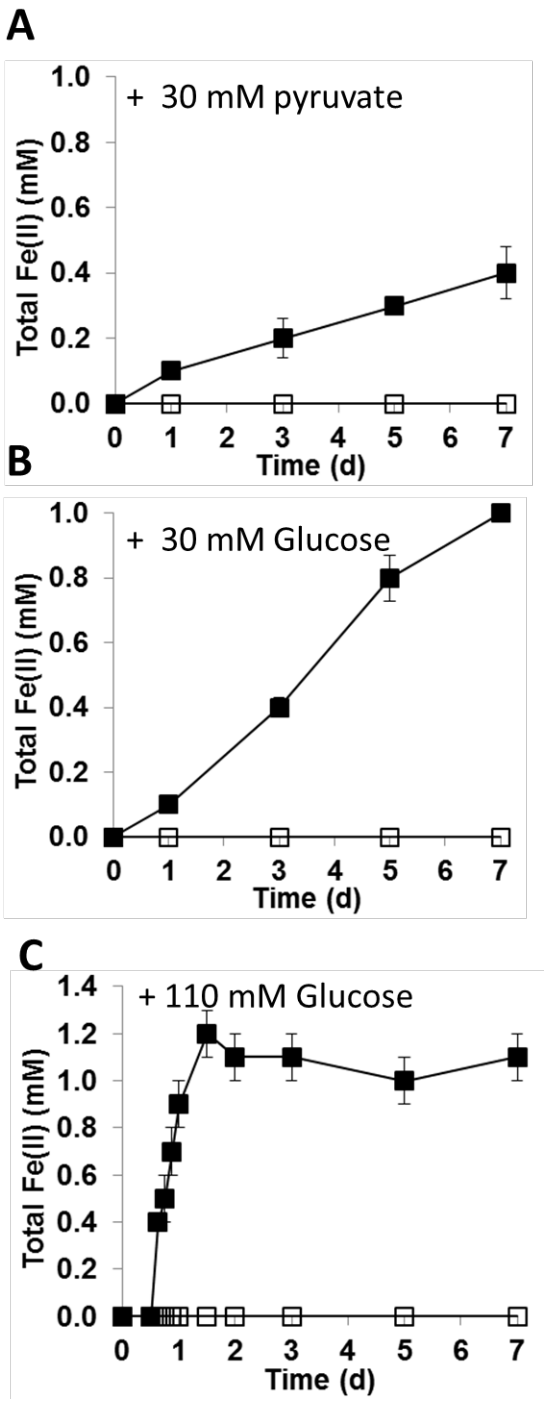

Figure 3.2. Ferrihydrite (1 mM) reduction by *Clostridium sp.* FGH when grown with 30 mM pyruvate(A), 30 mM glucose (B), or 110 mM glucose (C). Cells were incubated with ferrihydrite in presence [■] or absence [□] of carbon source. Points and error bars represent the means and standard deviations of duplicate cultures.

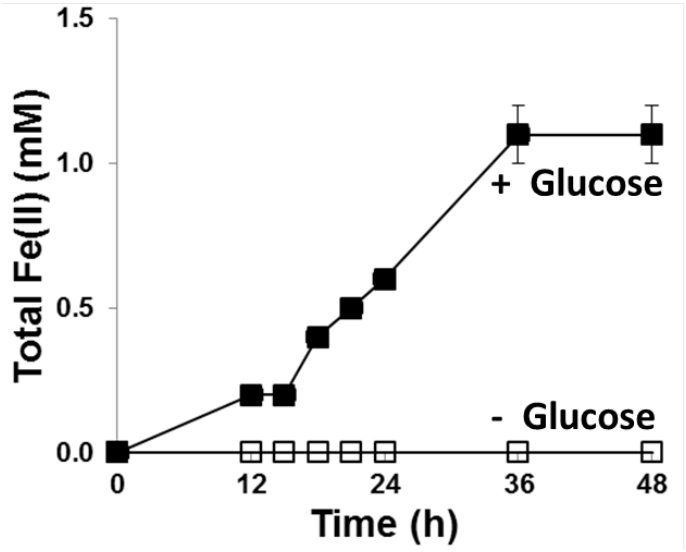

Figure 3.3. Ferrihydrite bead reduction by *Clostridium sp.* FGH during glucose (110 mM) fermentation. 1 mM ferrihydrite beads were provided. Cells were incubated with iron oxide in the presence [■] or absence [□] of glucose. Points and error bars represent the means and standard deviations of triplicate cultures.

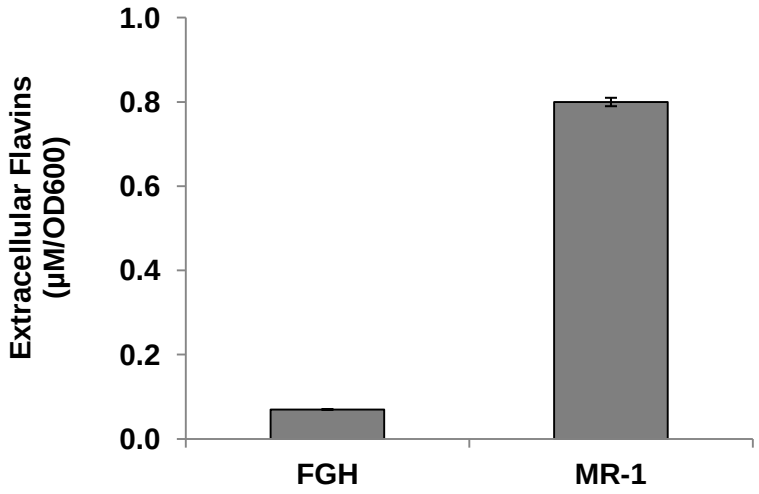

Figure 3.4. Extracellular flavin production by *Clostridium sp.* FGH. *Shewanella oneidensis* MR-1 was used as a positive control. Error bars represent the standard deviations of duplicate cultures.

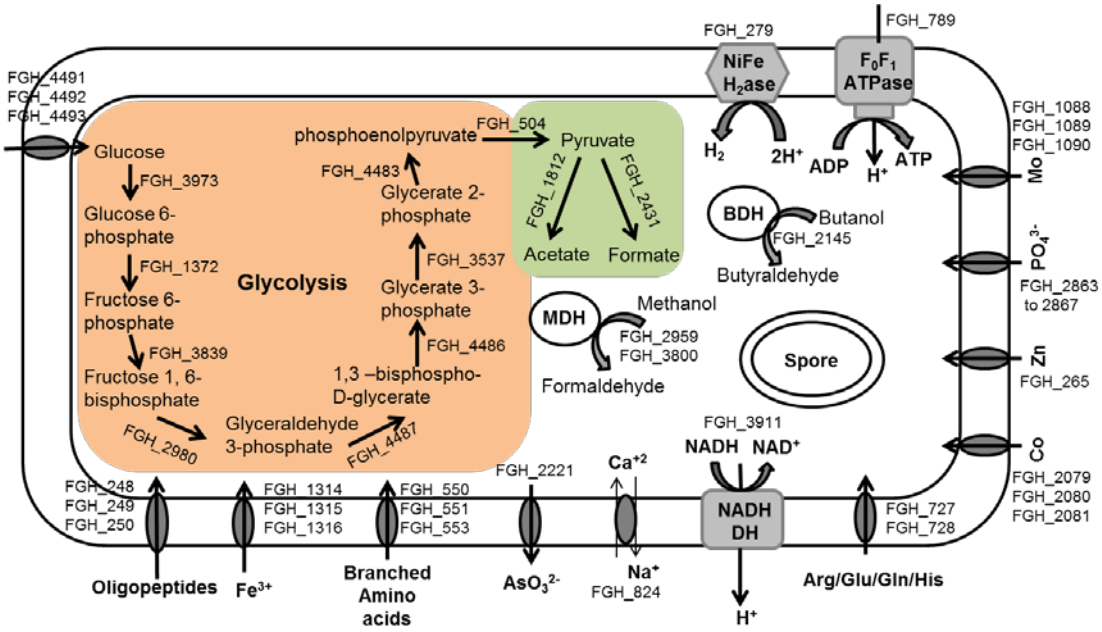

Figure 3.5. Schematic representation of genes and metabolism pathways in the genome of *Clostridium sp.* FGH

Table 3.1. Growth of *Clostridium sp*. FGH on various substrates[1] in presence or absence of sulfate[2].

Carbon source	Growth [O. D. (A_{600})]			Substrates utilized [mM] [7D]	
	1 D	3 D	7 D	Without SO_4^{2-}	With SO_4^{2-}
Glucose	+	++++	+++	ND[3]	ND
Pyruvate	++	+++	+++	30	30
Succinate	-	-	-	0	0
Lactate	-	-	-	0	0
Malate	-	-	-	0	0
Citrate	-	-	-	0	0

[1] 30 mM substrate and 0.05 g/l of yeast extract were added

[2] 5 mM sulfate was added as electron acceptor

[3] ND Not determined

- No growth + Weak growth ++ Moderate growth +++ Good growth ++++ Strong growth

Table 3.2. Spend media* reaction with ferrihydrite (30 mM).

Time	Total Fe(II)	Dissolved Fe(III)
h	µM	µM
0	27	10
2	26	7
6	26	8
12	25	8
24	22	10

* *Clostridium sp*. FGH was grown with 110 mM glucose

Table 3.3. Summary of c-type cytochromes in the genome of *Clostridium sp*. FGH and in the complete genome of other organisms.

Organisms	c-type cytochromes	Multiheme c-type cytochromes	Average heme per cytochrome
Clostridium sp. FGH	0	0	-
Clostridium beijerinckii NCIMB 8052	2	0	1
Clostridium cellulolyticum H10	0	0	-
Clostridium cellulovorans 743B	1	0	1
Clostridium lentocellum	0	0	-
Clostridium phytofermentans ISDg	0	0	-
Clostridium saccharolyticum WM1	0	0	-
Clostridium sp. BNL1100	0	0	-
Clostridium thermocellum ATCC27405	0	0	-
Thermicola potens[a]	41	32	11.9
Geobacter sulfurreducens PCA[b]	89	78	7.5
Geobacter metallireducens [b]	76	66	7.3
Shewanella oneidensis MR-1[c]	39	23	6.4

[a] Data from Wrighton et al., 2011 and Carlson et al., 2012

[b] Data from Butler et al., 2010

[c] Data from Heidelberg et al., 2002 and Wrighton et al., 2011

CHAPTER 4

Genomic characterization of a novel gram negative, spore forming *Veillonellaceae* derived from subsurface sediments

Abstract

Recently *Veillonellaceae* have been recognized to be active members of microbial communities at contaminated subsurface sites during vegetable oil amendments. In this study, we sequenced and analyzed the genome of strain RU4, a novel *Veillonellaceae* enriched from subsurface sediments of Oak Ridge, TN. Genomic characterization of strain RU4 revealed the presence of a β oxidation pathway for fatty acid metabolism. In addition to this, strain RU4 possesses several genes for fermenting glucose, pyruvate, succinate, malate, and formate. Strain RU4 carries genes for hydrogen oxidation and sulfate reduction. The RU4 genome encodes [NiFe]- and [FeFe]-hydrogenases for H_2 oxidation. The sulfate reduction pathway genes in the RU4 genome display low protein sequence homology with other known sulfate reducers such as *Desulfotomaculum* and *Desulfovibrio*. Genes coding for sulfide and polysulfide reductases are also present in the RU4 genome. Strain RU4 has about 60% protein sequence similarity and similar operon structure to sulfite reducing *Desulfotomaculum gibsoniae* and *Desulfotomaculum nigrificans*. The polysulfide reductase operon structure in strain RU4 is very similar to that in the polysulfide respiring bacteria *Wolinella succinogenes* and share high protein sequence similarity. Genomic characterization of strain RU4 broadens our knowledge on what biogeochemical and ecological role *Veillonellaceae* might play in the subsurface environment.

Introduction

The stimulation of the indigenous subsurface microbial community seems to be promising for reduction and immobilization of contaminants in groundwater. Recent pyrosequencing studies have shown that a limited microbial consortium is responsible for extended bioreduction of uranium in a contaminated aquifer at Oak Ridge, TN (Gihring et al., 2011). Quantitative PCR and pyrosequencing of 16S rRNA gene revealed that members of family *Veillonellaceae* are found to be active during metal reduction at bioremediation field sites. These organisms dominated after injection of vegetable oil in the ground and most likely catalyzed the initial oil decomposition. Subsurface sediment incubations from Rifle, CO, also showed that emulsified vegetable oil (EVO) and hydrogen release compound (HRC) additions were more effective in stimulating U(VI) removal (Barlett et al., 2012). Members of family *Veillonellaceae* dominated during addition of vegetable oil and HRC based on phospholipid fatty acid analysis and quantitative 16SrRNA gene specific PCR . However, the role of *Veillonellaceae* is poorly understood in the subsurface environments.

Members of the *Veillonellaceae* family have been mostly cultured from living animal hosts (Carlier et al., 2002; Jumas-Bilak et al., 2004; Marchandin et al., 2003; Moore et al., 1987). Previous studies primarily focused on the effect of *Veillonellaceae* on humans and animals (Bhatti and Frank, 2000; Hughes et al., 1988; Nisbet and Martin, 1990; Sawanon et al., 2011; Tanner et al., 2012; Valm et al., 2011). Characteristic features of members of this family are fermentation of sugars, carboxylic acids, and alcohols. Genomes of only two organisms, *Veillonella parvula* and *Pelosinus sp.* in this family have been analyzed (Beller et al., 2013; Gronow et al., 2010). *Veillonella parvula* are colonizers of the human oral cavity and are important in oral biofilm formation. The only characterized genome of subsurface *Veillonellaceae* is for *Pelosinus sp.* strain HCF1, which was recently isolated from a Cr contaminated site (Beller et al., 2013).

Since very few subsurface Veillonellaceae are cultured and studied, it is difficult to elucidate their biogeochemical and ecological role in the environment. Genomic characterization of subsurface *Veillonellaceae* would fill an important knowledge gap and may assist in the design of insitu bioremediation strategies at contaminated field sites.

Previously we enriched for a novel *Veillonellaceae* (designated as strain RU4) from Oak Ridge subsurface saprolite sediments (Shah et al., submitted). Based on 16S rRNA gene analysis, strain RU4 clusters with members of the family *Veillonellaceae* with low 16S rRNA gene sequence similarity (91% to closest relative). This organism may represent a novel genus in family *Veillonellaceae*. Phylogenetic analysis reveals that strain RU4 is distantly related to members of genus *Sporomusa* and *Propionispora* in family *Veillonellaceae* (Shah et al., submitted). Strain RU4 has low 16S rRNA gene sequence similarity (91%) to the well characterized strain *Pelosinus fermentens*. Strain RU4 is not closely related to any cultured and well-studied isolates. In contrast, analysis of 16S rRNA gene sequences revealed that strain RU4 clusters with many uncultured organisms enriched from subsurface environments. In this study, we sequenced and analyzed the draft genome of this novel *Veillonellaceae* enriched from saprolite sediment. Genome characterization of this novel genus provides insight in physiology of these organisms and its role in the subsurface environments.

Methods

Growth conditions. Enrichment culture was grown in defined minimal media at 28°C. Minimal media used to cultivate the enrichment culture was composed of 0.75 mM NH_4Cl, 0.1 mM NaCl, 0.34 mM KH_2PO_4, 0.38 mM $MgCl_2.6H_2O$, 0.34 mM $CaCl_2.2H_2O$, 10 mM PIPES buffer, 0.05 g/L yeast extract. Medium was supplemented with 10 ml per liter of Wolfe's vitamin mix and a modified mineral solution (Shah et al., submitted).

Enrichment culture was grown with 30mM fumarate as the carbon source. Cells were washed prior to inoculation by centrifugation at 9167 g for 10 mins and incubated in fresh medium. Growth was monitored by measuring the optical density of the cultures at 600 nm wavelength.

Electron microscopy. Thin sections for transmission electron microscopy were prepared with fumarate grown strain RU4 enrichment cultures at exponential (5 d) and stationary phase (7 d). Preparation of thin sections involved cell fixation and embedding in Epon-Araldite. Cells were first pelleted at exponential and stationary phase by centrifuging at 9167 g for 10 mins. The cell pellets were then fixed in Karnovsky's fixative (formaldehyde, 4% v/v and glutaraldehyde, 1% v/v, in 0.1 M Millonig's phosphate buffer, pH 7.3) for 3 h (Shah et al., submitted). After fixation, they were incubated in 1% osmium tetroxide for 1 h and dehydrated in a graded ethanol series. The fixed and dehydrated cell pellets were embedded in Epon–Araldite and sectioned with a diamond knife. For visualizing cells, the embedded cell pellets were stained for 15 mins in 5% (w/v) uranyl acetate solution and then for 2 mins in 0.5% (w/v) lead citrate solution. Imaging of the cells was conducted by using a transmission electron microscope (JEOL JEM 100 CX).

Genome sequencing and analysis. For sequencing the genome of strain RU4, genomic DNA was extracted from fumarate fermenting strain RU4 cultures using the PowerSoil DNA Kit (MoBio, Carlsbad, CA). The isolated DNA was then purified by a ultraclean DNA purification kit (MoBio, Carlsbad, CA) and concentration of DNA was determined by NanoDrop spectrophotometer (ND-1000). Illumina Nextera kit was used to prepare a paired end library. DNA sequencing was then performed with the help of an Illumina Genome Analyzer IIX. After obtaining reads from illumina sequencing, the DNA sequences were assembled by using the CLC Genomics Workbench 5.1 (Shah et al.,

submitted). The genome assembly contains a group of contigs that are formed by overlapping reads representing a consensus DNA sequence. After obtaining the genome assembly, G+C content and tetranucleotide frequences of contigs were determined distinguish genomic fragments of strain RU4 from *Clostridium sp.* strain FGH (other member of the enrichment culture). The G+C content of each contig was calculated using a tool from the EMBOSS package called GeeCee. In addition to G+C content, the tetranucleotide frequency of both strands on each contig was calculated with TETRA (Teeling et al., 2004). These tetranucleotide frequencies were then clustered with Cluster3.0 and visualized with JavaTreeView.

After comprising the draft genome for strain RU4, we analyzed the genome for presence of genes with known functions. The comparison of genes were conducted based on National Center for Biotechnology Information (NCBI) database and Basic Local Alignment Search Tool (BLAST) (Altschul et al., 1997). The sequence homology of protein sequences from strain RU4 to those found in the NCBI database were also performed by using blastp. Annotation of genes in the RU4 genome were performed using BLAST, KEGG Automatic Annotation Server (KAAS) (Moriya et al., 2007) and Rapid Annotation using Subsystem Technology (RAST) (Aziz et al., 2008). Metabolic pathway genes in the genome were viewed by seed viewer in RAST and KAAS. These tools were also applied to the genome to identify genes that are present in an operon as well as compare these operon structures to other completely sequences genomes in the NCBI database.

For constructing sulfate, sulfite and polysulfide reduction operons, protein sequences from sequenced known sulfate reducers were obtained from NCBI database. Protein sequences were collected from genomes of *Desulfotomaculum reducens* MR-1, *Desulfotomaculum gibsoniae* DSM 7213, *Desulfotomaculum nigrificans* DSM 574, *Desulfovibrio vulgaris* Hildenborough and *Wolinella succinogenes* DSM 1740. Blastp

was used to compare gene sequences from RU4 genome against genomes of known sulfate, sulfite and polysulfide reducing organisms in Genbank.

Results and Discussion

Enrichment Culture. When the consortium was grown with fumarate under strict anaerobic conditions, one cell type dominated. Vegetative cells exhibited a gram negative cell wall (Figure 4.1A). Stationary phase cultures displayed extensive endospore structures (Figure 4.1B). The 16SrRNA gene sequence analysis of this fumarate grown culture revealed the presence of a novel *Veillonellaceae* (designated as strain RU4). The other member of the consortium (*Clostridium sp.* FGH) was not detected by PCR amplification of 16S rRNA gene indicating that more than 98% of the fumarate grown culture was dominated by strain RU4 (Shah et al., submitted).

Genome assembly and general features. The genome assembly resulted in 28 contiguous sequences (contigs) containing a total of 3,977,975 base pairs. G+C content of these contigs was determined to eliminate contigs that might belong to *Clostridium sp.* FGH. Strain FGH had a G+C content of 30% (Shah et al., submitted), whereas strain RU4's G+C content is 46%. Two out of twenty eight contigs in the genome assembly had G+C content close to 30% (Table 4.1). These two contigs were therefore eliminated from the genome assembly. Since G+C content is known to vary quite a bit within a given genome, we analyzed the tetranucleotide frequency for each contig to assign genomic fragments to strain RU4. Tetranucleotide frequency analysis is currently being used for metagenomics studies to bin genomic fragments and assign them to specific organism.This approach uses frequencies of oligonucleotides in genomic sequences that are known to carry species-specific signals to bin genomic fragments. Therefore,

tetranucleotide frequency represents a more pronounced phylogenetic signal. A total of 17 contigs in the genome assembly were found to have similar tetranucleotide frequency (Table 4.1). These contigs were large in size and had coverage over 600X. These 17 contigs constitute the draft genome for strain RU4. There are 3411 open reading frames (ORFs) in the draft genome of strain RU4.

Gram negative and gram positive features. Strain RU4 possesses a gram-negative cell wall (Figure 4.1A) and is also found to produce spores (Figure 4.1B). Members of family *Veillonellaceae* are phylogenetically closely related to Firmicutes, but have a gram-negative type cell wall. The strain RU4 genome possesses genes for lipopolysaccharide biosynthesis protein (RU4_1668) and lipopolysaccharide heptosyltransferase II (RU4_106) that are essential for outermembrane formation in gram-negative bacteria. Several genes such as lipid A biosynthesis acetyltransferase (RU4_1616 and 1631) and lipid A disaccharide synthase (RU4_1623) are present in RU4 genome. An *msb*A related protein (RU4_519) found in the RU4 genome is required for flipping lipid A from the cytosolic side of the inner membrane to the outer side of the inner membrane as in other gram negative bacteria. In addition to this, the RU4 genome consists of an outermembrane chaperone skp (OmpH), a periplasmic protein that is involved in folding and transport of several proteins to the outer membrane. *Veillonellaceae* is recognized as a Firmicutes lineage with gram-negative cell type. The gram negative cell phenotype is found in all members of family *Veillonellaceae*, suggesting that lipid A biosynthesis genes are acquired by vertical transfer.

Strain RU4 possesses a number of sporulation specific genes. This is consistent with electron microcopic images showing endospore formation by strain RU4 at stationary phase (Figure 4.1B). The genome of strain RU4 contains sporulation transcriptional activator Spo0A (RU4_1049), sporulation related transcriptional regulator

(RU4_1528 and 1591) as well as spore germination proteins (RU4_145, 144, and 2773). Sigma factors such as σ^E (RU4_603) and σ^G (RU4_604) are found in the genome and are thought to in part govern the developmental program of sporulation. Several stage specific sporulation (stage II, III, IV, V) genes are present in the RU4 genome. Many sporulation genes are present in an operon or are found in close vicinity in the genome. Sporulation in family *Vellionellaceae* is only found in some genera such as *Sporomusa*, *Desulfosporomusa*, *Propionispora*, *Pelosinus*, *Acetonema* and *Dendrosporobacter* (Biebl et al., 2000).

Fatty acid oxidation. Genome analysis of strain RU4 revealed a complete beta oxidation pathway for fatty acids degradation (Figure 4.2). Members of family *Veillonellaceae* are found to be active during EVO degradation at contaminated sites but have not been studied for fatty acid metabolism ability. *Pelosinus fermentans* is capable of utilizing several fermentable substrates but not tested for long chain fatty acid metabolism (Shelobolina et al., 2007). The genome of strain RU4 reveals the presence of an entire β oxidation pathway suggesting that this organism has the ability to oxidize fatty acids and produce acetate or propionate.

The fatty acid-oxidation genes in the RU4 genome include genes encoding for the acyl-CoA synthetases (RU4_153 and RU4_2443), acyl-CoA dehydrogenases (RU4_2157 and RU4_3260), enoyl-CoA hydratase (RU4_1715), 3-hydroxyacyl-CoA dehydrogenase (RU4_1716), and acetyl CoA acetyltransferase (thiolase) (RU4_1717). Of these genes, enoyl-CoA hydratase, 3-hydroxyacyl-CoA dehydrogenase and thiolase are found in an operon. Transporters for fatty acids (RU4_2019 and RU4_2457) were also found in the RU4 genome. Figure 4.2 illustrates a schematic of the beta oxidation pathway in strain RU4, indicating which gene products are believed to catalyze each reaction. This pathway would enable strain RU4 to break down fatty acids to acetyl-CoA.

Acetyl CoA could then feed into the citric acid cycle to obtain energy or be converted to acetate via acetate kinase (RU4_855). Production of acetate by this organism can stimulate growth of several acetate oxidizing metal reducers in the subsurface.

Fermentation. Central metabolic pathways such as the Embden-Meyerhof-Parnas (glycolysis) pathway is present in the RU4 genome (Figure 4.3). Genes for the entire glycolysis pathway were present in the RU4 genome, including the hexokinase (RU4_1242), glucose-6-phosphate isomerase (RU4_1692), 6-phosphofructokinase (RU4_3351), fructose bisphosphate aldolase (RU4_3657), glyceraldehyde 3-phosphate dehydrogenase (RU4_197), phosphoglycerate kinase (RU4_2557), phosphoglycerate mutase (RU4_578), phosphopyruvate hydratase (RU4_2554) and pyruvate kinase (RU4_2619) genes. This glucose fermentation pathway could lead to production of pyruvate with acetate, formate, lactate, hydrogen and carbon dioxide.

Pyruvate is an intermediate in the oxidation of several carbon sources (glucose, propionate, and lactate) in addition to being itself an electron donor and fermentative substrate. The RU4 genome has pyruvate ferrodoxin oxidoreductase (RU4_1452) and pyruvate formate-lyase (RU4_2237) genes for pyruvate metabolism. In the fermentation pathway, pyruvate can be converted into acetyl-CoA by pyruvate-ferredoxin oxidoreductase, producing CO_2 and reduced ferredoxin as an electron donor for hydrogenases. On the other hand, pyruvate can also be converted to formate and acetyl-CoA by the activity of pyruvate formate –lyase. The acetyl-CoA generated during pyruvate metabolism can then be further converted to acetate by acetate kinase (RU4_855). This step will generate ATP by substrate level phosphorylation.

The RU4 genome also has genes for utilizing fumarate, malate, formate and succinate which can act as fermentation substrates or electron donors for growth. Fumarate reductase (RU4_3012 and RU4_3013) is found in the RU4 genome, which

enables strain RU4 to degrade fumarate. Major products of fumarate fermentation may be succinate and acetate. The genome of RU4 also includes genes coding for malate dehydrogenase (RU4_1915 and RU4_2146), which catalyzes the oxidation of malate to oxaloacetate. Succinate dehydrogenase (RU4_2022, RU4_ 2023 and RU4_2024), a membrane bound enzyme that catalyzes the oxidation of succinate to fumarate were also present in the genome. Formate oxidation to carbon dioxide is enabled by formate dehydrogenase (RU4_75), which is a part of RU4 genome.

Strain RU4 genome revealed genes for metabolizing diverse substrates such as glucose, pyruvate, fumarate, succinate, formate, and malate (Figure 4.3). Most of these fermentation pathways lead to production of acetate, propionate and hydrogen. Members of genus *Sporomusa* can also produce acetate and propionate, while fermenting fumarate, malate and succinate (Boga et al., 2003; Dehning et al., 1989). *Pelosinus fermentans* also possesses genes for acetate and propionate fermentation from lactate and pyruvate (Beller et al., 2013).

The RU4 genome did not encode for genes in carbon dioxide pathway suggesting that this organisms is not capable of autotrophic growth.

Hydrogen metabolism. The genome of strain RU4 encodes for [NiFe] (RU4_3275) and [Fe] (RU4_383, 1127 and 1130) hydrogenases that mediate the consumption and production of hydrogen gas. Several proteins play an important role in formation of these hydrogenase complexes. Proteins such as HypA, HypB, HypC, HypD, HypE and HypF function in isoenyme and expression formation, assembly chaperon and maturation of [NiFe] hydrogenases. These hydrogenases enable strain RU4 to utilize hydrogen as an electron donor. As shown in previous study, we observed that growth of strain RU4 was enhanced in the presence of hydrogen, and therefore, strain RU4 is a hydrogen oxidizer (Shah et al., submitted).

Sulfate Reduction. An entire sulfate reduction pathway has been found in the genome of RU4. Strain RU4 produces sulfide when grown with sulfate (Shah et al., submitted). Based on current literature, *Desulfosporomusa polyptropa* is the only organism in family *Veillonellaceae* known to reduce sulfate but is unable to reduce sulfite and elemental sulfur (Sass et al., 2004). The genome of *Desulfosporomusa polyptropa* has not been sequenced. The APS reductase and sulfate adenylyltransferase genes are found in an operon in strain RU4. Sulfate adenylyltransferase, *sat*AB (RU4_3103 and RU4_3102) activates sulfate to form APS (adenosine-5'-phosphosulfate). APS is further reduced to sulfite by an APS reductase, *apr*AB (RU4_3100 and 3101). Proton translocating pyrophosphatase (RU4_54) is also found in RU4 genome which enables sulfurylation of ATP to completion. The organization and size of *apr*AB in strain RU4 were similar to those of known sulfate reducers *Desulfotomaculum reducens* MR-1 and *Desulfovibrio vulgaris* Hildenborough (Figure 4.4).

The protein sequence of the alpha subunit of APS reductase (*apr*A) from RU4 genome was 34% identical to *apr*A of *Desulfotomaculum reducens* MR-1 and 28% identical to *apr*A of *Desulfovibrio vulgaris* Hildenborough. A sulfate adenylyltransferase gene was found adjacent to APS reductase in strain RU4 similar to *Desulfotomaculum reducens* MR-1 but the sequence homology was very low. However, most of the genes in the neighborhood of the APS reductase in strain RU4 differ from known sulfate reducers *Desulfotomaculum reducens* MR-1 and *Desulfovibrio vulgaris* Hildenborough. The strain RU4 genome consists of several sulfate and thiosulfate transport genes (RU4_3096 to RU4_3099) that were not found to be in the close vicinity to the APS reductase in *Desulfotomaculum reducens* MR-1 and *Desulfovibrio vulgaris* Hildenborough genomes (Figure 4.4). APS reductase is associated with *qmo*ABC, alpha, beta and gamma subunits of the quinone-interacting membrane-bound oxidoreductase

in *Desulfovibrio vulgaris* Hildenborough (Junier et al., 2010). *Desulfotomaculum reducens* MR-1 genome also encoded for *qmo*AB that was associated with APS reductase. These *qmo*ABC genes were not present in close vicinity to APS reductase in strain RU4.

Reduction of sulfite to sulfide is catalyzed by sulfite reductase, *dsr*ABC (RU4_1903, RU4_1904 and RU4_1905) which are also found in the RU4 genome. Sulfite reduction pathway genes were found in an operon in strain RU4 (Figure 4.5). Sulfite reductase genes *dsr*ABC shared high protein sequence identity (55 – 60%) to *dsr*ABC gene from dissimilatory sulfite reducers *Desulfotomaculum gibsoniae* DSM 7213 and *Desulfotomaculum nigrificans* DSM 574. The operon structure was also very similar between strain RU4 and sulfite reducers *Desulfotomaculum gibsoniae* DSM 7213 and *Desulfotomaculum nigrificans* DSM 574 (Figure 4.5). A sulfite exporter (RU4_3104) was present in RU4 genome.

Polysulfide Reductase. Apart from genes for sulfate and sulfite reduction, RU4 also contains polysulfide reduction genes. The polysulfide reduction operon consists of three genes that function in reduction of polysulfide to sulfide. Strain RU4 consists of polysulfide reductase genes *psr*ABC (RU4_922, RU4_921 and RU4_920) that are present in an operon (Figure 4.6). The organization and size of *psr*ABC genes in strain RU4 are very similar to *psr*ABC genes in well studied polysulfide respiring *Wolinella succinogenes* DSM 1740. The protein sequences of *psr* subunit A, B and C genes from RU4 genome are 48%, 61% and 53% identical to *psr* subunit A, B and C genes in *Wolinella succinogenes* DSM 1740.

Electron transport Chain. RU4 genome contain genes encoding for electron transport chain components. Components of the electron transport chain such as electron transfer

flavoprotein (RU4_451, 452, 3261, 3262 and 2061), proton translocating NADH ubiquinone oxidoreductases and plastoquinone oxidoreductase and quinones were found in an operon (RU4_940 to RU4_950). Genes for F0F1 ATP synthase (RU4_1579, 1581, 1582, 1583, 1584, 1585, and 1586) are present in an operon in the RU4 genome. The genome of strain RU4 encodes for TatC and TatA/E that are a part of TAT secretion system as well as transporters for molybdenum uptake ModABC (RU4_123, 124 and 125).

Genome of RU4 contains a partial citric acid pathway that oxidizes acetyl-CoA to carbon dioxide. Enzymes involved in the citric acid cycle such as citrate synthase (RU4_112), aconitate hydratase (RU4_2854 and RU4_3161), 2-oxoglutarate ferredoxin oxidoreductase (RU4_866, RU4_864 and RU4_2358), succinate dehydrogenase (RU4_2022, RU4_2023 and RU4_2024), fumarate hydratase (RU4_2020) and malate dehydrogenase (RU4_1915) are present in the genome. However, two enzymes isocitrate dehydrogenase and succinate thiokinase, are not found in the draft genome of RU4, suggesting that these genes might be in the gaps of the genome or not present. The presence of components of an electron transport chain and genes involved in the citric acid cycle suggest that strain RU4 can grow by respiration.

Environmental Implications.

Genome characterization of this novel strain RU4 suggests that its metabolic capabilities include fatty acid oxidation, fermentation pathways, hydrogen utilization, and respiration of inorganic sulfur compounds. Breakdown of fatty acids may produce products utilized by metal reducing bacteria. RU4 can produce sulfide which can react with metals and alter the fate and transport of those contaminants in the subsurface. Fermentation, hydrogen oxidation and sulfate reduction by strain RU4 may affect the

biogeochemical cycling of carbon and sulfur in the subsurface. Future studies should be aimed at understanding the regulation and expression of RU4 genes under environmentally relevant conditions.

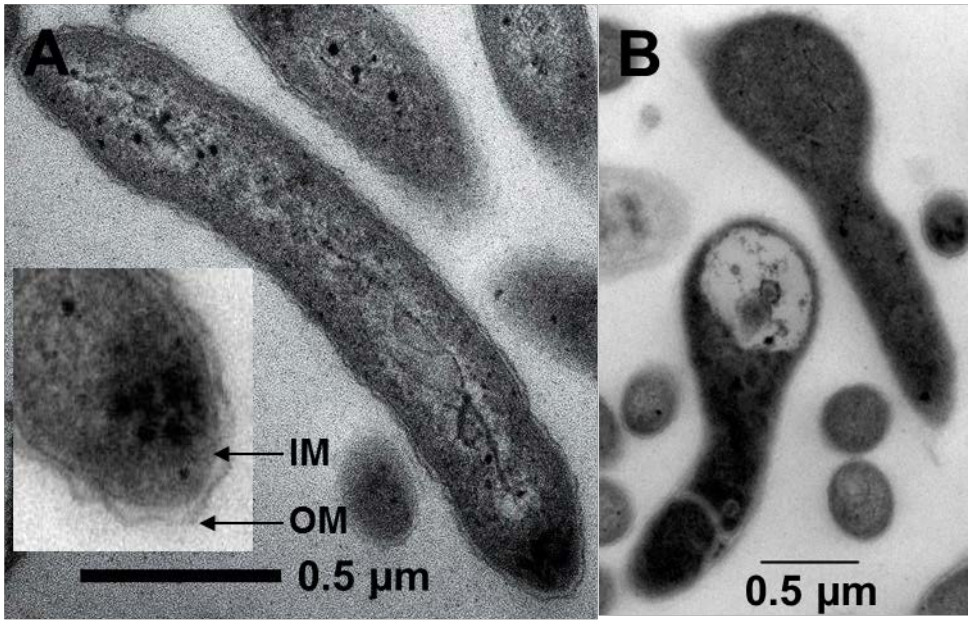

Figure 4.1. Transmission electron micrographs of Strain RU4. (A) Exponential phase culture showing gram-negative cell wall with an IM-Inner Membrane and OM-Outer Membrane; and (B) Stationary phase culture showing endopsore formation.

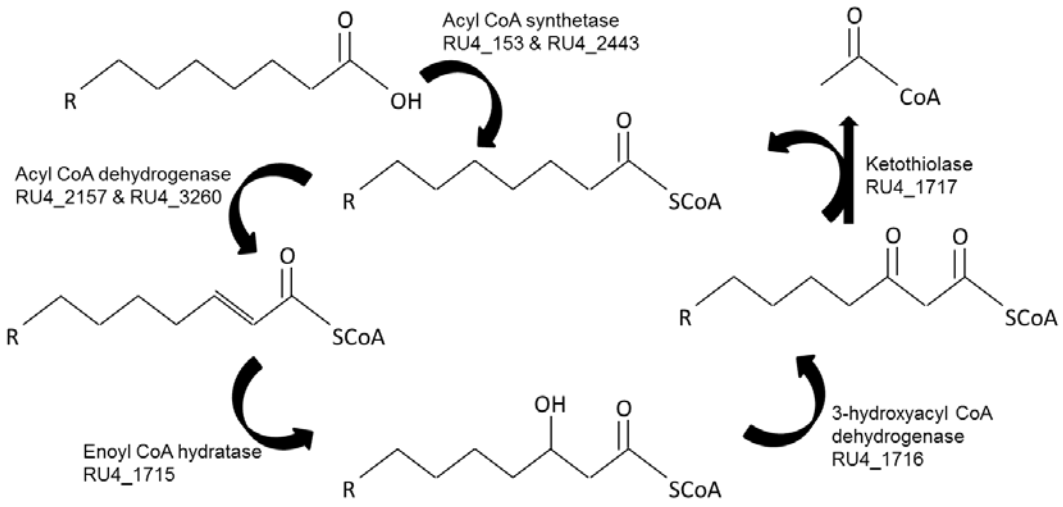

Figure 4.2. Beta oxidation pathway in strain RU4.

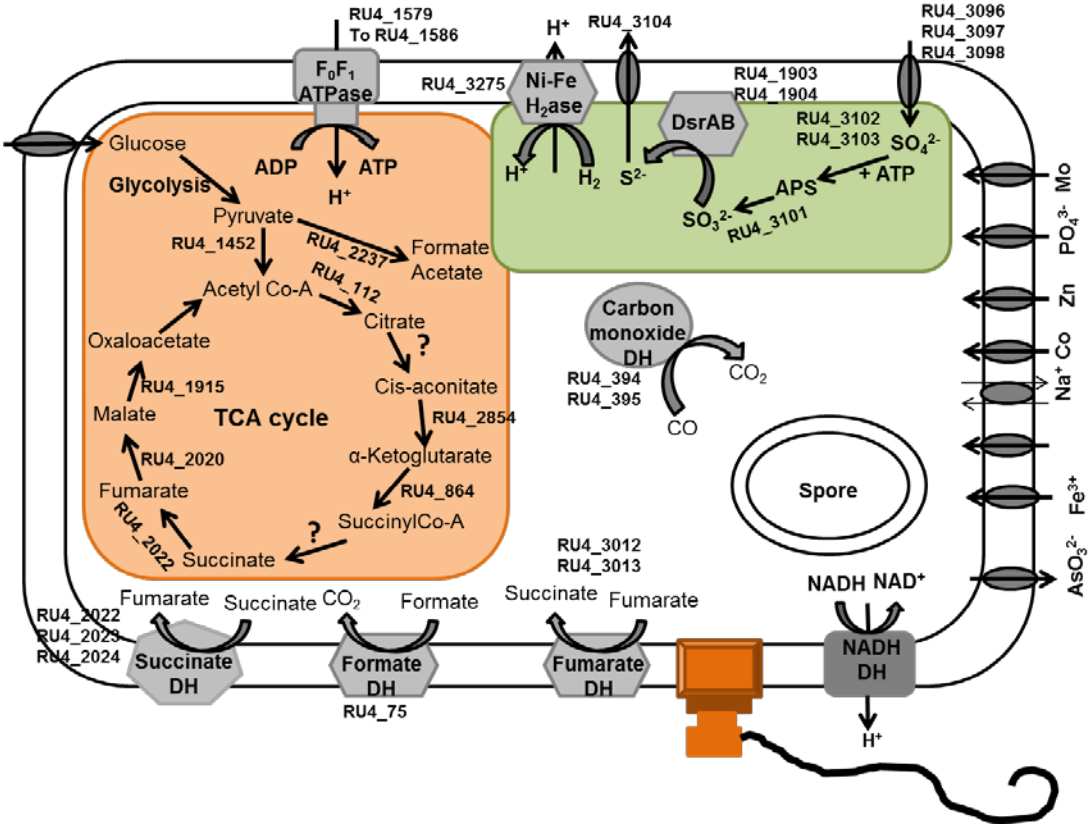

Figure 4.3. Schematic representation of genes and metabolism pathways in the genome of strain RU4.

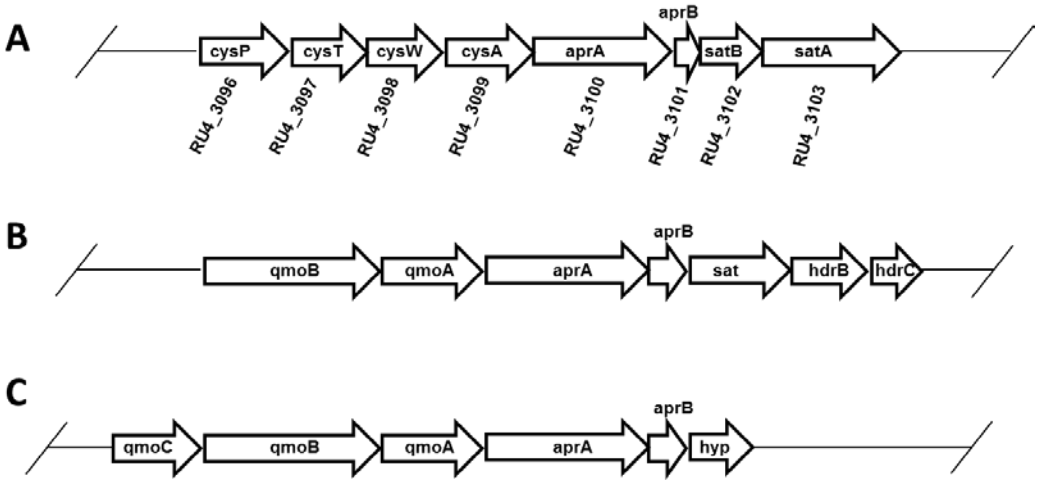

Figure 4.4. Sulfate reduction operon structure in (A) strain RU4, (B) *Desulfotomaculum reducens* strain MR-1 and (C) *Desulfovibrio vulgaris* strain Hildenborough. *apr*AB, alpha and beta subunit of the APS reductase; *sat*AB, alpha and beta subunit of the sulfate adenylyltransferase; *qmo*ABC, alpha, beta and gamma subunits of the quinone-interacting membrane-bound oxidoreductase; *hdr*B, heterodisulfide reductase; and hyp, hypothetical protein.

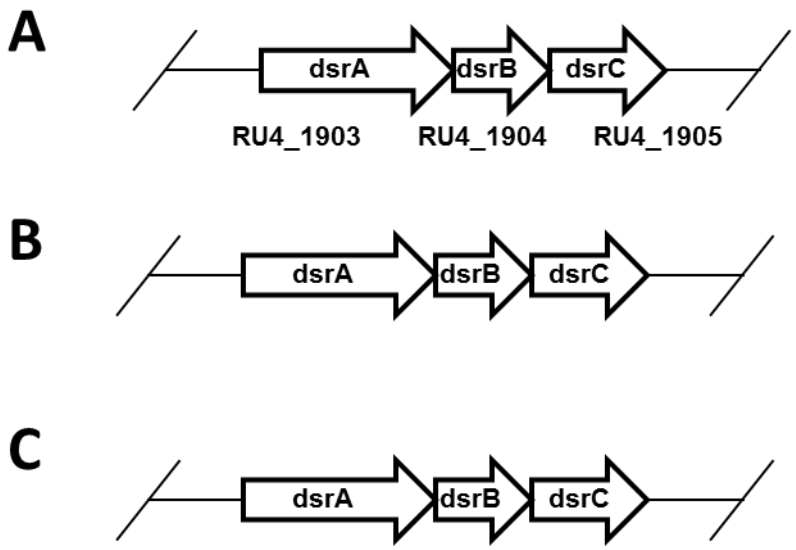

Figure 4.5. Sulfite reductase operon structure in (A) strain RU4, (B) *Desulfotomaculum gibsoniae* strain DSM 7213 and (C) *Desulfotomaculum nigrificans* strain DSM 574. dsrABC, sulfite reductase subunit A, B and C.

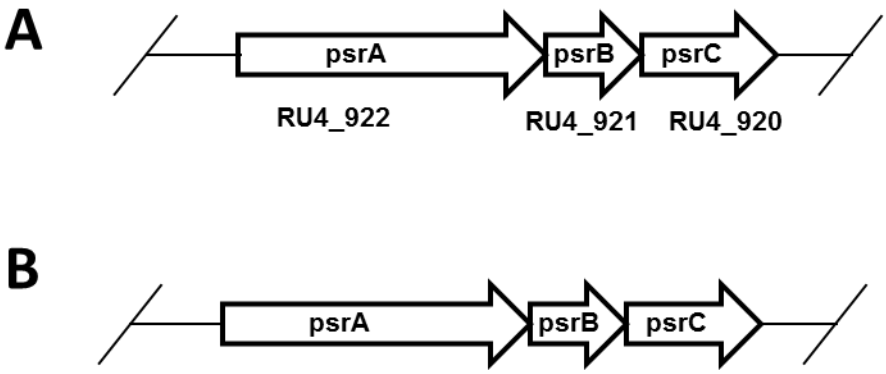

Figure 4.6. Polysulfide reduction operon structure in (A) strain RU4 and (B) *Wolinella succinogenes* strain DSM 1740. psrABC, polysulfide reductase subunit A, B and C.

Table 4.1. General features of the contigs in the genome assembly. Contigs highlighted in grey have similar tetranucleotide frequencies.

Contigs	G+C (%)	Coverage (X)	Size (bp)
Contig 1	47	754	412410
Contig 2	49	869	1880
Contig 3	47	701	744659
Contig 4	48	741	1059111
Contig 5	48	742	344244
Contig 6	46	719	214327
Contig 7	46	713	390707
Contig 8	47	712	239682
Contig 9	46	731	135797
Contig 10	55	3928	1733
Contig 11	49	231	3523
Contig 12	47	742	80728
Contig 14	46	705	152087
Contig 16	54	5388	2604
Contig 17	46	695	52803
Contig 18	47	722	15804
Contig 29	47	698	49567
Contig 34	47	734	7840
Contig 36	48	1408	2853
Contig 37	47	722	24954
Contig 40	31	138	1296
Contig 49	49	980	899
Contig 54	44	739	4018
Contig 55	54	1407	1061
Contig 66	48	1235	401
Contig 82	41	195	8931
Contig 111	52	629	782
Contig 184	31	139	1453

CHAPTER 5

CONCLUSIONS

Contribution to Knowledge

The research presented in this dissertation describes iron oxide reduction by a fermentative and sulfate reducing clostridial consortium. The experimental studies were focused on iron oxide reduction by different groups of microorganisms (fermentative and sulfate reducing) in contrast to traditional dissimilatory iron reducing *Geobacter* and *Shewanella*. The data demonstrated extensive crystalline iron oxide reduction and secondary biomineralization by the clostridial consortium. The results also provided new insights in the role of syntrophy in rapid iron oxide reduction by the consortium. Furthermore, genome of the two members of this consortium were sequenced and analyzed.

Chapter 2 described amorphous and crystalline iron oxide reduction by a clostridial consortium cultivated from subsurface sediments. The major finding reported in this chapter was rapid crystalline iron oxide reduction by the consortium. Extensive amounts of goethite and hematite were reduced by the consortium in comparison to a pure culture of *Clostridium sp*. FGH. *Clostridium sp*. FGH was able to reduce an extensive amount of ferrihydrite but not goethite and hematite. These results suggest that the ability of rapid crystalline iron oxide reduction was enabled when *Clostridium sp*. FGH was grown with strain RU4. Another finding was that *Clostridium sp*. FGH produced hydrogen during fermentative growth. It was also observed that growth and activity of sulfate reducing strain RU4 was substantially enhanced in presence of hydrogen. Strain RU4 produced reactive sulfide that mediated chemical reduction of iron oxides. These results indicate that syntrophy plays an important role in rapid iron oxide reduction by the

consortium. Overall, iron oxide reduction by the consortium was driven by multiple pathways, iron oxide reduction by *Clostridium sp*. FGH as well as biotic/abiotic reactions catalyzed by the activity of sulfide producing strain RU4. Secondary biominerals produced during iron oxide reduction by the consortium were analyzed with the help of X-ray diffraction analysis, transmission electron microscopy, and X-ray photoelectron spectroscopy. The results from these analyses revealed that most of the ferrous iron produced by the consortium was bound in solid-phase. In addition to lots of solid-phase Fe(II), nanoparticulate magnetite was formed during ferrihydrite reduction, and the precipitation of iron sulfide was observed during goethite and hematite reduction. The main conclusion of this chapter was that syntrophic interactions between fermentative and sulfate reducing bacteria represents an important pathway for crystalline iron oxide reduction and secondary mineralization.

Chapter 3 described the physiological and genomic characterization of fermentative *Clostridium sp*. strain FGH. In this study we isolated a fermentative *Clostridium sp.*, designated as strain FGH in pure culture and characterized its iron reduction ability. Main results of this study highlight that *Clostridium sp.* FGH is capable of reducing iron oxides in defined media and does not require direct contact with the iron oxide for reduction ability. Further experiments with spent medium show that reaction of cell-free spent medium with Fe(III) oxides did not result in Fe(II) production or Fe(III) solubilization. Therefore, strain FGH did not produce ligands to solubilize Fe(III) nor extracellular flavins like *Shewanella* for iron oxide reduction. Part of this study focused on genome analysis of strain FGH, which provided more insight into the physiology of this organism as well as the mechanism of iron oxide reduction. Genome sequencing and analysis revealed the presence of glucose and pyruvate metabolism genes in *Clostridium sp.* FGH. It also indicated the presence of [Fe] and [NiFe] hydrogenase in the genome of hydrogen producing *Clostridium sp.* FGH. Absence of multiheme c-type

cytochromes was revealed by genome analysis of strain FGH. Comparative genome analysis confirms that c-type cytochromes are rare in complete genomes of many *Clostridium sp*. in contrast to dissimilatory iron reducing bacteria such as *Geobacter*, *Shewanella* and *Thermincola*. The main conclusion of this study is that *Clostridium sp.* FGH reduces iron oxides at a distance and a cytochrome-independent mechanism is involved in iron oxide reduction.

Chapter 4 described the genomic characterization of a novel *Veillonellaceae* (strain RU4) that was enriched from subsurface sediments. Strain RU4 coexists with *Clostridium sp.* FGH in an anaerobic enrichment culture. The genome of strain RU4 in enrichment culture was sequenced in this study. The genomic fragments of strain RU4 were separated from *Clostridium sp.* FGH based on G+C content and tetranucleotide frequency analysis of contigs in the genome assembly. Genomic characterization of strain RU4 revealed metabolic capabilities of this organism. A β oxidation pathway for fatty acid metabolism was found in the RU4 genome. The strain RU4 genome also encodes for genes involved in fermentation of glucose, pyruvate, succinate, malate, and formate. Genes coding for [NiFe] hydrogenases that are involved in hydrogen oxidation were found in the genome of strain RU4. Interestingly, strain RU4 possesses genes for sulfate, sulfite and polysulfide reduction that have not been studied in members of family *Veillonellaceae*. These genes are present in an operon. APS reductase aprAB, has about 34% and 28% protein sequence identity with known sulfate reducers such as *Desulfotomaculum reducens* MR-1 and *Desulfovibrio vulgaris* Hildenborough, respectively. The genes upstream and downstream of APS reductase in strain RU4 are different from known sulfate reducers such as *Desulfotomaculum reducens* MR-1 and *Desulfovibrio vulgaris* Hildenborough. The sulfite reduction operon in strain RU4 has identical gene organization and high protein sequence similarity to other sulfite reducing bacteria *Desulfotomaculum gibsonia* DSM 7213 and *Desulfotomaculum nigrificans* DSM

574. The RU4 genome also encodes for polysulfite reductase that is present in an operon very similar to the one in polysulfide respiring *Wolinella succinogenes* DSM 1740 with 48 – 61% protein sequence similarity. Fermentation, hydrogen oxidation and sulfate reduction by strain RU4 may affect the biogeochemical cycling of carbon and sulfur in the subsurface. Results of this study broaden our knowledge on what biogeochemical and ecological role this novel subsurface *Veillonellaceae* might play in the subsurface environments.

Suggestions for Future Research

Research described in this dissertation elucidates rapid iron oxide reduction by the consortium. However, the relative abundance and spatial relationships of the two organisms in the consortium are still poorly understood. The relative abundance of strain FGH and strain RU4 can be determined by desiging strain specific primers and using quantitative PCR. Cell-cell and cell-mineral interactions can be studied by the fluoresence in-situ hybridization (FISH) approach. It will enable us to study molecular scale interactions between two different cell types or between cells and mineral surfaces.

This research demonstrated that direct contact was not required for iron reduction by fermentative *Clostridium sp*. FGH and that cells were needed for iron oxide reduction. However, future research is necessary to understand the nature of the redox active molecules that might be involved in iron oxide reduction by strain FGH. It is likely that strain FGH produces a redox active reduced molecule that can reduce any electron acceptor and is not specific for iron oxides. Experiments can be conducted to test this hypothesis by growing strain FGH with manganese oxide. After understanding the nature of extracellular molecule produced by strain FGH, future experiments can be focused on testing if strain FGH is capable of uranium reduction. If yes, does it involve

an extracellular factor as shown uranium reduction by *Clostridium acetobutylicum* and *Desulfotomaculum reducens* spores.

Future research needs to be conducted to identify the genes that are involved in iron oxide reduction by strain FGH. Since the genome of this organism is sequenced, we can do a transcriptome analysis of strain FGH cultures grown in the presence and absence of iron. This study would reveal the genes that are upregulated or downregulated under these conditions and provide insight about which genes are likely to be involved in iron reduction by strain FGH. Furthermore, we can test to see if there is a difference in genes that are expressed during soluble iron reduction and iron oxide reduction with the help of transcriptome analysis. If a set of the genes are found to be upregulated during iron reduction by strain FGH, a mutagenesis approach can be applied to test the function of these genes.

We need to isolate strain RU4 in pure culture. Isolation of strain RU4 would enable testing for metabolic capabilities that have been revelaed by genome analysis. Genome analysis of strain RU4 provided information about the potential metabolic ability of this organism that can assist the isolation approach for this organism. Further experimentation is also required to confirm if these genes are functional in this genome. A transcriptome study of strain RU4 grown under environmentally relevant conditions will provide insight into the role of this organism in metal reduction.

REFERENCES

Akob, D.M., Mills, H.J., Gihring, T.M., Kerkhof, L., Stucki, J.W., Anastacio, A.S., Chin, K.J., Kusel, K., Palumbo, A.V., Watson, D.B., Kostka, J.E., 2008. Functional diversity and electron donor dependence of microbial populations capable of U(VI) reduction in radionuclide-contaminated subsurface sediments. Applied and Environmental Microbiology 74, 3159-3170.

Akob, D.M., Mills, H.J., Kostka, J.E., 2007. Metabolically active microbial communities in uranium-contaminated subsurface sediments. FEMS Microbiology Ecology 59, 95-107.

Altschul, S.F., Madden, T.L., Schaffer, A.A., Zhang, J.H., Zhang, Z., Miller, W., Lipman, D.J., 1997. Gapped BLAST and PSI-BLAST: a new generation of protein database search programs. Nucleic Acids Research 25, 3389-3402.

Aziz, R.K., Bartels, D., Best, A.A., DeJongh, M., Disz, T., Edwards, R.A., Formsma, K., Gerdes, S., Glass, E.M., Kubal, M., Meyer, F., Olsen, G.J., Olson, R., Osterman, A.L., Overbeek, R.A., McNeil, L.K., Paarmann, D., Paczian, T., Parrello, B., Pusch, G.D., Reich, C., Stevens, R., Vassieva, O., Vonstein, V., Wilke, A., Zagnitko, O., 2008. The RAST server: Rapid annotations using subsystems technology. BMC Genomics 9, 15.

Barlett, M., Moon, H.S., Peacock, A.A., Hedrick, D.B., Williams, K.H., Long, P.E., Lovley, D., Jaffe, P.R., 2012. Uranium reduction and microbial community development in response to stimulation with different electron donors. Biodegradation 23, 535-546.

Beliaev, A.S., Saffarini, D.A., McLaughlin, J.L., Hunnicutt, D., 2001. MtrC, an outer membrane decahaem c cytochrome required for metal reduction in *Shewanella putrefaciens* MR-1. Molecular Microbiology 39, 722-730.

Beller, H.R., Han, R.Y., Karaoz, U., Lim, H., Brodie, E.L., 2013. Genomic and Physiological Characterization of the Chromate-Reducing, Aquifer-Derived Firmicute *Pelosinus sp* Strain HCF1. Applied and Environmental Microbiology 79, 63-73.

Bhatti, M.A., Frank, M.O., 2000. *Veillonella parvula* meningitis: Case report and review of *Veillonella* infections. Clinical Infectious Diseases 31, 839-840.

Biebl, H., Schwab-Hanisch, H., Sproer, C., Lunsdorf, H., 2000. *Propionispora vibrioides*, nov gen., nov sp., a new gram-negative, spore-forming anaerobe that ferments sugar alcohols. Archives of Microbiology 174, 239-247.

Boetius, A., Ravenschlag, K., Schubert, C.J., Rickert, D., Widdel, F., Gieseke, A., Amann, R., Jorgensen, B.B., Witte, U., Pfannkuche, O., 2000. A marine microbial consortium apparently mediating anaerobic oxidation of methane. Nature 407, 623-626.

Boga, H.I., Ludwig, W., Brune, A., 2003. *Sporomusa aerivorans* sp nov., an oxygen-reducing homoacetogenic bacterium from the gut of a soil-feeding termite. International Journal of Systematic and Evolutionary Microbiology 53, 1397-1404.

Bretschger, O., Obraztsova, A., Sturm, C.A., Chang, I.S., Gorby, Y.A., Reed, S.B., Culley, D.E., Reardon, C.L., Barua, S., Romine, M.F., Zhou, J., Beliaev, A.S., Bouhenni, R., Saffarini, D., Mansfeld, F., Kim, B.H., Fredrickson, J.K., Nealson, K.H., 2007. Current production and metal oxide reduction by *Shewanella oneidensis* MR-1 wild type and mutants. Applied and Environmental Microbiology 73, 7003-7012.

Butler, J.E., Kaufmann, F., Coppi, M.V., Nunez, C., Lovley, D.R., 2004. MacA a diheme c-type cytochrorne involved in Fe(III) reduction by *Geobacter sulfurreducens*. Journal of Bacteriology 186, 4042-4045.

Caccavo, F., Coates, J.D., RosselloMora, R.A., Ludwig, W., Schleifer, K.H., Lovley, D.R., McInerney, M.J., 1996. *Geovibrio ferrireducens*, a phylogenetically distinct dissimilatory Fe(III)-reducing bacterium. Archives of Microbiology 165, 370-376.

Caccavo, F., Lonergan, D.J., Lovley, D.R., Davis, M., Stolz, J.F., McInerney, M.J., 1994. *Geobacter sulfurreducens* sp. nov, A hydrogen oxidizing and acetate oxidizing dissimilatory metal reducing microorganisms. Applied and Environmental Microbiology 60, 3752-3759.

Caffrey, S.M., Voordouw, G., 2010. Effect of sulfide on growth physiology and gene expression of *Desulfovibrio vulgaris* Hildenborough. Antonie Van Leeuwenhoek International Journal of General and Molecular Microbiology 97, 11-20.

Cardenas, E., Wu, W.M., Leigh, M.B., Carley, J., Carroll, S., Gentry, T., Luo, J., Watson, D., Gu, B.H., Ginder-Vogel, M., Kitanidis, P.K., Jardine, P.M., Zhou, J.Z., Criddle, C.S., Marsh, T.L., Tiedje, J.M., 2010. Significant Association between Sulfate-Reducing Bacteria and Uranium-Reducing Microbial Communities as Revealed by a Combined Massively Parallel Sequencing-Indicator Species Approach. Applied and Environmental Microbiology 76, 6778-6786.

Carlier, J.P., Marchandin, H., Jumas-Bilak, E., Lorin, V., Henry, C., Carriere, C., Jean-Pierre, H., 2002. *Anaeroglobus geminatus* gen. nov., sp nov., a novel member of the family *Veillonellaceae*. International Journal of Systematic and Evolutionary Microbiology 52, 983-986.

Carlson, H.K., Iavarone, A.T., Gorur, A., Yeo, B.S., Tran, R., Melnyk, R.A., Mathies, R.A., Auer, M., Coates, J.D., 2012. Surface multiheme c-type cytochromes from *Thermincola potens* and implications for respiratory metal reduction by Gram-positive bacteria. Proceedings of the National Academy of Sciences of the United States of America 109, 1702-1707.

Castro, H.F., Williams, N.H., Ogram, A., 2000. Phylogeny of sulfate-reducing bacteria. FEMS Microbiology Ecology 31, 1-9.

Chenna, R., Sugawara, H., Koike, T., Lopez, R., Gibson, T.J., Higgins, D.G., Thompson, J.D., 2003. Multiple sequence alignment with the Clustal series of programs. Nucleic Acids Research 31, 3497-3500.

Cline, J.D., 1969. Spectrophotometric determination of hydrogen sulfide in natural waters. Limnology and Oceanography 14, 454-458.

Coleman, M.L., Hedrick, D.B., Lovley, D.R., White, D.C., Pye, K., 1993. Reduction of Fe(II) in sediments by sulfate-reducing bacteria. Nature 361, 436-438.

Coursolle, D., Baron, D.B., Bond, D.R., Gralnick, J.A., 2010. The Mtr Respiratory Pathway Is Essential for Reducing Flavins and Electrodes in *Shewanella oneidensis*. Journal of Bacteriology 192, 467-474.

Covington, E.D., Gelbmann, C.B., Kotloski, N.J., Gralnick, J.A., 2010. An essential role for UshA in processing of extracellular flavin electron shuttles by *Shewanella oneidensis*. Molecular Microbiology 78, 519-532.

Dalla Vecchia, E.C., Veeramani, H., Suvorova, E.I., Wigginton, N.S., Bargar, J.R., Bernier-Latmani, R., 2010. U(VI) reduction by spores of *Clostridium acetobutylicum*. Research in Microbiology 161, 765-771.

Daniel, R., Warnecke, F., Potekhina, J.S., Gottschalk, G., 1999. Identification of the syntrophic partners in a coculture coupling anaerobic methanol oxidation to Fe(III) reduction. FEMS Microbiology Letters 180, 197-203.

Daumas, S., Cordruwisch, R., Garcia, J.L., 1988. *Desulfotomaculum geothermicum* sp. nov,. A thermophilic,fatty acid degrading, sulfate-reducing bacterium isolated with H_2 from geothermal groundwater. Antonie Van Leeuwenhoek Journal of Microbiology 54, 165-178.

Dehning, I., Stieb, M., Schink, B., 1989. *Sporomusa malonica* sp. nov. A homoacetogenic bacterium growing by decarboxylation of malonate or succinate. Archives of Microbiology 151, 421-426.

Dobbin, P.S., Carter, J.P., San Juan, C.G.S., Von Hobe, M., Powell, A.K., Richardson, D.J., 1999. Dissimilatory Fe(III) reduction by *Clostridium beijerinckii* isolated from freshwater sediment using Fe(III) maltol enrichment. FEMS Microbiology Letters 176, 131-138.

Elsner, M., Schwarzenbach, R.P., Haderlein, S.B., 2004. Reactivity of Fe(II)-bearing minerals toward reductive transformation of organic contaminants. Environmental Science & Technology 38, 799-807.

Francis, A.J., Dodge, C.J., Lu, F.L., Halada, G.P., Clayton, C.R., 1994. XPS and XANES studies of uranium reduction by *Clostridium sp.* Environmental Science & Technology 28, 636-639.

Fredrickson, J.K., Zachara, J.M., Kennedy, D.W., Dong, H.L., Onstott, T.C., Hinman, N.W., Li, S.M., 1998. Biogenic iron mineralization accompanying the dissimilatory

reduction of hydrous ferric oxide by a groundwater bacterium. Geochimica et Cosmochimica Acta 62, 3239-3257.

Fredrickson, J.K., Zachara, J.M., Kennedy, D.W., Kukkadapu, R.K., McKinley, J.P., Heald, S.M., Liu, C.X., Plymale, A.E., 2004. Reduction of TcO_4^- by sediment-associated biogenic Fe(II). Geochimica et Cosmochimica Acta 68, 3171-3187.

Gao, W.M., Francis, A.J., 2008. Reduction of uranium(VI) to uranium(IV) by clostridia. Applied and Environmental Microbiology 74, 4580-4584.

Gavrilov, S.N., Slobodkin, A.I., Robb, F.T., de Vries, S., 2007. Characterization of membrane-bound Fe(III)-EDTA reductase activities of the thermophilic gram-positive dissimilatory iron-reducing bacterium *Thermoterrabacterium ferrireducens.* Microbiology 76, 139-146.

Geets, J., Borrernans, B., Diels, L., Springael, D., Vangronsveld, J., van der Lelie, D., Vanbroekhoven, K., 2006. *DsrB* gene-based DGGE for community and diversity surveys of sulfate-reducing bacteria. Journal of Microbiological Methods 66, 194-205.

Gihring, T.M., Zhang, G.X., Brandt, C.C., Brooks, S.C., Campbell, J.H., Carroll, S., Criddle, C.S., Green, S.J., Jardine, P., Kostka, J.E., Lowe, K., Mehlhorn, T.L., Overholt, W., Watson, D.B., Yang, Z.M., Wu, W.M., Schadt, C.W., 2011. A Limited Microbial Consortium Is Responsible for Extended Bioreduction of Uranium in a Contaminated Aquifer. Applied and Environmental Microbiology 77, 5955-5965.

Gregory, K.B., Larese-Casanova, P., Parkin, G.F., Scherer, M.M., 2004. Abiotic transformation of hexahydro-1,3,5-trinitro-1,3,5-triazine by fell bound to magnetite. Environmental Science & Technology 38, 1408-1414.

Gronow, S., Welnitz, S., Lapidus, A., Nolan, M., Ivanova, N., Del Rio, T.G., Copeland, A., Chen, F., Tice, H., Pitluck, S., Cheng, J.F., Saunders, E., Brettin, T., Han, C., Detter, J.C., Bruce, D., Goodwin, L., Land, M., Hauser, L., Chang, Y.J., Jeffries, C.D., Pati, A., Mavromatis, K., Mikhailova, N., Chen, A., Palaniappan, K., Chain, P., Rohde, M., Goker, M., Bristow, J., Eisen, J.A., Markowitz, V., Hugenholtz, P., Kyrpides, N.C., Klenk, H.P., Lucas, S., 2010. Complete genome sequence of *Veillonella parvula* type strain (Te3(T)). Standards in Genomic Sciences 2, 57-65.

Hammann, R., Ottow, J.C.G., 1974. Reductive Dissolution of Fe_2O_3 by Saccharolytic Clostridia and *Bacillus polymyxa* under anaerobic conditions. Journal of Plant Nutrition and Soil Science 137, 108-115.

Hansel, C.M., Benner, S.G., Fendorf, S., 2005. Competing Fe(II)-induced mineralization pathways of ferrihydrite. Environmental Science & Technology 39, 7147-7153.

Hansel, C.M., Benner, S.G., Neiss, J., Dohnalkova, A., Kukkadapu, R.K., Fendorf, S., 2003. Secondary mineralization pathways induced by dissimilatory iron reduction of ferrihydrite under advective flow. Geochimica et Cosmochimica Acta 67, 2977-2992.

Heidelberg, J.F., Paulsen, I.T., Nelson, K.E., Gaidos, E.J., Nelson, W.C., Read, T.D., Eisen, J.A., Seshadri, R., Ward, N., Methe, B., Clayton, R.A., Meyer, T., Tsapin, A., Scott, J., Beanan, M., Brinkac, L., Daugherty, S., DeBoy, R.T., Dodson, R.J., Durkin, A.S., Haft, D.H., Kolonay, J.F., Madupu, R., Peterson, J.D., Umayam, L.A., White, O., Wolf, A.M., Vamathevan, J., Weidman, J., Impraim, M., Lee, K., Berry, K., Lee, C., Mueller, J., Khouri, H., Gill, J., Utterback, T.R., McDonald, L.A., Feldblyum, T.V., Smith, H.O., Venter, J.C., Nealson, K.H., Fraser, C.M., 2002. Genome sequence of the dissimilatory metal ion-reducing bacterium *Shewanella oneidensis*. Nature Biotechnology 20, 1118-1123.

Holmes, D.E., Chaudhuri, S.K., Nevin, K.P., Mehta, T., Methe, B.A., Liu, A., Ward, J.E., Woodard, T.L., Webster, J., Lovley, D.R., 2006. Microarray and genetic analysis of electron transfer to electrodes in *Geobacter sulfurreducens*. Environmental Microbiology 8, 1805-1815.

Hughes, C.V., Kolenbrander, P.E., Andersen, R.N., Moore, L.V.H., 1988. Coaggregation properties of human oral *Veillonella spp* - Relationship to colonization site and oral ecology. Applied and Environmental Microbiology 54, 1957-1963.

Hyun, S.P., Davis, J.A., Sun, K., Hayes, K.F., 2012. Uranium(VI) Reduction by Iron(II) Monosulfide Mackinawite. Environmental Science & Technology 46, 3369-3376.

Jumas-Bilak, E., Carlier, J.P., Jean-Pierre, H., Teyssier, C., Gay, B., Campos, J., Marchandin, H., 2004. *Veillonella montpellierensis* sp nov., a novel, anaerobic, Gram-negative coccus isolated from human clinical samples. International Journal of Systematic and Evolutionary Microbiology 54, 1311-1316.

Junier, P., Frutschi, M., Wigginton, N. S., Schofield, E. J., Bargar, J. R., and Bernier-Latmani, R., 2009. Metal reduction by spores of *Desulfotomaculum reducens*. Environmental Microbiology 11, 3007-3017.

Junier, P., Junier, T., Podell, S., Sims, D.R., Detter, J.C., Lykidis, A., Han, C.S., Wigginton, N.S., Gaasterland, T., Bernier-Latmani, R., 2010. The genome of the Gram-positive metal- and sulfate-reducing bacterium *Desulfotomaculum reducens* strain MI-1. Environmental Microbiology 12, 2738-2754.

Kappler, A., Straub, K.L., 2005. Geomicrobiological cycling of iron. Molecular Geomicrobiology 59, 85-108.

Kashefi, K., Lovley, D.R., 2000. Reduction of Fe(III), Mn(IV), and toxic metals at 100 degrees C by *Pyrobaculum islandicum*. Applied and Environmental Microbiology 66, 1050-1056.

Kashefi, K., Lovley, D.R., 2003. Extending the upper temperature limit for life. Science 301, 934-934.

Kerkhof, L., Ward, B.B., 1993. Comparison of nucleic acid hybridization and fluorometry for measurement of the relationship between RNA/RNA ration and growth rate in a marine bacterium. Applied and Environmental Microbiology 59, 1303-1309.

Klausen, J., Trober, S.P., Haderlein, S.B., Schwarzenbach, R.P., 1995. Reduction of substituted nitrobenzenes by Fe(II) in aqueous mineral suspensions. Environmental Science & Technology 29, 2396-2404.

Klouche, N., Fardeau, M.L., Lascourreges, J.F., Cayol, J.L., Hacene, H., Thomas, P., Magot, M., 2007. *Geosporobacter subterraneus* gen. nov., sp nov., a spore-forming bacterium isolated from a deep subsurface aquifer. International Journal of Systematic and Evolutionary Microbiology 57, 1757-1761.

Kostka, J.E., Dalton, D.D., Skelton, H., Dollhopf, S., Stucki, J.W., 2002. Growth of iron(III)-reducing bacteria on clay minerals as the sole electron acceptor and comparison of growth yields on a variety of oxidized iron forms. Applied and Environmental Microbiology 68, 6256-6262.

Kotloski, N.J., Gralnicka, J.A., 2013. Flavin Electron Shuttles Dominate Extracellular Electron Transfer by *Shewanella oneidensis*. mBio, pp. 1-4.

Kukkadapu, R.K., Zachara, J.M., Fredrickson, J.K., McKinley, J.P., Kennedy, D.W., Smith, S.C., Dong, H.L., 2006. Reductive biotransformation of Fe in shale-limestone saprolite containing Fe(III) oxides and Fe(II)/Fe(III) phyllosilicates. Geochimica et Cosmochimica Acta 70, 3662-3676.

Kunapuli, U., Lueders, T., Meckenstock, R.U., 2007. The use of stable isotope probing to identify key iron-reducing microorganisms involved in anaerobic benzene degradation. ISME Journal 1, 643-653.

Leang, C., Adams, L.A., Chin, K.J., Nevin, K.P., Methe, B.A., Webster, J., Sharma, M.L., Lovley, D.R., 2005. Adaptation to disruption of the electron transfer pathway for Fe(III) reduction in *Geobacter sulfurreducens*. Journal of Bacteriology 187, 5918-5926.

Leang, C., Coppi, M.V., Lovley, D.R., 2003. OmcB, a c-type polyheme cytochrome, involved in Fe(III) reduction in *Geobacter sulfurreducens*. Journal of Bacteriology 185, 2096-2103.

Lee, W., Batchelor, B., 2002. Abiotic, reductive dechlorination of chlorinated ethylenes by iron-bearing soil minerals. 2. Green rust. Environmental Science & Technology 36, 5348-5354.

Lehours, A.C., Batisson, I., Guedon, A., Mailhot, G., Fonty, G., 2009. Diversity of Culturable Bacteria, from the Anaerobic Zone of the Meromictic Lake Pavin, Able to Perform Dissimilatory-Iron Reduction in Different in Vitro Conditions. Geomicrobiology Journal 26, 212-223.

Li, Y.L., Vali, H., Yang, J., Phelps, T.J., Zhang, C.L., 2006. Reduction of iron oxides enhanced by a sulfate-reducing bacterium and biogenic H_2S. Geomicrobiology Journal 23, 103-117.

Lies, D.P., Hernandez, M.E., Kappler, A., Mielke, R.E., Gralnick, J.A., Newman, D.K., 2005. *Shewanella oneidensis* MR-1 uses overlapping pathways for iron reduction

at a distance and by direct contact under conditions relevant for biofilms. Applied and Environmental Microbiology 71, 4414-4426.

Liger, E., Charlet, L., Van Cappellen, P., 1999. Surface catalysis of uranium(VI) reduction by iron(II). Geochimica et Cosmochimica Acta 63, 2939-2955.

Lin, B., Hyacinthe, C., Bonneville, S., Braster, M., Van Cappellen, P., Roling, W.F.M., 2007. Phylogenetic and physiological diversity of dissimilatory ferric iron reducers in sediments of the polluted Scheldt estuary, Northwest Europe. Environmental Microbiology 9, 1956-1968.

Lin, L.H., Wang, P.L., Rumble, D., Lippmann-Pipke, J., Boice, E., Pratt, L.M., Lollar, B.S., Brodie, E.L., Hazen, T.C., Andersen, G.L., DeSantis, T.Z., Moser, D.P., Kershaw, D., Onstott, T.C., 2006. Long-term sustainability of a high-energy, low-diversity crustal biome. Science 314, 479-482.

Liu, C.G., Zachara, J.M., Gorby, Y.A., Szecsody, J.E., Brown, C.F., 2001a. Microbial reduction of Fe(III) and sorption/precipitation of Fe(II) on *Shewanella putrefaciens* strain CN32. Environmental Science & Technology 35, 1385-1393.

Liu, C.X., Kota, S., Zachara, J.M., Fredrickson, J.K., Brinkman, C.K., 2001b. Kinetic analysis of the bacterial reduction of goethite. Environmental Science & Technology 35, 2482-2490.

Liu, Y.T., Karnauchow, T.M., Jarrell, K.F., Balkwill, D.L., Drake, G.R., Ringelberg, D., Clarno, R., Boone, D.R., 1997. Description of two new thermophilic *Desulfotomaculum spp.*, *Desulfotomaculum putei* sp. nov, from a deep terrestrial subsurface, and *Desulfotomaculum luciae* sp. nov, from a hot spring. International Journal of Systematic Bacteriology 47, 615-621.

Lloyd, J.R., Leang, C., Myerson, A.L.H., Coppi, M.V., Cuifo, S., Methe, B., Sandler, S.J., Lovley, D.R., 2003. Biochemical and genetic characterization of PpcA, a periplasmic c-type cytochrome in *Geobacter sulfurreducens*. Biochemical Journal 369, 153-161.

Lovley, D.R., 1987. Organic matter mineralization with the reduction of ferric iron - A review. Geomicrobiology Journal 5, 375-399.

Lovley, D.R., 1995. Microbial reduction of iron, manganese and other metals. Advances in Agronomy 54, 175-231.

Lovley, D.R., Coates, J.D., BluntHarris, E.L., Phillips, E.J.P., Woodward, J.C., 1996. Humic substances as electron acceptors for microbial respiration. Nature 382, 445-448.

Lovley, D.R., Holmes, D.E., Nevin, K.P., 2004. Dissimilatory Fe(III) and Mn(IV) reduction. Advances in Microbial Physiology, 49, 219-286.

Lovley, D.R., Phillips, E.J.P., 1986. Organic matter mineralization with reduction of ferric iron in anaerobic sediments. Applied and Environmental Microbiology 51, 683-689.

Lovley, D.R., Phillips, E.J.P., 1989. Requirement for a microbial consortium to completely oxidize glucose in Fe(III)-reducing sediments. Applied and Environmental Microbiology 55, 3234-3236.

Lovley, D.R., Phillips, E.J.P., Lonergan, D.J., 1991. Enzymatic versus nonenzymatic mechanisms for Fe(III) reduction in aquatic sediments. Environmental Science & Technology 25, 1062-1067.

Lovley, D.R., Roden, E.E., Phillips, E.J.P., Woodward, J.C., 1993. Enzymatic iron and uranium reduction by sulfate-reducing bacteria. Marine Geology 113, 41-53.

Lovley, D.R., Stolz, J.F., Nord, G.L., Phillips, E.J.P., 1987. Anaerobic production of magnetite by a dissimilatory iron reducing microorganisms. Nature 330, 252-254.

Madden, A.S., Palumbo, A.V., Ravel, B., Vishnivetskaya, T.A., Phelps, T.J., Schadt, C.W., Brandt, C.C., 2009. Donor-dependent Extent of Uranium Reduction for Bioremediation of Contaminated Sediment Microcosms. Journal of Environmental Quality 38, 53-60.

Marchandin, H., Jumas-Bilak, E., Gay, B., Teyssier, C., Jean-Pierre, H., de Buochberg, M.S., Carriere, C., Carlier, J.P., 2003. Phylogenetic analysis of some *Sporomusa* sub-branch members isolated from human clinical specimens: description of *Megasphaera micronuciformis* sp nov. International Journal of Systematic and Evolutionary Microbiology 53, 547-553.

Marsili, E., Baron, D.B., Shikhare, I.D., Coursolle, D., Gralnick, J.A., Bond, D.R., 2008. *Shewanella* Secretes flavins that mediate extracellular electron transfer. Proceedings of the National Academy of Sciences of the United States of America 105, 3968-3973.

McCormick, M.L., Bouwer, E.J., Adriaens, P., 2002. Carbon tetrachloride transformation in a model iron-reducing culture: Relative kinetics of biotic and abiotic reactions. Environmental Science & Technology 36, 403-410.

McInerney, M.J., Beaty, P.S., 1988. Anaerobic community structure from a nonequilibrium thermodynamic perspective. Canadian Journal of Microbiology 34, 487-493.

McInerney, M.J., Sieber, J.R., Gunsalus, R.P., 2009. Syntrophy in anaerobic global carbon cycles. Current Opinion in Biotechnology 20, 623-632.

McInerney, M.J., Struchtemeyer, C.G., Sieber, J., Mouttaki, H., Stams, A.J.M., Schink, B., Rohlin, L., Gunsalus, R.P., 2008. Physiology, ecology, phylogeny, and genomics of microorganisms capable of syntrophic metabolism. Incredible Anaerobes: from Physiology to Genomics to Fuels 1125, 58-72.

Mehta, T., Coppi, M.V., Childers, S.E., Lovley, D.R., 2005. Outer membrane c-type cytochromes required for Fe(III) and Mn(IV) oxide reduction in *Geobacter sulfurreducens*. Applied and Environmental Microbiology 71, 8634-8641.

Mehta-Kolte, M.G., Bond, D.R., 2012. *Geothrix fermentans* Secretes Two Different Redox-Active Compounds To Utilize Electron Acceptors across a Wide Range of Redox Potentials. Applied and Environmental Microbiology 78, 6987-6995.

Methe, B.A., Nelson, K.E., Eisen, J.A., Paulsen, I.T., Nelson, W., Heidelberg, J.F., Wu, D., Wu, M., Ward, N., Beanan, M.J., Dodson, R.J., Madupu, R., Brinkac, L.M., Daugherty, S.C., DeBoy, R.T., Durkin, A.S., Gwinn, M., Kolonay, J.F., Sullivan, S.A., Haft, D.H., Selengut, J., Davidsen, T.M., Zafar, N., White, O., Tran, B., Romero, C., Forberger, H.A., Weidman, J., Khouri, H., Feldblyum, T.V., Utterback, T.R., Van Aken, S.E., Lovley, D.R., Fraser, C.M., 2003. Genome of *Geobacter sulfurreducens*: Metal reduction in subsurface environments. Science 302, 1967-1969.

Moore, L.V.H., Johnson, J.L., Moore, W.E.C., 1987. Selenomonas noxia sp. nov, Selenomonas flueggei sp. nov, Selenomonas infelix sp. nov, Selenomonas dianae sp. nov, and Selenomonas artemidis sp. nov, from the human gingival crevice. International Journal of Systematic Bacteriology 37, 271-280.

Moriya, Y., Itoh, M., Okuda, S., Yoshizawa, A.C., Kanehisa, M., 2007. KAAS: an automatic genome annotation and pathway reconstruction server. Nucleic Acids Research 35, W182-W185.

Moser, D.P., Onstott, T.C., Fredrickson, J.K., Brockman, F.J., Balkwill, D.L., Drake, G.R., Pfiffner, S.M., White, D.C., Takai, K., Pratt, L.M., Fong, J., Lollar, B.S., Slater, G., Phelps, T.J., Spoelstra, N., Deflaun, M., Southam, G., Welty, A.T., Baker, B.J., Hoek, J., 2003. Temporal shifts in the geochemistry and microbial community structure of an ultradeep mine borehole following isolation. Geomicrobiology Journal 20, 517-548.

Munch, J.C., Ottow, J.C.G., 1980. Preferential Reduction of Amorphous to Crystalline Iron Oxides by Bacterial Activity. Soil Science 129, 15-29.

Munch, J.C., Ottow, J.C.G., 1983. Reductive Transformation Mechanism of Ferric Oxides in Hydromorphic Soils. Ecological Bulletins 35, 383-394.

Muyzer, G., Dewaal, E.C., Uitterlinden, A.G., 1993. Profiling of complex microbial populations by Denaturing Gradient Gel Electrophoresis analysis of polymerase chain reaction amplified genes coding for 16S ribosomal RNA. Applied and Environmental Microbiology 59, 695-700.

Muyzer, G., Smalla, K., 1998. Application of denaturing gradient gel electrophoresis (DGGE) and temperature gradient gel electrophoresis (TGGE) in microbial ecology. Antonie Van Leeuwenhoek International Journal of General and Molecular Microbiology 73, 127-141.

Myers, C.R., Myers, J.M., 1993. Role of menaquinone in the reduction of fumarate, nitrate, iron(III) and manganese(IV) by *Shewanella putrefaciens* MR-1. FEMS Microbiology Letters 114, 215-222.

Myers, C.R., Myers, J.M., 1997. Cloning and sequence of *cymA* a gene encoding a tetraheme cytochrome c required for reduction of iron(III), fumarate, and nitrate by *Shewanella putrefaciens* MR-1. Journal of Bacteriology 179, 1143-1152.

Myers, J.M., Myers, C.R., 2000. Role of the tetraheme cytochrome CymA in anaerobic electron transport in cells of *Shewanella putrefaciens* MR-1 with normal levels of menaquinone. Journal of Bacteriology 182, 67-75.

Nevin, K.P., Finneran, K.T., Lovley, D.R., 2003. Microorganisms associated with uranium bioremediation in a high-salinity subsurface sediment. Applied and Environmental Microbiology 69, 3672-3675.

Nevin, K.P., Lovley, D.R., 2000. Lack of production of electron-shuttling compounds or solubilization of Fe(III) during reduction of insoluble Fe(III) oxide by *Geobacter metallireducens*. Applied and Environmental Microbiology 66, 2248-2251.

Nevin, K.P., Lovley, D.R., 2002. Mechanisms for accessing insoluble Fe(III) oxide during dissimilatory Fe(III) reduction by *Geothrix fermentans*. Applied and Environmental Microbiology 68, 2294-2299.

Newman, D.K., Kolter, R., 2000. A role for excreted quinones in extracellular electron transfer. Nature 405, 94-97.

Nico, P.S., Stewart, B.D., Fendorf, S., 2009. Incorporation of Oxidized Uranium into Fe (Hydr)oxides during Fe(II) Catalyzed Remineralization. Environmental Science & Technology 43, 7391-7396.

Nisbet, D.J., Martin, S.A., 1990. Effect of dicarboxylic acids and Aspergillus Oryzae fermentation extract on Lactate uptake by the ruminal bacterium *Selenomonas ruminantium*. Applied and Environmental Microbiology 56, 3515-3518.

North, N.N., Dollhopf, S.L., Petrie, L., Istok, J.D., Balkwill, D.L., Kostka, J.E., 2004. Change in bacterial community structure during in situ Biostimulation of subsurface sediment cocontaminated with uranium and nitrate. Applied and Environmental Microbiology 70, 4911-4920.

Peretyazhko, T.S., Zachara, J.M., Kukkadapu, R.K., Heald, S.M., Kutnyakov, I.V., Resch, C.T., Arey, B.W., Wang, C.M., Kovarik, L., Phillips, J.L., Moore, D.A., 2012. Pertechnetate (TcO_4^-) reduction by reactive ferrous iron forms in naturally anoxic, redox transition zone sediments from the Hanford Site, USA. Geochimica et Cosmochimica Acta 92, 48-66.

Petrie, L., North, N.N., Dollhopf, S.L., Balkwill, D.L., Kostka, J.E., 2003. Enumeration and characterization of iron(III)-reducing microbial communities from acidic subsurface sediments contaminated with uranium(VI). Applied and Environmental Microbiology 69, 7467-7479.

Pitts, K.E., Dobbin, P.S., Reyes-Ramirez, F., Thomson, A.J., Richardson, D.J., Seward, H.E., 2003. Characterization of the *Shewanella oneidensis* MR-1 decaheme cytochrome MtrA. Journal of Biological Chemistry 278, 27758-27765.

Poulton, S.W., Krom, M.D., Raiswell, R., 2004. A revised scheme for the reactivity of iron (oxyhydr)oxide minerals towards dissolved sulfide. Geochimica et Cosmochimica Acta 68, 3703-3715.

Qafoku, N.P., Kukkadapu, R.K., McKinley, J.P., Arey, B.W., Kelly, S.D., Wang, C.M., Resch, C.T., Long, P.E., 2009. Uranium in Framboidal Pyrite from a Naturally Bioreduced Alluvial Sediment. Environmental Science & Technology 43, 8528-8534.

Raiswell, R., Canfield, D.E., 1998. Sources of iron for pyrite formation in marine sediments. American Journal of Science 298, 219-245.

Rastogi, G., Osman, S., Kukkadapu, R., Engelhard, M., Vaishampayan, P.A., Andersen, G.L., Sani, R.K., 2010. Microbial and Mineralogical Characterizations of Soils Collected from the Deep Biosphere of the Former Homestake Gold Mine, South Dakota. Microbial Ecology 60, 539-550.

Reguera, G., 2005. Extracellular electron transfer via microbial nanowires. Nature 435, 1098-1101.

Rosnes, J.T., Torsvik, T., Lien, T., 1991. Spore-forming thermophilic sulfate-reducing bacteria isolated from North sea oil field waters. Applied and Environmental Microbiology 57, 2302-2307.

Sass, H., Overmann, J., Rutters, H., Babenzien, H.D., Cypionka, H., 2004. *Desulfosporomusa polytropa* gen. nov., sp nov., a novel sulfate-reducing bacterium from sediments of an oligotrophic lake. Archives of Microbiology 182, 204-211.

Sawanon, S., Koike, S., Kobayashi, Y., 2011. Evidence for the possible involvement of *Selenomonas ruminantium* in rumen fiber digestion. FEMS Microbiology Letters 325, 170-179.

Scala, D.J., Hacherl, E.L., Cowan, R., Young, L.Y., Kosson, D.S., 2006. Characterization of Fe(III)-reducing enrichment cultures and isolation of Fe(III)-reducing bacteria from the Savannah River site, South Carolina. Research in Microbiology 157, 772-783.

Schink, B., Stams, A.J.M., 2006. Syntrophism among Prokaryotes. Prokaryotes 2, 309-335.

Schwertmann, U., Cornell, R.M., 1991. Iron Oxides in the Laboratory - Preparation and Characterization. WILEY-VCH, New York.

Scott, T.B., Allen, G.C., Heard, P.J., Randell, M.G., 2005. Reduction of U(VI) to U(IV) on the surface of magnetite. Geochimica et Cosmochimica Acta 69, 5639-5646.

Senko, J.M., Zhang, G.X., McDonough, J.T., Bruns, M.A., Burgos, W.D., 2009. Metal Reduction at Low pH by a *Desulfosporosinus species*: Implications for the Biological Treatment of Acidic Mine Drainage. Geomicrobiology Journal 26, 71-82.

Shah, M., Lin, C-C., Kukkadapu, R., Engelhard, M., Zhao, X., Wang, Y., Barkay, T., and Yee, N. Syntrophic Effects in a Subsurface Clostridia Consortium on Fe(III)-(Oxyhydr)oxide Reduction and Secondary Mineralization. Submitted to Geomicrobiology Journal.

Shah, M., Barkay, T., and Yee, N. Physiological and Genomic Characterization of an Iron-Reducing, Saprolite-derived *Clostridium sp*. Strain FGH. Submitted to Geobiology Journal.

Shelobolina, E.S., Nevin, K.P., Blakeney-Hayward, J.D., Johnsen, C.V., Plaia, T.W., Krader, P., Woodard, T., Holmes, D.E., VanPraagh, C.G., Lovley, D.R., 2007. *Geobacter pickeringii* sp nov., *Geobacter argillaceus* sp nov and *Pelosinus fermentans* gen. nov., sp nov., isolated from subsurface kaolin lenses. International Journal of Systematic and Evolutionary Microbiology 57, 126-135.

Shi, L.A., Richardson, D.J., Wang, Z.M., Kerisit, S.N., Rosso, K.M., Zachara, J.M., Fredrickson, J.K., 2009. The roles of outer membrane cytochromes of *Shewanella* and *Geobacter* in extracellular electron transfer. Environmental Microbiology Reports 1, 220-227.

Shimizu, T., Ohtani, K., Hirakawa, H., Ohshima, K., Yamashita, A., Shiba, T., Ogasawara, N., Hattori, M., Kuhara, S., Hayashi, H., 2002. Complete genome sequence of *Clostridium perfringens*, an anaerobic flesh-eater. Proceedings of the National Academy of Sciences of the United States of America 99, 996-1001.

Stams, A.J.M., 2006. Exocellular electron transfer in anaerobic microbial communities. Environmental Microbiology 8, 371-382.

Stams, A.J.M., de Bok, F.A.M., Plugge, C.M., van Eekert, M.H.A., Dolfing, J., Schraa, G., 2006. Exocellular electron transfer in anaerobic microbial communities. Environmental Microbiology 8, 371-382.

Stams, A.J.M., Plugge, C.M., 2009. Electron transfer in syntrophic communities of anaerobic bacteria and archaea. Nature Reviews Microbiology 7, 568-577.

Starkey, R.L., Halvorson, H.O., 1927. Studies on transformation of iron in nature: II. Concerning the importance of microorganisms in solution and precipitation of iron. Soil Science 24, 381-402.

Stewart, B.D., Nico, P.S., Fendorf, S., 2009. Stability of Uranium Incorporated into Fe (Hydr)oxides under Fluctuating Redox Conditions. Environmental Science & Technology 43, 4922-4927.

Straub, K.L., Schink, B., 2004. Ferrihydrite-dependent growth of *Sulfurospirillum deleyianum* through electron transfer via sulfur cycling. Applied and Environmental Microbiology 70, 5744-5749.

Stumm, W., Morgan, J., 1996. Aquatic Chemistry: Chemical Equilibria and Rates in Natural Waters. John Wiley & Sons, Inc., New York.

Summers, Z.M., Fogarty, H.E., Leang, C., Franks, A.E., Malvankar, N.S., Lovley, D.R., 2010. Direct Exchange of Electrons Within Aggregates of an Evolved Syntrophic Coculture of Anaerobic Bacteria. Science 330, 1413-1415.

Tamura, K., Dudley, J., Nei, M., Kumar, S., 2007. MEGA4: Molecular evolutionary genetics analysis (MEGA) software version 4.0. Molecular Biology and Evolution 24, 1596-1599.

Tanner, A.C.R., Sonis, A.L., Holgerson, P.L., Starr, J.R., Nunez, Y., Kressirer, C.A., Paster, B.J., Johansson, I., 2012. White-spot Lesions and Gingivitis Microbiotas in Orthodontic Patients. Journal of Dental Research 91, 853-858.

Tebo, B.M., Obraztsova, A.Y., 1998. Sulfate-reducing bacterium grows with Cr(VI), U(VI), Mn(IV), and Fe(III) as electron acceptors. FEMS Microbiology Letters 162, 193-198.

Teeling, H., Waldmann, J., Lombardot, T., Bauer, M., Glockner, F.O., 2004. TETRA: a web-service and a stand-alone program for the analysis and comparison of tetranucleotide usage patterns in DNA sequences. BMC Bioinformatics 5, 7.

Thabet, O.B., Fardeau, M.L., Joulian, C., Thomas, P., Hamdi, M., Garcia, J.L., Ollivier, B., 2004. *Clostridium tunisiense* sp nov., a new proteolytic, sulfur-reducing bacterium isolated from an olive mill wastewater contaminated by phosphogypse. Anaerobe 10, 185-190.

Turick, C.E., Tisa, L.S., Caccavo, F., 2002. Melanin production and use as a soluble electron shuttle for Fe(III) oxide reduction and as a terminal electron acceptor by *Shewanella algae* BrY. Applied and Environmental Microbiology 68, 2436-2444.

Valm, A.M., Welch, J.L.M., Rieken, C.W., Hasegawa, Y., Sogin, M.L., Oldenbourg, R., Dewhirst, F.E., Borisy, G.G., 2011. Systems-level analysis of microbial community organization through combinatorial labeling and spectral imaging. Proceedings of the National Academy of Sciences of the United States of America 108, 4152-4157.

Vargas, M., Kashefi, K., Blunt-Harris, E.L., Lovley, D.R., 1998. Microbiological evidence for Fe(III) reduction on early Earth. Nature 395, 65-67.

Viollier, E., Inglett, P.W., Hunter, K., Roychoudhury, A.N., Van Cappellen, P., 2000. The ferrozine method revisited: Fe(II)/Fe(III) determination in natural waters. Applied Geochemistry 15, 785-790.

Von Canstein, H., Ogawa, J., Shimizu, S., Lloyd, J.R., 2008. Secretion of flavins by *Shewanella species* and their role in extracellular electron transfer. Applied and Environmental Microbiology 74, 615-623.

White, D., 2007. The Physiology and Biochemistry of Prokaryotes. Oxford University Press, Inc., New York.

Wiatrowski, H.A., Das, S., Kukkadapu, R., Ilton, E.S., Barkay, T., Yee, N., 2009. Reduction of Hg(II) to Hg(O) by Magnetite. Environmental Science & Technology 43, 5307-5313.

Widdel, F., Pfenning, N., 1977. A New Anaerobic, Sporing, Acetate-Oxidizing, Sulfate-Reducing Bacterium, *Desulfotomaculum* (emend.) *acetoxidans* Archives of microbiology 112, 119-122.

Wu, T., Shelobolina, E., Xu, H.F., Konishi, H., Kukkadapu, R., Roden, E.E., 2012. Isolation and Microbial Reduction of Fe(III) Phyllosilicates from Subsurface Sediments. Environmental Science & Technology 46, 11618-11626.